COMMENTARY ON THE GUIDE FOR

BUCKLING AND ULTIMATE STRENGTH ASSESSMENT FOR OFFSHORE STRUCTURES

MARCH 2005 (Updated March 2018 – see next page)

American Bureau of Shipping
Incorporated by Act of Legislature of
the State of New York 1862

ABS Plaza
16855 Northchase Drive
Houston, TX 77060 USA

Updates

March 2018 consolidation includes:

- February 2014 version plus Corrigenda/Editorials

February 2014 consolidation includes:

- March 2005 version plus Corrigenda/Editorials

Foreword

This Commentary provides the fundamental principles and technical background, including sources and additional details, for the ABS *Guide for Buckling and Ultimate Strength Assessment for Offshore Structures*, April 2004, which is referred to herein as "the ABS *Buckling Guide*". The Commentary presents supplementary information to better explain the basis and intent of the criteria that are used in the ABS *Buckling Guide*. The accuracy for determining buckling and the ultimate strength predictions obtained from the application of the ABS *Buckling Guide* is established by the comparison of its results against a very extensive database of test results assembled by ABS and also from the results of nonlinear finite element analysis. Results obtained using the criteria in the ABS *Buckling Guide* are also compared against existing recognized offshore standards, such as the ABS *MODU Rules*, API RP 2A WSD, API Bulletins 2U and 2V, DnV CN30.1, and AISC LRFD [references 1, 3, 5, 6, 7, 30].

It should be understood that the Commentary is applicable only to the indicated version of the ABS *Buckling Guide*. The order of presentation of the material in this Commentary generally follows that of the ABS *Buckling Guide*. The major topic headings of the Sections in both, the ABS *Buckling Guide* and the Commentary are the same, but the detailed contents of the individual Subsections will not typically have a one-to-one correspondence between the ABS *Buckling Guide* and the Commentary.

In case of a conflict between anything presented herein and the ABS Rules or Guides, precedence is given to the ABS Rules or Guides.

ABS welcomes comments and suggestions for improvement of this Commentary. Comments or suggestions can be sent electronically to *rsd@eagle.org*.

COMMENTARY ON THE GUIDE FOR

BUCKLING AND ULTIMATE STRENGTH ASSESSMENT FOR OFFSHORE STRUCTURES

CONTENTS

This Page Intentionally Left Blank

SECTION C1 Introduction

C1 General

An important aspect in the design of an offshore steel structure is the buckling and ultimate strength behavior of its fundamental structural components. To ensure high technical quality, ABS consulted a number of internationally recognized experts in the theoretical and experimental study of buckling and ultimate strength behaviors for offshore structures. This Commentary has been compiled to give background information on the formulations and design guidance presented in the ABS *Buckling Guide* to help engineers better understand some of the fundamental principles that form the basis of that Guide.

The Commentary follows the same format and the section numbering of the ABS *Buckling Guide*. The same nomenclature is adopted in most cases, and new symbols are defined where they are used in the Commentary. Some sections that are deemed to be sufficiently clear in the ABS *Buckling Guide* will be intentionally left blank in this Commentary.

The design criteria adopted in the ABS *Buckling Guide* use a working stress format, where the acting stresses are to be less than or equal to the allowable stresses. The working stress format is deterministic; therefore, uncertainties in loads and resistances are not specially addressed, but are inherently incorporated into the maximum strength allowable utilization factors.

The formulations proposed are generally based on the premises that:

- They should not depart significantly from the formulations presented in ABS existing Rules and Guides and be consistent throughout the whole Guide;
- Where departures from existing ABS formulations are recommended, they should tend towards a formulation presented in other widely used design standards, such as API RP 2A-WSD;
- Where appropriate, improvement in formulation accuracy, whether the starting point is ABS *MODU Rules*[1], ABS *Steel Vessel Rules*[2] or API RP 2A-WSD[3], should be included in the proposed formulations.

In order to validate the two- or three-dimensional interaction equations of buckling and ultimate strength proposed in the Guide, a modeling uncertainty is introduced, which was suggested by Hoadley and Yura(1985)[4]. The modeling uncertainty is the ratio of the distance from the origin to the test data point in question, L_1, over the distance from the origin to the interaction curve, L_2, and is written by:

Modeling Uncertainty = L_1/L_2

An example of the modeling uncertainty is shown in Section C1, Figure 1. From this definition, the buckling and ultimate strength prediction is conservative if modeling uncertainty is greater than 1.0. The modeling uncertainty is especially useful because it can be used in one, two and three dimensions, and it is not a function of the exponent of each term in the interaction equation. In addition, it can be used to determine the amount of conservatism in a state limit when the experimental points are outside the range of the interaction equation when excluding factors of safety.

This concept is also extended to determine the amount of conservatism of a design when design loads are inside the range of the interaction equation including factors of safety. In spreadsheets developed by the ABS Offshore Technology Department, the so-called ‘unity check’ method is used. In this method, the unity check is done by calculating the ratio of the distance, Q_1, from the origin to the design load point *A*, over the distance, Q_2 from the origin to the point *B* on the interaction curve, as shown schematically in Section C1, Figure 2 and written by:

Unity ratio = Q_1/Q_2

The design is acceptable if the unity ratio is less than 1.0.

FIGURE 1
Definition of Modeling Uncertainty

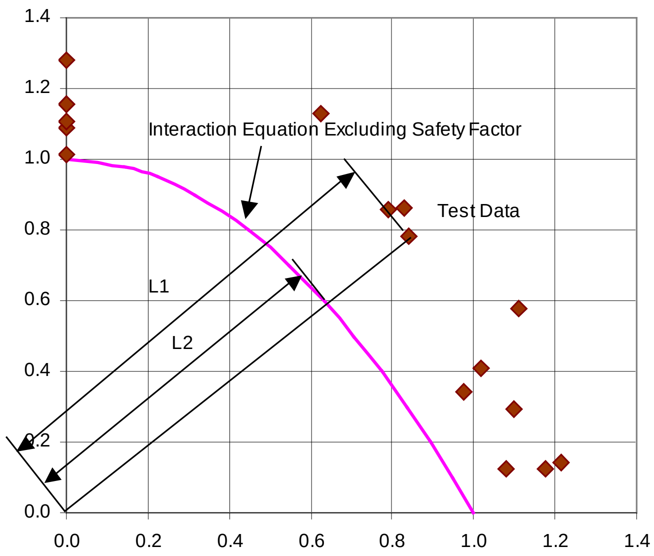

FIGURE 2
Definition of Unity Ratio

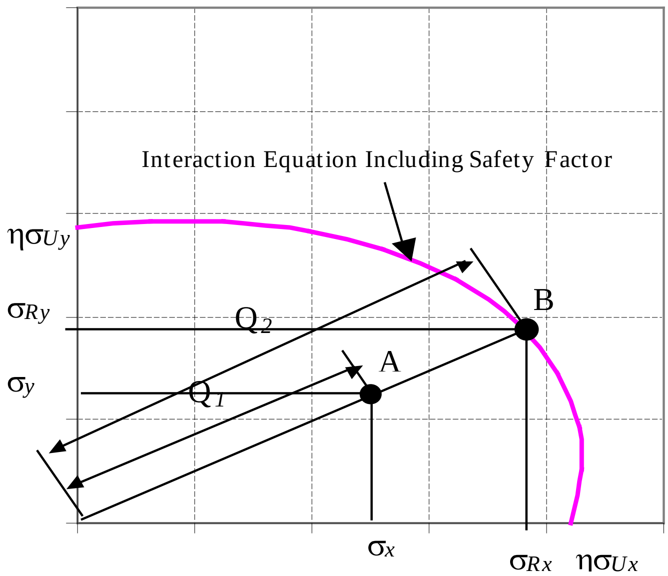

C3 Scope of This Commentary

The information in this Commentary is presented so that it can be helpful to engineers and designers in several ways. First, the comparison between the Guide's predictions and experimental and/or nonlinear FEM analysis results provides confidence about the application of the ABS *Buckling Guide*. Also the information can be useful in cases where the design parameters fall outside the range of validating test data. In such circumstances, engineers should seek to develop properly validated information. However, it is also possible to extrapolate the trends of the present criteria in initial design. It is expected that the background data presented here will be valuable in the extrapolation process.

The ABS *Buckling Guide* includes criteria for commonly used structural components in offshore structures such as:

i) Individual Structural Members

ii) Plates, Stiffened Panels and Corrugated Panels

iii) Stiffened Circular Cylindrical Shells

iv) Tubular Joints

In order to verify and validate the criteria, the ABS Offshore Technology Department gathered information and constructed a comprehensive test database in conjunction with a large amount of nonlinear buckling analysis results using the ANSYS program. The proposed criteria are also compared with results obtained from existing offshore codes, including API RP 2A WSD[3], API Bulletin 2U[5] and 2V[6], and DnV CN30.1[7], DnV RP C201[8] and DnV RP C202[142], etc.

The ABS *Buckling Guide* also provides guidelines on the use of an alternative Buckling Analysis by FEM, when adequate documentation is presented. It is important that new analysis methods be compared to recognized test results and/or service experience before they are declared fit for use.

C5 Tolerances and Imperfections

Determining the critical load of structural components subjected to compressive loads generally requires that major imperfections along with loading eccentricities be taken into account. However, there is a general lack of information about all of the aspects of initial geometric imperfections and residual stresses which could exist in actual structure. Because of their effect on strength, it is important that imperfections be monitored and repaired, as necessary, not only during construction, but also in the completed structure to ensure that the structural components satisfy tolerance limits. The tolerances on imperfections to which the strength criteria are considered valid are listed, for example, in the ABS IACS Recommendation No. 47 "Shipbuilding and Repair Quality Standard" [9]. Imperfections exceeding such published tolerances are not acceptable unless it is shown using a recognized method that the strength capacity and the utilization factor of the imperfect structural component are within proper target safety levels.

C7 Corrosion Wastage

Offshore structures are exposed to the marine environment requiring the use of counteractive corrosion measures such as: a cathodic protection system, protective coatings or both to prevent corrosion damage. Despite these measures, there are numerous cases where offshore structural components have suffered from unexpected corrosion damage. Testing of a corroded member indicates that even nominal values of corrosion can result in lost capacity up to 35% to 50% (Ricles et al[10]). Therefore, special care should be taken in the buckling and ultimate strength assessment of corroded components. It is recommended that actual as-gauged minimum thickness be used in the buckling and ultimate strength assessment in order to keep the corroded components within the acceptable safety level.

C9 Loadings

Offshore structures should be designed for the appropriate loading conditions, which produce the most severe, probable effects on the structure. For more detail information on loadings and loading conditions, refer to relevant ABS offshore Rules/Guides and API Recommended Practices.

C11 Maximum Allowable Strength Utilization Factors

Major industry codes and the ABS criteria are used as references to establish the allowable utilization factors. In these codes and the ABS *Buckling Guide*, the design basis is working stress design, which implies that the acting stresses cannot exceed specified allowable values. The permissible stresses depend on the allowable utilization factor, η, or factor of safety, and structural critical strength. The relation between factor of safety and allowable utilization factor is as follows:

$$\eta = \frac{1}{\text{Factor of Safety}}$$

The establishment of the allowable utilization factors is not a trivial matter. Allowable utilization factors are a function of the loading conditions, the type of the structural components and the possible consequences of failure. They must take into account such matters as the following: the accuracy of the determined loads, inaccuracies in construction/quality of workmanship, variations in the properties of the material, deterioration due to corrosion or other environmental effects, accuracy of the method of analysis, consequences of failure (minor damage or major catastrophe) and so on.

The allowable utilization factors vary among different design codes. One design code can permit more or less risk than another. Besides, the design codes use different formulations for the prediction of the buckling and ultimate strength of structural components. Depending on the formulation of the strength used the utilization factor might be higher or lower, but typically not by much.

The allowable utilization factors may be divided into two parts in the current offshore codes. The first part corresponds to the basic utilization factors, which are very consistent among the codes and depend merely on the load conditions (See Section C1, Tables 1 to 4). The second part is related to the adjustment factors. These factors are different among the current offshore codes and will be discussed in subsequent sections. The allowable utilization factors are the product of basic utilization factors and adjustment factors. In the ABS *Buckling Guide*, the maximum allowable strength utilization factors have the following values.

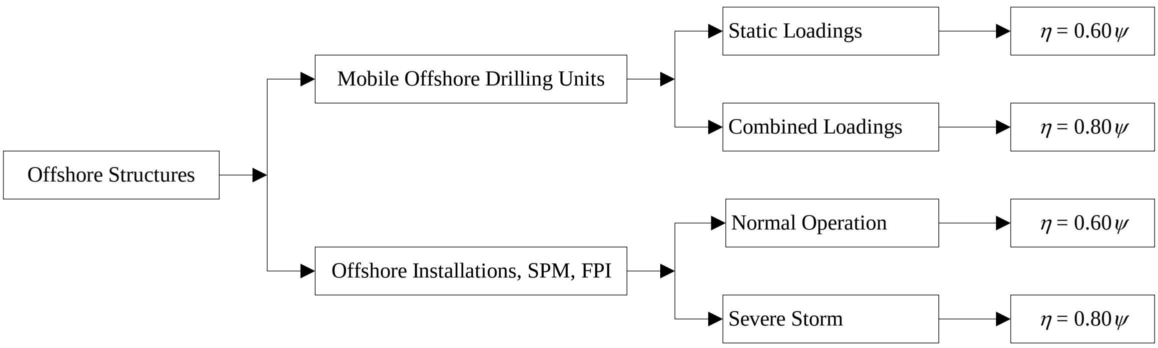

where

ψ = adjustment factor

TABLE 1
Basic Utilization Factors in ABS MODU Rules[1]

Load Conditions	*Environmental Events*	*Basic Utilization Factors*
Static Loadings	Operational gravity loads and the weight of the unit	0.60
Combined Loadings	Static loads combined with relevant environmental loads	0.80

TABLE 2
Basic Utilization Factors in ABS FPI Rules[11]

Load Conditions	*Environmental Events*	*Basic Utilization Factors*
Loadout	Calm	0.60
Ocean Transit	10-year-return storm for the selected route condition (Owner specified)	0.80
Field Transit	1-year-return storm for the selected route condition (Owner specified)	0.80
Deck Installation	Calm	0.60
In-place Design Operating	1-year-return storm (minimum)	0.60
In-place Design Environmental	100-year-return storm at specific site	0.80
In-place Damaged	1-year-return storm	0.80

TABLE 3
Basic Utilization Factors in API 2A WSD[3], Bulletin 2U[4] and 2V[5]

Load Conditions	*Environmental Events*	*Basic Utilization Factors*
Operations	Operating environmental conditions combined with dead loads and maximum live loads appropriate to normal operations of the platform.	0.60
Design Environments	Design environmental conditions with dead loads and maximum live loads appropriate for combining with extreme conditions.	0.80
Earthquake	Earthquake induced loading combined with gravity, hydrostatic pressure and buoyancy	1.0

TABLE 4
Basic Utilization Factors in DnV MOU Rules[13]

Load Conditions	*Basic Utilization Factors*
Functional loads	0.60
Maximum environmental loads and associated functional loads	0.80
Accidental loads and associated functional loads	0.80
Environmental loads corresponding to a return period of 1 year and associated functional loads after credible failure, or accidental events	1.00
Environmental loads corresponding to a return period of 1 year and associated functional loads in a heeled condition corresponding to accidental flooding.	1.00

SECTION C2 Individual Structural Members

C1 General

Many assemblies used in offshore structures are made up of a variety of sectional shapes joined together by bolts, rivets or welds. For example in a jack-up (self-elevating) unit, the bracing members of a latticed leg are typically hollow tubular members while the leg chords have a variety of shapes such as tubulars, split tubulars around solid rack plates, and even hollow prismatic chord members .

A WSD methodology is widely used in the design check process as embodied in the ABS existing Rules/Guides. The WSD approach is also widely used in the design of tubulars in jacket structures via API RP 2A-WSD[3].

C1.1 Geometries and Properties of Structural Members

The ABS *Buckling Guide* covers structural members that have at least a single axis symmetry.

It is noted that the formulations for the calculations of geometrical properties listed in Section 2, Table 1 of the ABS *Buckling Guide* are derived based on the assumption that the wall thickness is relatively small. For sections with relatively thick wall or sections not listed in this table, the key geometrical properties are to be calculated based on acceptable formulations.

C1.3 Load Application

<No Commentary>

C1.5 Failure Modes

The failure modes specifically addressed in the existing ABS *MODU Rules* are:

- Axial tension
- Axial compression including overall buckling
- Bending
- Shear
- Combined axial tension and bending moment
- Combined axial compression and bending moment
- Combined axial tension, bending moment and hydrostatic pressure
- Combined axial compression, bending moment and hydrostatic pressure

Other possible failure modes might include local buckling under axial compression or bending and any loading condition involving external or hydrostatic pressure. However, for a jack-up unit, these failure modes are not necessarily of critical concern for two reasons. Firstly, the cross-sectional slenderness of tubular sections used in jack-up construction is usually so low as to preclude any local buckling considerations. Secondly, for the water depths in which present-day jack-ups operate and again because of the low tubular slenderness involved, any pressure effects in respect to affecting tubular strength under axial, bending and shear loading conditions are minimal.

In relation to the appropriateness of the provisions specifically addressed in the present ABS *MODU Rules*, most of these are soundly based: although some aspects do need consideration as discussed below. However, in relation to bending, the major omission is the lack of provisions that allow the development of any plastic hinge capacity for tubular members. As will be seen later, this represents an extremely conservative approach when designing particularly low slenderness tubular for bending.

In identifying the requirements for revised design criteria for tubular members of ABS *MODU Rules*[1], the aim is to overcome the more relevant of the weaknesses listed above. Local buckling under axial compression and bending is of importance in this respect. Also is the need to deal with hydrostatic pressure.

For the structural members with rolled and fabricated plate section, the failure modes of torsional buckling and lateral-torsional buckling also need to be taken into account (Timenshenko and Gere[15]).

C1.7 Cross Section Classification

Cross-sections should be classified based on whether local buckling limits the maximum attainable strength. The assessment of each element of a cross-section subjected to compression due to a bending moment or an axial force should be based on its outer diameter-to-thickness ratio for tubular members or width-to-thickness ratio for rolled or fabricated-plate sections. The dimensions of these compression elements should be taken from Section 2, Table 1 of the ABS *Buckling Guide*. Each element of a cross-section is generally of constant thickness. A distinction should be made between the following types of element:

C1.7.1 Tubular Members

The compact limit for tubular section is defined by:

$$\frac{D}{t} \le \frac{E}{9\sigma_0}$$

where

D	=	outer diameter
t	=	wall thickness
E	=	Young's modulus
σ_0	=	yield strength

C1.7.2 Rolled or Fabricated-Plate Sections

C1.7.2(a) Outstand elements attached to an adjacent element at one edge only, with the other edge free. The compact limit is defined by:

$$\frac{b_2}{t_f} \le 0.4\sqrt{\frac{E}{\sigma_0}}$$

where

b_2	=	width of outstand.
t_f	=	thickness of outstand.

C1.7.2(b) Internal elements attached to other elements on both longitudinal edges and including:

- Webs consisting of internal elements perpendicular to the axis of bending
- Flanges consisting of internal elements parallel to the axis of bending

The compact limit is defined by:

$$\frac{a}{t_f}, \frac{d}{t_w} \le 1.5\sqrt{\frac{E}{\sigma_0}}$$

where

a	=	width of an internal flange
t_f	=	thickness of an internal flange
d	=	height of webs
t_w	=	thickness of webs

C1.9 Adjustment Factors

The adjustment factors for the allowable basic utilization factors in the existing offshore codes are provided in Section C2, Table 1 and Section C2, Figure 1. The adjustment factors for beam-column buckling and tension/bending from various codes are remarkably identical and the difference is less than 3.5%.

TABLE 1
Adjustment Factors

	Beam-Column Buckling	*Tension/ Bending*	*Local Buckling*
ABS Buckling Guide	$\psi = 0.87$ if $\sigma_{EA} \le P_r\sigma_0$ $= 1 - 0.13\sqrt{P_r\sigma_0 / \sigma_{EA}}$ if $\sigma_{EA} > P_r\sigma_0$	$\psi = 1.0$	$\psi = 0.833$ if $\sigma_{Ci} \le 0.55\sigma_0$ $= 0.629 + 0.371\sigma_{Ci}/\sigma_o$ if $\sigma_{Ci} > 0.55\sigma_0$
ABS MODU Rules[1]/ SPM Rules[14]	$\psi = 0.87$ if $\sigma_{EA} \le 0.5\sigma_0$ $=1/(1 + 0.15\sqrt{0.5\sigma_0 / \sigma_{EA}})$ if $\sigma_{EA} > 0.5\sigma_0$	$\psi = 1.0$	N/A
API RP WSD 2A (AISC)[3]	$\psi = 0.87$ if $\sigma_{EA} \le 0.5\sigma_0$ $= \dfrac{1}{1+0.1588\left(\dfrac{\sigma_0}{\sigma_{EA}}\right)^{0.5} - 0.0529\left(\dfrac{\sigma_0}{\sigma_{EA}}\right)^{1.5}}$ if $\sigma_{EA} > 0.5\sigma_0$	$\psi = 1.0$	$\psi = 0.8333\sim1.0$ for axial compression $\psi = 0.8333$ for external pressure
DnV MOU Rules[13]	$\psi = 1.0$ if $\sigma_{EA} \ge 25\sigma_0$ $= 1.025 - 0.125\sqrt{\sigma_0 / \sigma_{EA}}$ if $\sigma_o < \sigma_{EA} \le 25\sigma_0$ $= 0.9$ if $\sigma_{EA} \le \sigma_0$	$\psi = 1.0$	N/A

FIGURE 1
Comparison of Adjustment Factor for Beam-Column Buckling

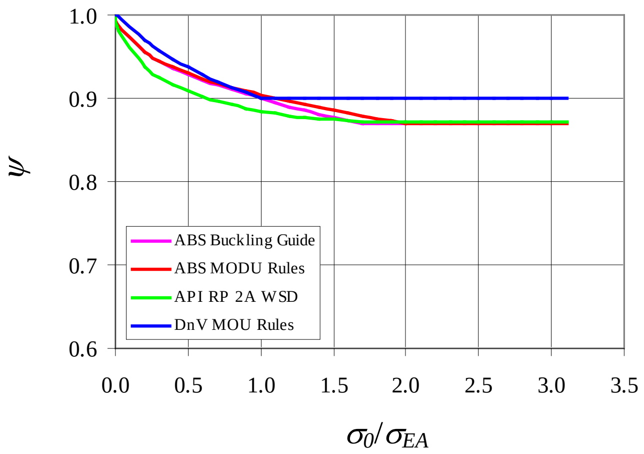

C3 Members Subjected to Single Actions

C3.1 Axial Tension

<No Commentary>

C3.3 Axial Compression

The proposed formulation includes flexural buckling and torsional buckling. The state limit is defined by the following equation:

$$\sigma_A / \eta_1 \sigma_{CA} \le 1$$

where σ_A is the axial compressive stress and σ_{CA} is the critical buckling stress:

$$\sigma_{CA} = \begin{cases} \sigma_{EA} & \text{if} \quad \sigma_{EA} \le P_r \sigma_F \\ \sigma_F \left[1 - P_r (1 - P_r) \dfrac{\sigma_F}{\sigma_{EA}} \right] & \text{if} \quad \sigma_{EA} > P_r \sigma_F \end{cases}$$

where

P_r = proportional linear elastic limit of the structures

σ_F = specified minimum yield strength for the compact section or local buckling stress for the non-compact section, as specified in 2/3.3 of the ABS *Buckling Guide*

σ_{EA} = elastic buckling stress, which is the least of the solutions of the following equation for an arbitrary thin-walled cross section (Timenshenko and Gere, 1961[15]):

$$\frac{I_o}{A}(\sigma_{EA} - \sigma_{Ey})(\sigma_{EA} - \sigma_{Ez})(\sigma_{EA} - \sigma_{ET}) - \sigma_{EA}{}^2 y_0{}^2(\sigma_{EA} - \sigma_{Ez}) - \sigma_{EA}{}^2 z_0{}^2(\sigma_{EA} - \sigma_{Ey}) = 0$$

where

σ_{Ey}, σ_{Ez} = Euler buckling stresses

σ_{ET} = torsional buckling stress given by:

$$= \frac{EK}{2.6 I_o} + \left(\frac{\pi}{kL}\right)^2 \frac{E\Gamma}{I_o}$$

y_0, z_0 = coordinates of shear center, as shown in Section C2, Figure 2

FIGURE 2
Geometry of Thin Walled Members

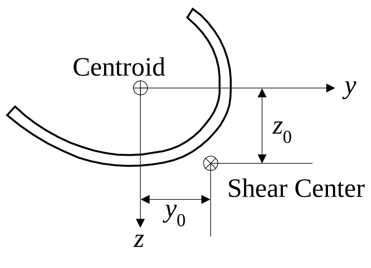

For a section with one plane of symmetry about a longitudinal axis, the elastic buckling stress can be solved from the following equation (Section 2/3.3 of the ABS *Buckling Guide*)

$$\frac{I_o}{A}(\sigma_{EA} - \sigma_{E\eta})(\sigma_{EA} - \sigma_{ET}) - \sigma_{EA}{}^2 d_{es}{}^2 = 0$$

For an arbitrary section with one plane of symmetry, assuming it to be through the *y*-axis, we obtain the equation for calculating the elastic buckling stress

$$\frac{I_o}{A}(\sigma_{EA} - \sigma_{Ey})(\sigma_{EA} - \sigma_{ET}) - \sigma_{EA}^2 y_0^2 = 0$$

The smaller of the roots and Euler buckling stress in the plane of symmetry represents the elastic buckling stress.

In the existing ABS Rules, API 2A WSD[3] and AISC[16], 0.5 is taken for P_r, but 0.6 is used in the Guide to be in agreement with ABS *Steel Vessel Rules*[2]. Using 0.6 instead of 0.5 does not provide a big difference in the predicted strength (See two thick lines in Section C2, Figure 3).

FIGURE 3
The Effect of P_r on the Critical Buckling Stress

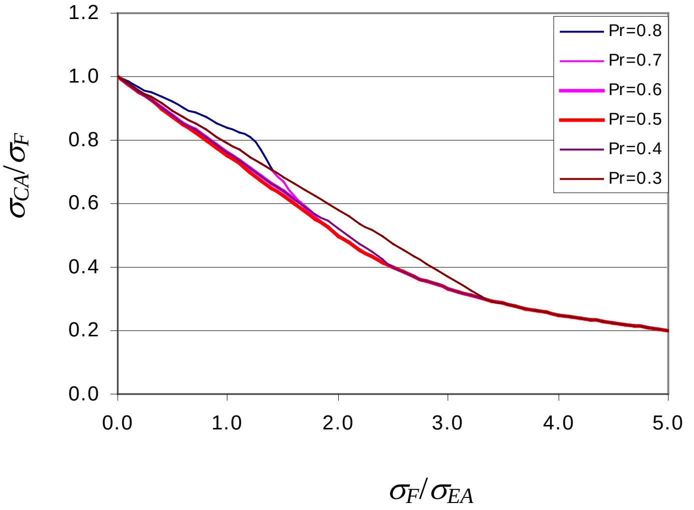

For tubular members, Section C2, Figure 4 presents a comparison of the ABS *MODU Rules*[1], API RP 2A-WSD[3] and the ABS *Buckling Guide* with test results. The column test database consists of 12 tests on fabricated tubular members, Chen and Ross[17] and Smith et al[18]; 2 on seamless pipe, Smith et al[19]; and 70 on ERW pipe, Steinmann and Vojta[20] and Yeomans[21]. This is considerably larger than that previously used to validate offshore tubular strength formulations. The increase is primarily due to the inclusion of relevant results from a large CIDECT test program (Yeomans[21]). The figure confirms that the ABS *MODU Rules*[1] and API RP 2A-WSD[3] formulations are identical. However, the statistics of the comparisons between the formulations and the test data indicate that differences do arise. For example, the means for the two formulations are 1.0736 and 1.0743 respectively. An examination of the calculation details reveals that differences arise because of an API RP 2A-WSD local strength requirement. This applies for $D/t \geq 60$; whereas the ABS *MODU Rules* local buckling limit is in excess of 60 (or using ABS *MODU Rules*[1] definitions, $D/t > 59$) for yield stresses up to 386 N/mm^2. The mean and COV of modeling uncertainty of various codes are given in Section C2, Table 2.

Section C2, Table 3 provides comparison between the ABS *Buckling Guide* and AISC Code[16] for two rolled-plate sections.

The allowable buckling stress from the ABS *Buckling Guide* is remarkably close to that from the AISC Code when local buckling is ignored, as is the case for compact sections. Differences arise for non-compact sections, in which the allowable buckling stress from the ABS *Buckling Guide* is considerably smaller than that from the AISC Code. This is reasonable because the ABS *Buckling Guide* includes the local buckling effect for non-compact sections.

TABLE 2
Mean/COV of Modeling Uncertainty for Column Buckling

	ABS MODU Rules	*API RP 2A WSD*	*ABS Buckling Guide*
Mean	1.0736	1.0743	1.0547
COV	7.56%	7.51%	5.28%

FIGURE 4
Column Buckling for Tubular Members

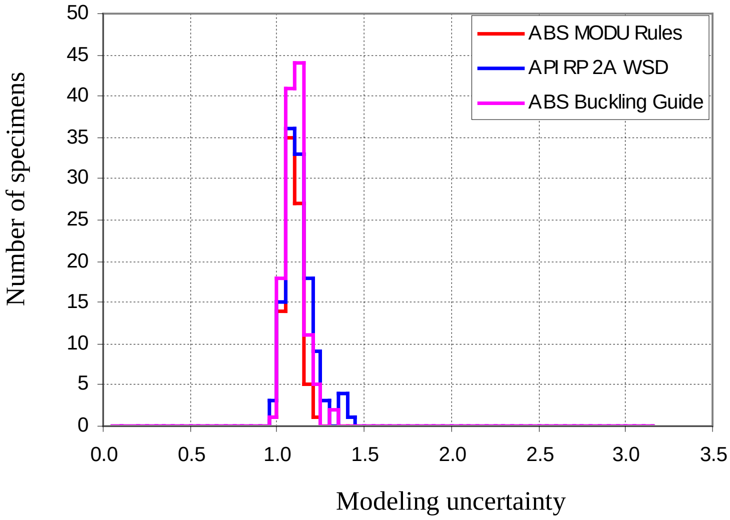

TABLE 3
Column Buckling for Rolled-plate Sections

		W-shape	*Square Hollow Section*
Geometry and Material			
Length	ℓ	144.00	144.00
Section shape type		2	4
Specified minimum yield point	σ_o	36.00	36.00
Modulus of elasticity	E	2.90E+04	2.90E+04
Poisson's ratio	ν	0.30	0.30
Flange width	b	3.75	7.96
Flange thickness	t_f	0.25	0.43
Web depth	d	3.75	9.75
Web thickness	t_w	0.25	0.29
Section classification		Non-compact	Compact
The ABS Buckling Guide			
Allowable buckling stress considering local buckling		13.73	—
Allowable buckling stress ignoring local buckling		16.14	19.90
AISC Code			
Allowable buckling stress ignoring local buckling		15.99	19.46

C3.5 Bending Moment

The ABS *Buckling Guide* includes two failure modes that take proper account of plastic moment capacity and lateral torsional buckling capacity for the members.

The proposed buckling state limit is defined by the following equation:

$$\sigma_b / \eta_2 \sigma_{CB} \leq 1$$

where

σ_b = bending stress due to bending moment

σ_{CB} = characteristic bending strength given as follows:

i) For tubular members, the critical bending strength is obtained from the equation in Section 2/9.3 of the ABS *Buckling Guide*, in which the fully plastic capacity of the section could be developed.

ii) For members with rolled or fabricated sections, the critical bending strength is determined by the critical lateral-torsional buckling stress.

The critical lateral-torsional buckling stress is obtained by:

$$\sigma_{C(LT)} = \begin{cases} \sigma_{E(LT)} & \text{if} \quad \sigma_{E(LT)} \leq P_r \sigma_F \\ \sigma_F \left[1 - P_r (1 - P_r) \dfrac{\sigma_F}{\sigma_{E(LT)}} \right] & \text{if} \quad \sigma_{E(LT)} > P_r \sigma_F \end{cases}$$

where

$\sigma_{E(LT)}$ = elastic lateral-torsional buckling stress, which is given below (Timenshenko and Gere[15])

$$= \sqrt{C} \, \frac{\pi^2 E I_\xi}{SM_c (kL)^2}$$

Comparisons are presented for tubular members in Section C2, Figure 5 between the existing ABS *MODU Rules*, API RP 2A-WSD and the ABS *Buckling Guide* for bending and the test data. The bending database consists of 57 results published by Steinmann and Vojta[20], Kiziltug et al[22], Sherman[23,24], Korol and Hudoba[25] and Korol[26]. In the ABS *MODU Rules*[1], bending strength is limited to the range where $D/t \leq E/9\sigma_0$ or $\sigma_0 D/Et \approx \leq 0.11$ and local buckling effect is ignored. Over this valid range, the ABS *MODU Rules*[1] underestimate the bending strength. Section C2, Table 4 presents the Mean/COV of modeling uncertainty of bending strength for tubular members.

TABLE 4
Mean/COV of Modeling Uncertainty of Bending Strength for Tubular Members

	ABS MODU Rules	*API RP 2A WSD*	*ABS Buckling Guide*
Mean	1.3678	1.1741	1.1463
COV	10.83%	9.40%	9.79%

FIGURE 5
Bending Strength for Tubular Members

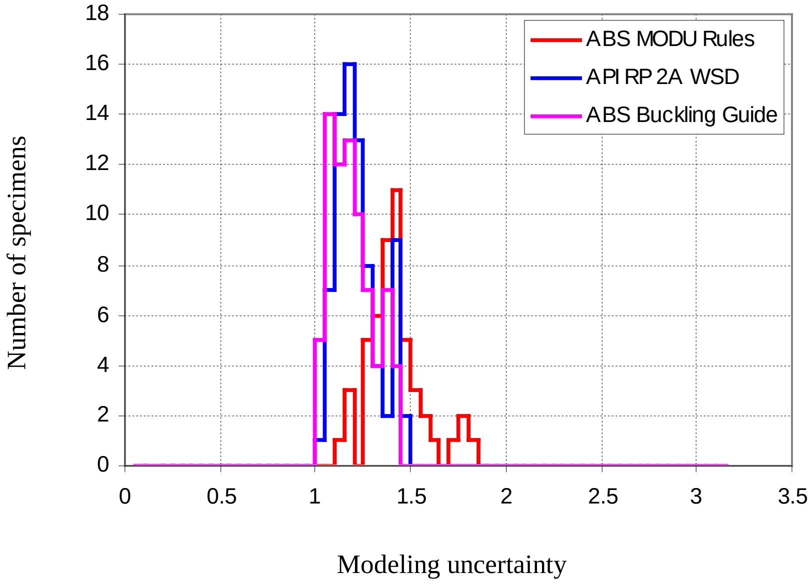

The critical bending strength for the beams with rolled or fabricated compact sections obtained from SSRC[28], ECCS[29], AISC LRFD[30], DnV CN30.1[7] and the ABS *Buckling Guide* is shown in Section C2, Figure 6. The criterion proposed in the ABS *Buckling Guide* is conservative for the short beam. In this case, the critical bending strength is governed by the development of full plasticity. The criterion proposed in the ABS *Buckling Guid*e is acceptable for the beams with rolled or fabricated compact sections in the practical range of slenderness ratio.

FIGURE 6
Comparison of Lateral-Torsional Buckling Strength

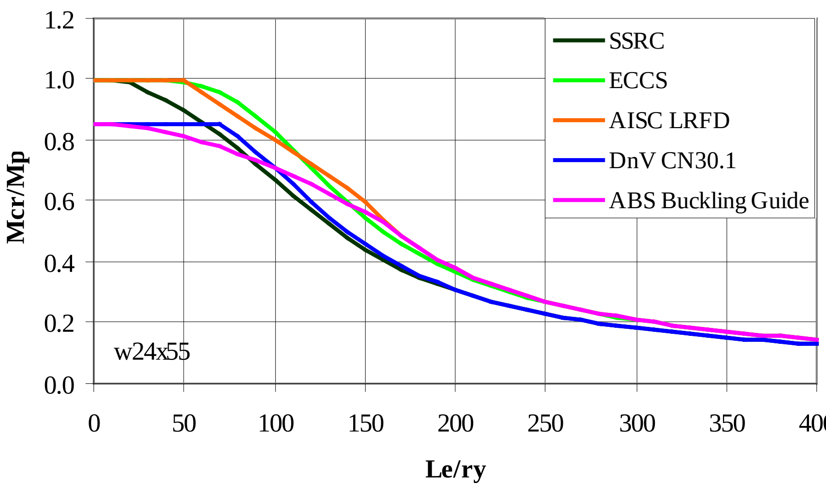

C5 Members Subjected to Combined Loads

C5.1 Axial Tension and Bending Moment

<No Commentary>

C5.3 Axial Compression and Bending Moment

The criteria for combined column buckling and bending moment in the ABS *Buckling Guide* is based on the individual formulation for column buckling and bending combined via the interaction equation involving Euler amplification of deflections by axial loading. This applies when the ratio of axial stress σ_a to the column strength σ_{CA} is greater than 0.15, i.e., the buckling failure is dominant. Otherwise, a relationship that does not involve the amplification is adopted, in which a yield failure governs. The equations in the ABS *Buckling Guide* are:

For tubular members:

$$\frac{\sigma_a}{\eta_1 \sigma_{CA}} + \frac{1}{\eta_2}\left\{\left[\frac{1}{\sigma_{CBy}} \frac{C_{my}\sigma_{by}}{1-\sigma_a/(\eta_1\sigma_{Ey})}\right]^2 + \left[\frac{1}{\sigma_{CBz}} \frac{C_{mz}\sigma_{bz}}{1-\sigma_a/(\eta_1\sigma_{Ez})}\right]^2\right\}^{0.5} \le 1 \qquad \text{when } \sigma_a/\sigma_{CA} > 0.15$$

$$\frac{\sigma_a}{\eta_1 \sigma_{CA}} + \frac{1}{\eta_2}\left[\left(\frac{\sigma_{by}}{\sigma_{CBy}}\right)^2 + \left(\frac{\sigma_{bz}}{\sigma_{CBz}}\right)^2\right]^{0.5} \le 1 \qquad \text{when } \sigma_a/\sigma_{CA} \le 0.15$$

For rolled or fabricated plate sections:

$$\frac{\sigma_a}{\eta_1 \sigma_{CA}} + \frac{1}{\eta_2 \sigma_{CBy}} \frac{C_{my}\sigma_{by}}{1-\sigma_a/(\eta_1\sigma_{Ey})} + \frac{1}{\eta_2 \sigma_{CBz}} \frac{C_{mz}\sigma_{bz}}{1-\sigma_a/(\eta_1\sigma_{Ez})} \le 1 \qquad \text{when } \sigma_a/\sigma_{CA} > 0.15$$

$$\frac{\sigma_a}{\eta_1 \sigma_{CA}} + \frac{\sigma_{by}}{\eta_2 \sigma_{CBy}} + \frac{\sigma_{bz}}{\eta_2 \sigma_{CBz}} \le 1 \qquad \text{when } \sigma_a/\sigma_{CA} \le 0.15$$

The comparisons between the ABS *Buckling Guide* for combined column buckling and bending and test data for tubular members are presented in Section C2, Figure 7. For overall buckling, 49 test results exist extracted from Prion and Birkemoe[31], Kiziltug et al[22], Ellis[32], Wagner et al[33], Kato and Akiyama[27] and Smith et al[18]: 34 results were rejected on the grounds of being too thin and inadequately documented. For local buckling, 19 data have been extracted from Kiziltug et al[22] and Prion and Birkemoe[31]: no data were rejected.

The mean and COV of modeling uncertainty of various codes are presented in Section C2, Table 5.

TABLE 5
Mean/COV of Modeling Uncertainty for Beam-Column Buckling

	ABS MODU Rules	*API RP 2A WSD*	*ABS Buckling Guide*
Mean	1.0811	1.0439	1.0180
COV	10.03%	9.52%	10.84%

FIGURE 7
Beam-Column Buckling for Tubular Members

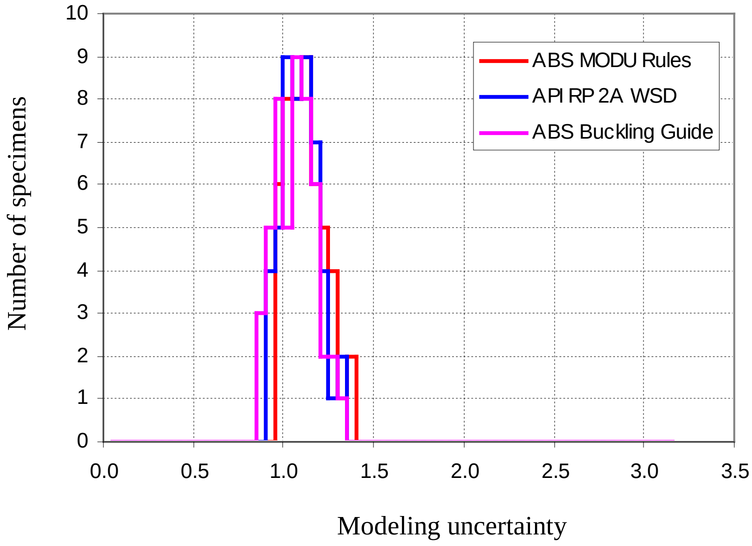

C7 Tubular Members Subjected to Combined Loads with Hydrostatic Pressure

Unstiffened tubular members under external hydrostatic pressure are subjected to elastic or inelastic local buckling of the shell wall between restraints. Once initiated, the collapse will tend to flatten the member from one end to the other. Similarly, ring-stiffened members are subject to local buckling of the shell wall between rings. The shell buckles between the rings, while the rings remain essentially circular. Consequently, it is desirable to provide rings with sufficient reserve strength to prevent general instability.

Strength design interaction equations for the cases in which a tubular member is subjected to axial tension or compression, and/or bending combined with external hydrostatic pressure have been proposed in API RP 2A WSD. The hoop compression is not explicitly included in the analysis, but its effect on member design is considered within the design interaction equations. The hoop collapse design check must be satisfied first. The method described is based on the explicit application of the capped-end axial compression, which allows for a more precise redistribution of the capped-end load based on the relative stiffness of the braces at a node. A collection of the test data and additional comparisons of the design equations to test data can be found in Miller and Salikis[34].

C7.1 Axial Tension, Bending Moment and Hydrostatic Pressure

The member net axial stress is the calculated value, σ_{tc}, since the effect of the capped-end axial compression is explicitly included in the design analysis. Therefore, the calculated axial tensile stress, σ_{tc}, can be used directly in the cross-sectional strength check.

Test data for tubular members subjected to combined axial tension, bending, and hydrostatic pressure can be found in Miller et al[35].

C7.3 Axial Compression, Bending Moment and Hydrostatic Pressure

In this method, the calculated axial stress, σ_{ac}, is the net axial compressive stress of the member since the capped-end axial compression is included in the design analysis. For the stability check, the axial compression to be used with the equation is the component that is in addition to the pure hydrostatic pressure condition (see Section C2, Figure 8). Therefore, the capped-end axial compression is subtracted from the net axial compressive stress. For the strength check, the net axial compressive stress is used. In addition, the cross-section elastic buckling criterion needs to be satisfied. The comparison between the ABS *Buckling Guide* and test data for tubular members subjected to combined axial compression, bending, and hydrostatic pressure can be found in Loh[36,37].

FIGURE 8
Capped-end Action Arising from Hydrostatic Pressure

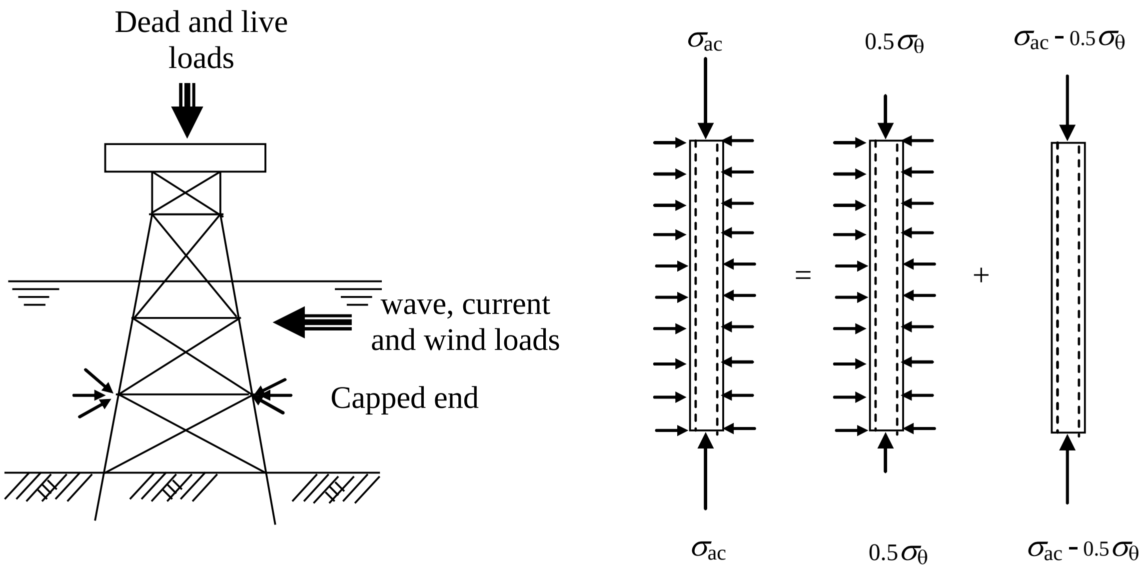

Tubular members subjected to combined compression, bending moment and hydrostatic pressure are to satisfy the following proposed equations at all cross-sections along their length.

When $\sigma_{ac}/\sigma_{CA\theta} > 0.15 > 0.15$ and $\sigma_{ac} > 0.5\sigma_\theta$:

$$\frac{\sigma_{ac} - 0.5\sigma_\theta}{\eta_1 \sigma_{CA\theta}} + \frac{1}{\eta_2 \sigma_{CB\theta}} \frac{C_m \sigma_b}{1 - (\sigma_{ac} - 0.5\sigma_\theta)/(\eta_1 \sigma_E)} \le 1$$

When $\sigma_{ac}/\sigma_{CA\theta} \le 0.15$:

$$\frac{\sigma_{ac}}{\eta_1 \sigma_{CA\theta}} + \frac{\sqrt{\sigma_{by}^2 + \sigma_{bz}^2}}{\eta_2 \sigma_{CB\theta}} \le 1$$

When $\sigma_x > 0.5\eta_1\sigma_{C\theta}$ and $\sigma_{Cx} > 0.5\sigma_{C\theta}$, the following local buckling state limit should also be satisfied:

$$\frac{\sigma_x - 0.5\eta_1 \sigma_{C\theta}}{\eta_1(\sigma_{Cx} - 0.5\sigma_{C\theta})} + \left[\frac{\sigma_\theta}{\eta_1 \sigma_{C\theta}}\right]^2 \le 1$$

The comparison of the characteristic buckling strength from the above interaction equation to test data is shown in Section C2, Figure 9. This is based on test data for $D/t \le 120$ from Das (2000)[38] and includes both stiffened and unstiffened members under hydrostatic pressure or combined loadings. The mean and COV of the modeling uncertainty are 1.0299 and 13.28% respectively.

FIGURE 9
Local Buckling under Hydrostatic Pressure and Combined Loadings

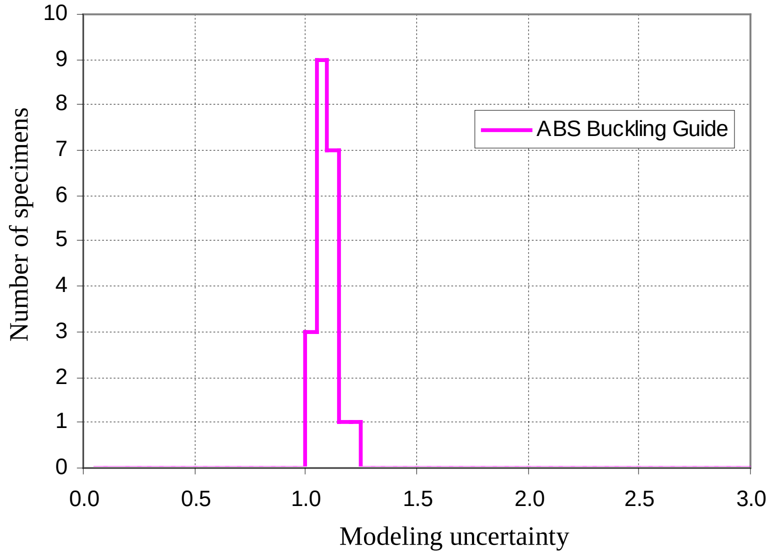

C9 Local Buckling

For a member with a non-compact section, the local buckling may occur before the member as a whole becomes unstable or before the yield point of the material is reached. Such behavior is characterized by local distortions of the cross section of the member. When a detailed analysis is not available, the equations given as below may be used to evaluate the local buckling stress for the member with a non-compact section.

C9.1 Tubular Members in Axial Compression

Because of the absence of any ABS *MODU Rule* local buckling requirement, and the absence of an appropriate form of non-dimensionalisation for API RP 2A-WSD[3] local buckling formulation, the formulation recommended for tubular members is,

$$\sigma_{Cx} = \begin{cases} \sigma_{Ex} & \text{if} \quad \sigma_{Ex} \le P_r \sigma_0 \\ \sigma_0 \left[1 - P_r (1 - P_r) \dfrac{\sigma_0}{\sigma_{Ex}} \right] & \text{if} \quad \sigma_{Ex} > P_r \sigma_0 \end{cases}$$

where

P_r = proportional linear elastic limit of the member, which may be taken as 0.6 for steel

σ_0 = specified minimum yield point

σ_{Ex} = elastic buckling stress, given by $0.6Et/D$ for tubular members, to account for the inevitable effects of initial imperfections on perfect cylinder compressive buckling strength.

Comparisons for local buckling of tubular members under axial compression. are presented in Section C2, Figure 10 The local buckling database consists of 38 results performed by several investigators Chen and Ross[17], Marzullo and Ostapenko[39], Ostapenko and Grimm[40], Prion and Birkemoe[31], Eder et al[41] and Kiziltug et al[22]. Twenty five test results were rejected as being too thin and/or not adequately documented. The mean and COV were found to be 1.1449 and 8.89%, respectively.

FIGURE 10
Local Buckling for Tubular Members under Axial Compression

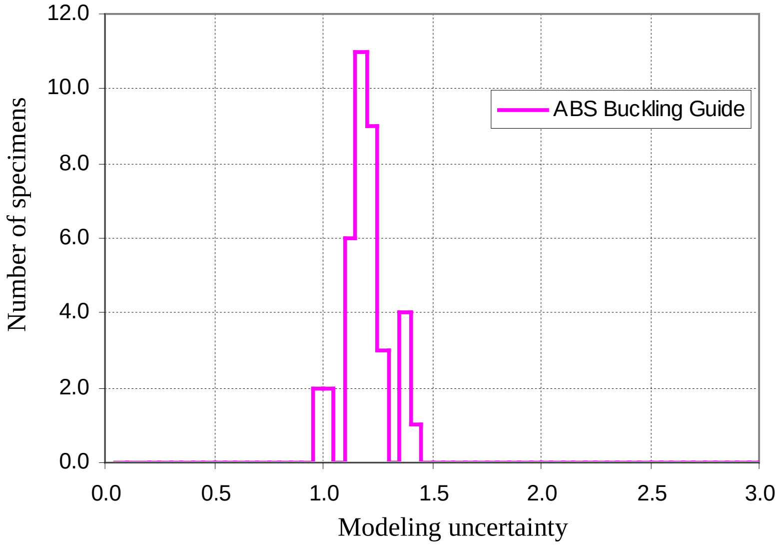

C9.3 Tubular Members Subjected to Bending Moment

<No Commentary>

C9.5 Tubular Members Subjected to Hydrostatic Pressure

<No Commentary>

C9.7 Plate Elements Subjected to Compression and Bending Moment

The critical local buckling of a member with W-shape, channel, T-section, rectangular hollow section or built-up sections may be taken as the smallest of local buckling stress of the plate elements. The local buckling stress of a plate element is obtained from the following equation with respect to uniaxial compression and in-plane bending moment:

$$\sigma_{Cx} = \begin{cases} \sigma_{Ex} & \text{if} \quad \sigma_{Ex} \le P_r \sigma_0 \\ \sigma_o \left[1 - P_r (1 - P_r) \dfrac{\sigma_0}{\sigma_{Ex}} \right] & \text{if} \quad \sigma_{Ex} > P_r \sigma_0 \end{cases}$$

where

σ_0 = specified minimum yield point

σ_{Ex} = elastic buckling stress, as given by:

$$= k_s \frac{\pi^2 E}{12(1-\nu^2)} \left(\frac{t}{s} \right)^2$$

The buckling coefficient k_s for a plate element are specified based on the ABS *Steel Vessel Rules*[2], Timoshenko and Gere[15] and Galambos[28].

SECTION C2 Appendix 1 – Examples of Buckling Analysis of Individual Structural Members

An MS EXCEL application, entitled, *ABS- Individual Structural Members*, has been developed to facilitate the use of the ABS *Buckling Guide*. There are three worksheets, namely “Input Data”, “Output Data” and “Intermediate Results”. In the worksheet “Input data”, the input data including the Member ID, Load case, Type of sectional shape, Geometries, Material parameters, Effective length factors, Moment reduction factors, Loadings and Basic utilization factor corresponding to the specified load case are provided by the user. Once the input data are entered, a macro represented by a large button “Structural Members” at the left-hand side corner is run. Buckling check results and intermediate results can be seen in the worksheets “Output” and “Intermediate Results”. All symbols used in the spreadsheet are consistent with those in the ABS *Buckling Guide*. Appendix C2A1, Table 1 shows several examples using tested tubular members.

TABLE 1
Examples Containing Detail Information for Tubular Members

Member ID			TEST-1	TEST-A3	TEST-2
Load Case			1	1	1
	Total length	L	5.49E+03	1.81E+03	1.57E+03
	Length between Transverse Frame or Diaphrams	ℓ	5486.40	1811.02	1567.00
	Section shape type		1	1	1
	Specified minimum yield stress	σ_0	271.03	337.93	216.20
	Modulus of elasticity	E	2.14E+05	2.00E+05	2.05E+05
	Poisson's ratio	ν	0.30	0.3	0.3
	Effective length factor along y-axis	k_y	1.00	1.00	1.00
	Effective length factor along z-axis	k_z	1.00	1.00	1.00
	Moment reduction factor around y-axis	C_{my}	1.00	1.00	1.00
	Moment reduction factor around z-axis	C_{mz}	1.00	1.00	1.00
Circular Tube (Shape type=1)					
	Outer diameter	D	381.00	458.47	114.30
	Thickness	t	8.03	16.54	3.51
Loading					
	Axial force	F_x	-2.47E+06	0.00E+00	-1.41E+05
	Bending moment about major axis	M_y	0.00E+00	1.20E+09	4.52E+06
	Bending moment about minor axis	M_z	0.00E+00	0.00E+00	0.00E+00
	External pressure	p	0.00	0.00	0.00
	Shear Force along major axis	F_y	0.00	0.00	0.00
	Shear Force along minor axis	F_z	0.00	0.00	0.00
	Torque	T	0	0.00	0.00
Maximum Allowable Strength Utilization Factor					
	Basic	η	1.00	1.00	1.00
Is the Section Compact?			Yes	Yes	Yes
Unity Check					
	Overall buckling		**1.03**	**1.11**	**1.08**
	Local buckling		**N/A**	**N/A**	**N/A**

Intermediate Results					
Geometry	Sectional Area	A	9404.78	22957.39	1221.68
	Moment of Inertia about y-axis	I_y	1.64E+08	5.61E+08	1.88E+06
	Sectional modulus about y-axis	SM_y	8.59E+05	2.45E+06	3.28E+04
	Moment of Inertia about z-axis	I_z	1.64E+08	5.61E+08	1.88E+06
	Sectional modulus about z-axis	SM_z	8.59E+05	2.45E+06	3.28E+04
	Radius of gyration about y-axis	r_y	131.90	156.36	39.19
	Radius of gyration about z-axis	r_z	131.90	156.36	39.19
	St. Venant torsional constant	K	3.27E+08	1.12E+09	3.75E+06
	Polar moment of inertia	I_o	3.27E+08	1.12E+09	3.75E+06
	Warping constant	G	0.00E+00	0.00E+00	0.00E+00
Stress	Normal stress due to axial force	σ_a	263.04	0.00	115.38
	Bending stress about y-axis	σ_{by}	0.00	489.60	137.60
	Bending stress about y-axis	σ_{bz}	0.00	0.00	0.00
	Shear stress along y-aixs	τ_y	0.00	0.00	0.00
	Shear stress along z-aixs	τ_z	0.00	0.00	0.00
	Torsional stress	t	0.00	0.00	0.00
Resistance					
	Euler buckling stress about y-axis	$\sigma_{(EC)y}$	1219.51	14713.53	1265.50
	Euler buckling stress about z-axis	$\sigma_{(EC)z}$	1219.51	14713.53	1265.50
	Elastic torsional buckling stress	$\sigma_{(ET)}$	8.22E+04	7.68E+04	7.88E+04
	Elastic local buckling stress	σ_{Ex}	2702.34	4327.98	3777.17
	Local axial buckling stress	σ_{Cx}	271.03	337.93	216.20
	Critical buckling stress about y-axis	σ_{CFfy}	256.58	336.07	207.34
	Critical buckling stress about z-axis	σ_{CFz}	256.58	336.07	207.34
	Critical buckling stress about minor-axis	σ_{CF}	256.58	336.07	207.34
	Critical torsional buckling stress	σ_{CT}	270.82	337.57	216.06
	Critical buckling stress	σ_{CA}	256.58	336.07	207.34
	Critical bending stress about y-axis	σ_{CBy}	341.45	442.07	287.30
	Critical bending stress about z-axis	σ_{CBbz}	341.45	442.07	287.30
Unity Check for each individual load					
	Axial stress		1.03	0.00	0.56
	Bending stress about y-axis		0.00	1.11	0.48
	Bending stress about z-axis		0.00	0.00	0.00

Units: Length – [mm], Area – [mm^2], Sectional Modulus – [mm^3], Sectional Moment of Inertia – [mm^4], St. Venant torsional constant – [mm^6], force – [N], Bending Moment – [N-mm], Stress and Pressure – [N/mm^2]

SECTION C3 Plates, Stiffened Panels and Corrugated Panels

C1 General

Plates, stiffened panels and corrugated panels are used extensively in offshore structures. The panels form basic members for the deck structures, some pontoon structures, habitation units and watertight bulkheads and shear diaphragms. There is an extensive history of the application of plates, stiffened panels and corrugated panels as major and secondary components of thin-walled structures due to their easy construction and good structural efficiency measured by the ratio of strength to weight.

The various aspects of stiffened panels have been widely investigated, and the results of the design formulas have been compared to available test results. In general, the design formulas are based on a most comprehensive set of test results and other data for panels subjected to a variety of loading conditions. The predictions for strength resulting from these recommendations should be sufficiently accurate.

The process of buckling and ultimate strength assessment of stiffened panels is shown in the flow chart of Section C3, Figure 1. It consists of three parts, which are plate panels, stiffened panels, and girders and webs. The objective of the check performed in each step is explained in the flow chart. The procedure has been incorporated into an MS Excel application developed by OTD, ABS Technology.

C1.1 Geometry of Plates, Stiffened Panels and Corrugated Panels

A rectangular plate is a flat structure characterized by having its length and breadth dimensions very much greater than its thickness. It is usually supported in-plane around all four edges and may also be flexurally restrained.

The stiffeners themselves can act as single or multiple plates, depending on their geometry. They may buckle independently or in conjunction with the plate sections between the stiffeners. The precise analysis of a stiffened panel should reflect the capacity of the panel to act as a member in overall buckling between its outer boundaries, in addition to the possibility of the plates buckling locally between stiffeners.

Knowledge of the general behavior of plate panels subjected to the common forms of in-plane loadings is essential to understanding their response. The plate aspect ratio and the geometrical slenderness ratio are the two governing geometrical parameters in the buckling and ultimate strength assessment. These two parameters of plate panels in offshore structures may be different from those in other metal structures. In order to achieve an appropriate balance between accuracy and simplicity, a statistical description for the aspect ratio and slenderness ratio for the four types of floating production installations (FPIs) is carried out[42]. The recorded values are the design values or so-called nominal values. The histograms of plate aspect ratio, ℓ/s, and the geometrical slenderness ratio, s/t, are shown in Section C3, Figures 2 and 3. The size of database for TLP, Spar and Semi-Submersible (Column Stabilized) is 8856, 7859 and 78639, respectively. The statistical data of FPSO is converted from Tankers, and the data source provided by Guedes Soares[43] is used. The statistical characteristics are given in Section C3, Table 1.

FIGURE 1
Flow Chart of Buckling and Ultimate Strength Checks for Plates, Stiffened Panels and Girders and Webs

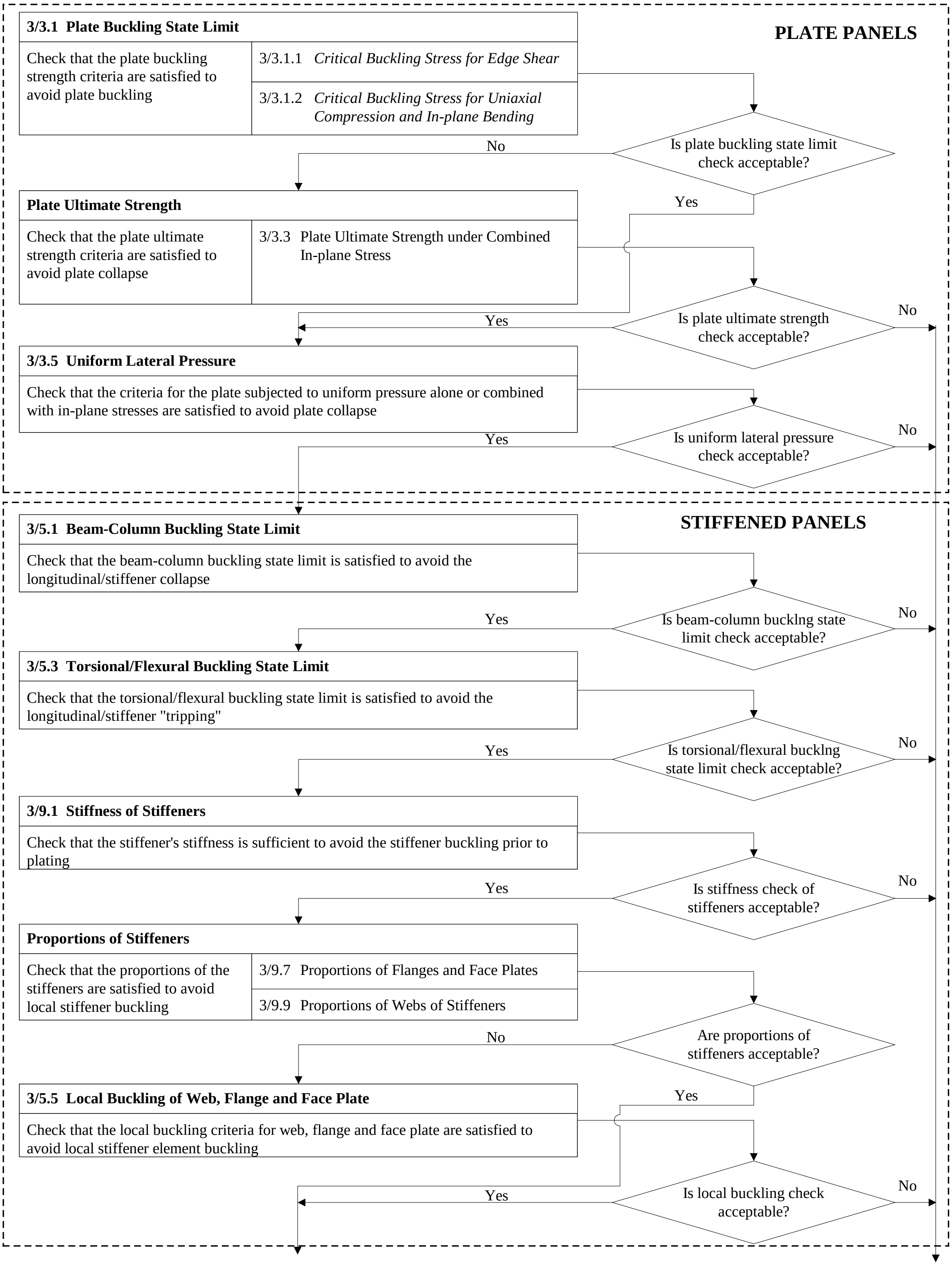

FIGURE 1 (continued) Flow Chart of Buckling and Ultimate Strength Checks for Plates, Stiffened Panels and Girders and Webs

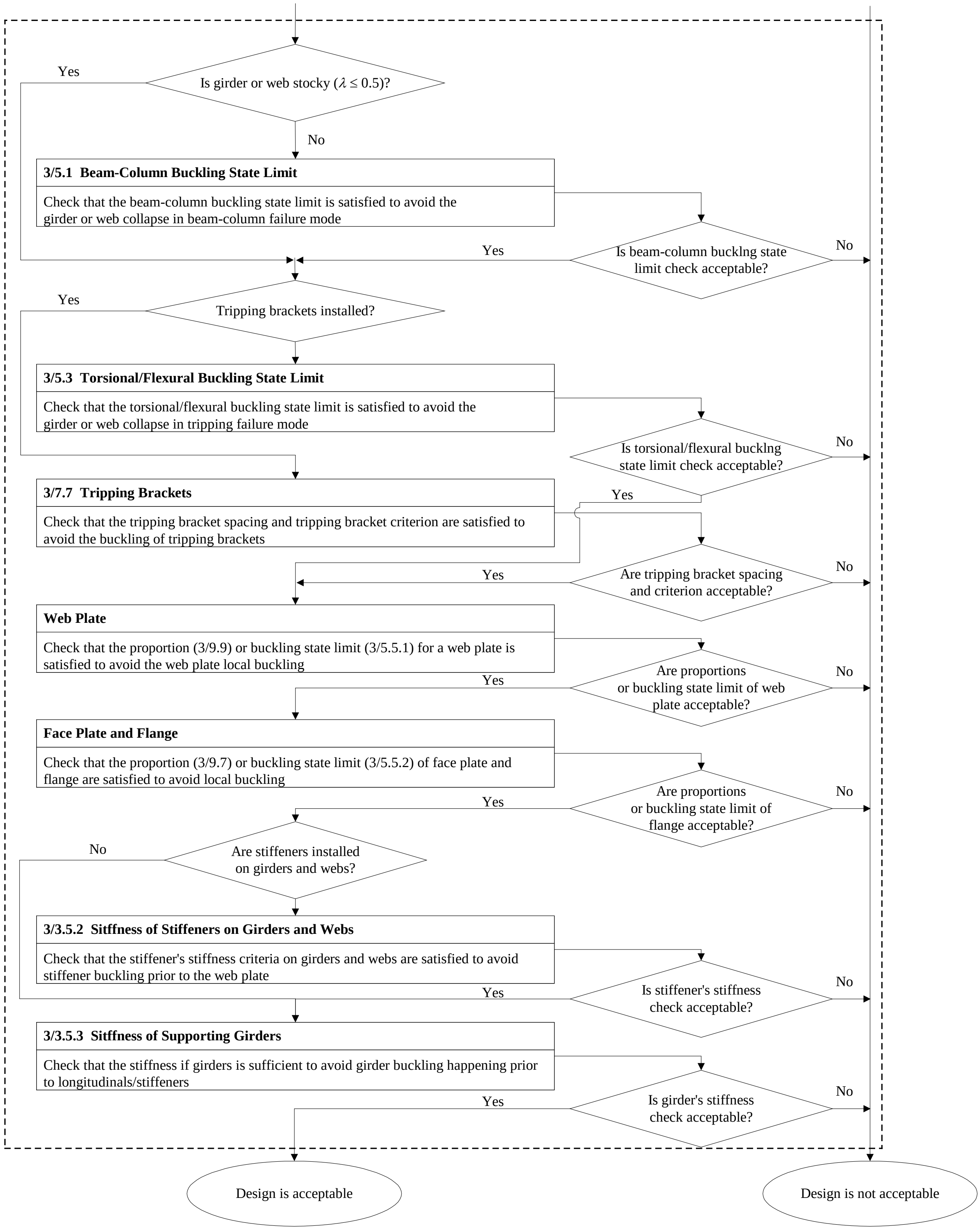

TABLE 1
Statistical Characteristics of Floating Production Installations (FPIs)

	Aspect Ratio(α)		*Slenderness Ratio(s/t)*	
	Mean	*COV*	*Mean*	*COV*
TLP	2.5	0.28	41	0.22
Spar	2.8	0.12	39	0.24
Semi	4.0	0.20	44	0.30
FPSO	4.7	0.16	46	0.25

According to design practice, the plate width (stiffener spacing) has relatively little variation. From Section C3, Table 1, it can be seen that the means of plate aspect ratio of TLP and Spar are very close, which implies that the plate length (transverse girder spacing) for these two types of structures is consistent. The COV of plate aspect ratio of TLP is greater than that of Spar, demonstrating the variation of girder spacing in a TLP is typically greater.

Semi-Submersible and FPSO have similar statistical characteristics on plate aspect ratio, implying that these two types of structures have the same design principles in the selection of a stiffening system.

All types of FPIs have identical statistical characteristics on plate slenderness ratio, implying that the longitudinal buckling and ultimate strength are in agreement with each other if the same steel grade is selected.

Corrugated panels in a watertight bulkhead are usually corrugated vertically without horizontal girders and supported by stools at upper and lower ends. Corrugated shear diaphragms typically omit the stool support structure. Based on experimental results, each corrugation of a corrugated panel deforms similarly under lateral pressure. This implies that the behavior of a unit corrugation can represent that of the entire corrugated panel when subjected to lateral pressure.

FIGURE 2
Statistical Depiction of Plate Aspect Ratio of FPIs

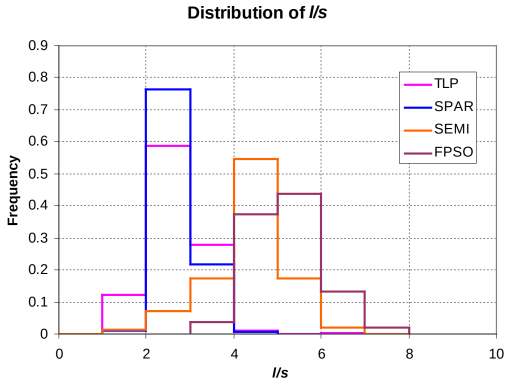

FIGURE 3
Statistical Depiction of Plate Slenderness Ratio of FPIs

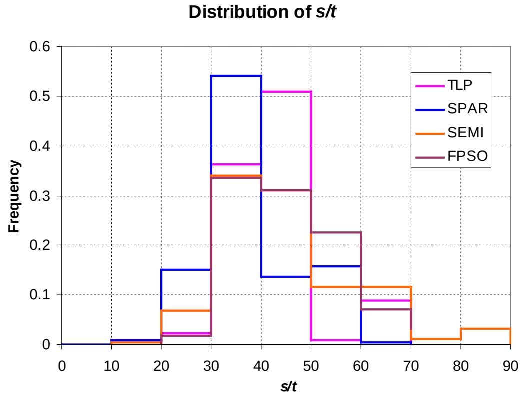

C1.3 Load Application

<No Commentary>

C1.5 Buckling Control Concepts

In the design of stiffened panels, one should keep in mind that there are three levels of failure mode, namely the plate level, the stiffened panel level and the entire grillage level; the higher level of failure usually leads more severe consequence than the preceding level. Therefore suitable scantling proportions between plates, stiffeners and girders are necessary to guarantee the sufficient safety of the stiffened panels.

Theoretically, plate panels exhibit a continued increase of resistance after the bifurcation point, before they finally reach the ultimate load carrying capacity. In other words, the plate panels have stable postbuckling behavior. Therefore, it is acceptable that plate panels are designed to reach the buckling state but not the ultimate state. The nominal load-deflection relationship of plate panels is shown schematically in Section C3, Figure 4.

FIGURE 4
Load-Deflection Relationship of Plate Panels

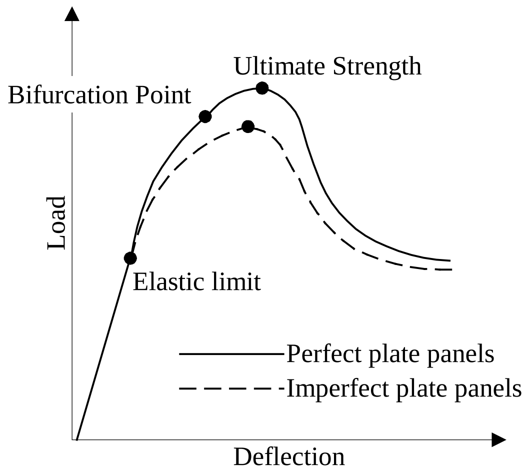

There are three types of buckling mode for stiffeners and girders, i.e., beam-column buckling, torsional-flexural buckling and local flange/web plate buckling. The buckling of stiffeners and girders is restricted because their resistance decreases quickly if any one of these three types of buckling occurs. Their buckling strength is regarded as the ultimate strength. If the associated plating of a stiffener buckles, but is below its ultimate state, the plating's effective width acting with the stiffener is to be applied.

Corrugated panels are 'self-stiffened' panels. There are three levels of failure mode, i.e., flange/web plate buckling, unit corrugation buckling and entire corrugation buckling. Depending on the loading type, corrugated panels may collapse into the different failure modes. For examples, axial compression mainly induces the flange/web buckling, lateral pressure induces the buckling of unit corrugation, and edge shear force leads to the buckling of entire panels. The buckling strength is the least value obtained from those established for the three failure modes considering any load type and load combination.

C1.7 Adjustment Factors

The adjustment factors for the allowable basic utilization factor in the existing offshore codes are provided in Section C3, Table 2.

TABLE 2
Adjustment Factor

	Plate Panels	*Stiffeners*	*Girders and Webs*	*Corrugated Panels*
ABS *Buckling Guide*	1.0	1.0	1.0	1.0
API RP WSD 2A (AISC)[3]	1.0	1.0	1.0	—
DnV MOU Rules[13]	1.1	1.0	1.0	—

DnV MOU Rules[13] suggests a higher adjustment factor for plate panels, as the ultimate strength in DnV CN30.1[7] is generally underestimated. The allowable ultimate strength requirements for plate panels from those three codes are very comparable, which will be demonstrated in the comparison study for a Spar in Section C3, Appendix 2.

C3 Plate Panels

C3.1 Buckling State Limit

A large amount of effort has been carried out over the past three decades and different interaction equations have been suggested. In the ABS *Buckling Guide*, the buckling state limit for plate panels between stiffeners is defined by the following equation:

$$\left(\frac{\sigma_{x\max}}{\eta\sigma_{Cx}}\right)^2 + \left(\frac{\sigma_{y\max}}{\eta\sigma_{Cy}}\right)^2 + \left(\frac{\tau}{\eta\tau_C}\right)^2 \le 1$$

where

σ_{Cx}, σ_{Cy} = critical buckling stresses for compressions

τ_C = critical buckling stress for edge shear

The critical buckling stress for edge shear, τ_C, may be taken as (Johnson-Ostenfeld formula):

$$\tau_C = \begin{cases} \tau_E & \textit{for} \quad \tau_E \le P_r\tau_o \\ \tau_o\left[1 - P_r(1-P_r)\dfrac{\tau_o}{\tau_E}\right] & \textit{for} \quad \tau_E > P_r\tau_o \end{cases}$$

In the above equations, the elastic buckling stress is:

$$\tau_E = k_s \frac{\pi^2 E}{12(1-\upsilon^2)}\left(\frac{t}{s}\right)^2$$

where

k_s = boundary dependent constant.

$$= \left[4\left(\frac{s}{\ell}\right)^2 + 5.34\right]C_1$$

The critical buckling stress in a given direction, σ_{Ci} ($i = x$ or y), for plates subjected to combined uniaxial compression and in-plane bending may be taken as (Johnson-Ostenfeld formula):

$$\sigma_{Ci} = \begin{cases} \sigma_{EI} & \textit{for} \quad \sigma_{EI} \le P_r\sigma_0 \\ \sigma_0\left[1 - P_r(1-P_r)\dfrac{\sigma_0}{\sigma_{EI}}\right] & \textit{for} \quad \sigma_{EI} > P_r\sigma_0 \end{cases}$$

The elastic buckling stress is given by

$$\sigma_E = k_s \frac{\pi^2 E}{12(1-\upsilon^2)}\left(\frac{t}{s}\right)^2$$

where

k_s = buckling coefficient

For loading applied along the short edge of the plating (long plate):

$$k_s = C_1\begin{cases} \dfrac{8.4}{\kappa + 1.1} & \text{for} \quad 0 \le \kappa \le 1 \\ 7.6 - 6.4\kappa + 10\kappa^2 & \text{for} \quad -1 \le \kappa < 0 \end{cases}$$

For loading applied along the long edge of the plating (wide plate)

$$k_s = C_2 \begin{cases} \left[1.0875 \cdot \left(1 + \frac{1}{\alpha^2}\right)^2 - 18\frac{1}{\alpha^2}\right] \cdot (1+\kappa) + 24\frac{1}{\alpha^2} & \text{for } \kappa < \frac{1}{3} \text{ and } 1 \le \alpha \le 2 \\ \left[1.0875 \cdot \left(1 + \frac{1}{\alpha^2}\right)^2 - 9\frac{1}{\alpha}\right] \cdot (1+\kappa) + 12\frac{1}{\alpha} & \text{for } \kappa < \frac{1}{3} \text{ and } \alpha > 2 \\ \left(1 + \frac{1}{\alpha^2}\right)^2 (1.675 - 0.675\kappa) & \text{for } \kappa \ge \frac{1}{3} \end{cases}$$

It should be noted that the formulation for k_s for wide plates is basically similar to K_i in 5-1-A2/3 of the ABS *Steel Vessel Rules*[2]. The difference is that ABS provides three points between which the designer is to use linear interpolation, while the formulation given above relies on a continuous curve.

Comparison Study – Buckling Strength

Test Database

The plate test database consists of 206 datasets for plates under uniaxial compression along short edges and 15 datasets for plates under uniaxial compression along long edges. The data were collected from numerous publications. No records related to plates under edge shear loading were included in the database.

Comparison Basis

Comparisons between the strength predictions of the existing formulations and test data are generally conducted on the basis of safety factors excluded (set to unity). In all cases, measured values of geometry and material properties were input to the strength equations. For single-acting loading conditions such as pure compression, the resultant strength was taken as the predicted value for the model in question. For assessing accuracy in terms of 'Modeling Uncertainty', as defined in Section 1, the test result is then divided by the value from the strength formulations. The average of all of these modeling uncertainty values is then calculated along with the standard deviation in order that the COV (coefficient of variation) can be determined as the ratio of (standard deviation) ÷ (average). The average (or mean or bias as it is more usually referred to) and COV provide the statistics by which the accuracy of the formulation can be quantified.

Comparison Results

- *Long Plates.* Section C3, Figure 5 shows the relation between σ_{Cx} and β for the long plates. Section C3, Figure 6 shows the distribution of modeling uncertainty. Section C3, Table 3 gives the statistical characteristics of the modeling uncertainty.

TABLE 3
Mean/COV of Modeling Uncertainty of Long Plates

	ABS Buckling Guide	*DnV CN30.1*	*API Bulletin 2V*
Mean	1.1149	1.1731	1.0747
COV	0.2845	0.2723	0.3050

FIGURE 5
Buckling Stress of Long Plates

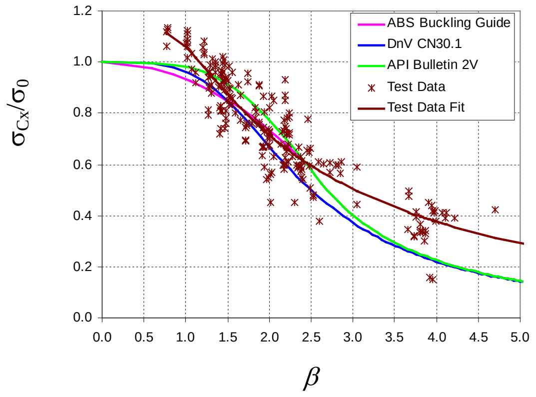

FIGURE 6
Modeling Uncertainty of Long Plates

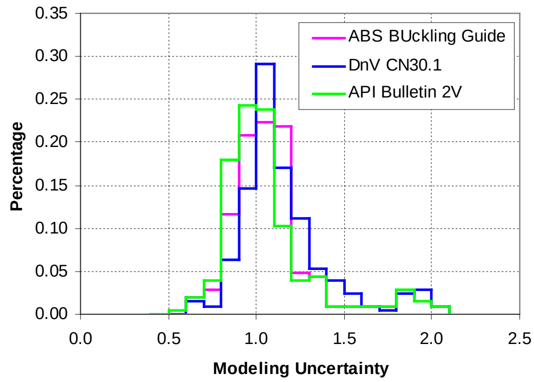

The mean of the modeling uncertainty in the three codes is greater than 1 and its COV is around 30%. The relatively large COV is not surprising because the test data have been collected from many different published sources. In general, the buckling strength evaluated by the three codes is conservative compared to the test data.

- *Wide Plates.* Section C3, Figure 7 shows graphically the relation between σ_{Cy} and β for the wide plates for two different aspect ratios according to the formulae of the ABS *Buckling Guide*, DnV CN30.1, API Bulletin 2V and test data. The results obtained from the formulae of the three codes are in good agreement with test data.

FIGURE 7
Buckling Stress of Wide Plates

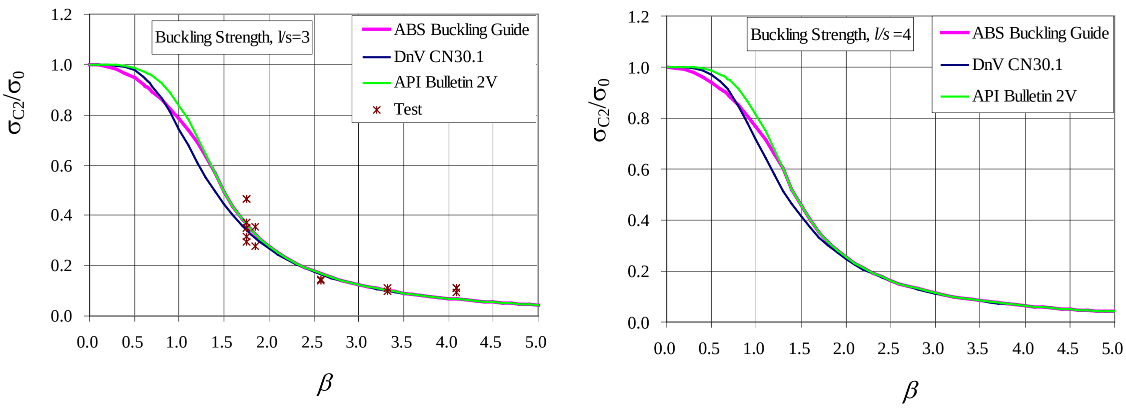

Section C3, Figure 8 shows the comparison of buckling coefficient for wide plates subjected to non-uniform compression on the long edges. The buckling coefficient value obtained from the ABS *Buckling Guide* is somewhat different from those from API Bulletin 2V and DnV CN 30.1 when the plate aspect ratio is less than 3 and the stress ratio is negative.

FIGURE 8
Buckling Coefficient of Wide Plates Subjected to Non-Uniform Stress

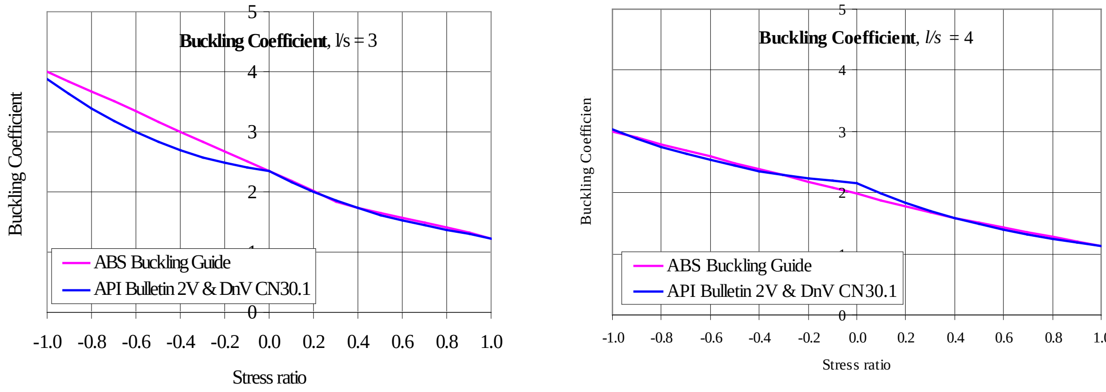

- *Edge Shear Loading.* Section C3, Figure 9 shows the relation between τ_C and β for the plates with different aspect ratios according to the ABS *Buckling Guide*, DnV CN30.1 and API Bulletin 2V. The difference among the three codes is negligible.

FIGURE 9
Buckling Stress under Shear Loading

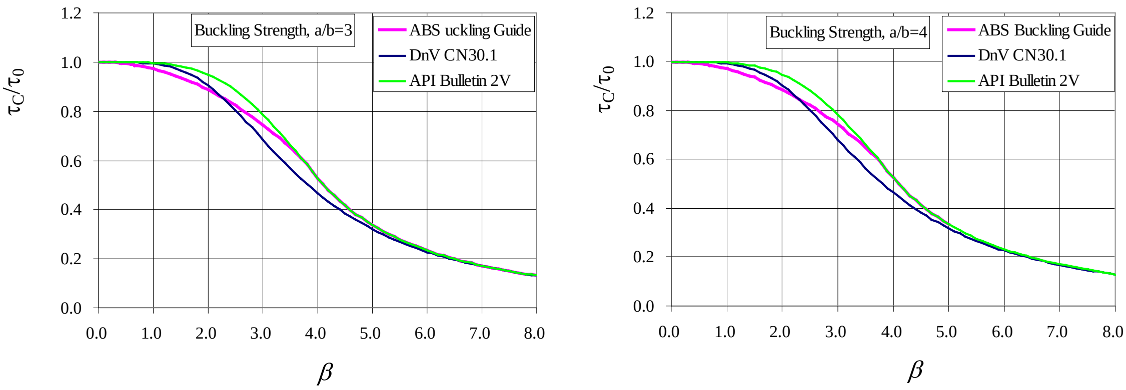

C3.3 Ultimate Strength under Combined In-plane Stresses

Unlike columns and cylinders, a buckled plate panel can sustain further loading until the ultimate strength is reached. The in-plane stiffness of the panel takes a negative slope in the post-ultimate phase, which implies a high degree of instability. The ultimate strength behavior of plate panels depends on many influential factors such as geometry and material properties, loading and boundary conditions and initial imperfections (i.e., initial deflection and residual stress).

A large amount of effort has been given to the ultimate strength assessment of plate panels. In the ABS *Buckling Guide*, the ultimate strength limit for plate panels between stiffeners is defined by the following equation:

$$\left(\frac{\sigma_{x\max}}{\eta\sigma_{Ux}}\right)^2 - \varphi\left(\frac{\sigma_{x\max}}{\eta\sigma_{Ux}}\right)\left(\frac{\sigma_{y\max}}{\eta\sigma_{Uy}}\right) + \left(\frac{\sigma_{y\max}}{\eta\sigma_{Uy}}\right)^2 + \left(\frac{\tau}{\eta\tau_U}\right)^2 \le 1$$

The ultimate strength for uniaxial compression in short edge was developed by Faulkner[44], which is written by:

$$\sigma_{Ux} = \sigma_0 C_x \text{ and}$$

$$C_x = \begin{cases} 1.0 & \text{for} \quad \beta < 1 \\ \dfrac{2}{\beta} - \dfrac{1}{\beta^2} & \text{for} \quad \beta \geq 1 \end{cases}$$

Following the ABS *Steel Vessel Rules*[2], the ultimate strength, σ_{Cy} should not be less than the critical buckling stress, σ_{Cx}. If the ultimate strength is less than the critical buckling stress, the ultimate strength should be set equal to the critical buckling stress.

The ABS *Steel Vessel Rules* adopted Frankland's formula, from which the ultimate strength is in general higher than that Faulkner's formula. The ABS *Steel Vessel Rules* uses net thickness to assess the buckling strength.

The ultimate strength for uniaxial compression along the long edge is given by:

$$\sigma_{U2} = \sigma_y C_y \geq \sigma_{C2}$$

where

$$C_y = C_x(s/\ell) + 0.1(1 - 1/\alpha)(1 + 1/\beta^2)^2$$

The basic philosophy behind the above formula is that the plate is divided into two separate regions (Valsgard[45]), as shown in Section C3, Figure 10. The shaded region along the transverse girders is supposed to be a quadratic area which carries the same amount of load as specified by square plates. The strength of the central region is corrected with the results by the lab tests and numerical experiments as provided in comparison study.

FIGURE 10
Ultimate Strength of Wide Plates

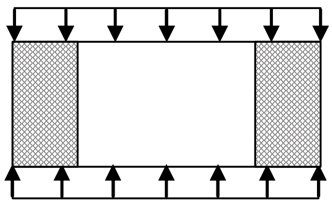

The ultimate shear strength of plate panels was developed by Porter et al[46], which was the correction of Basler's approach[47], as given by:

$$\tau_U = \tau_C + \frac{\sqrt{3}}{2\sqrt{1 + \alpha + \alpha^2}}(\tau_0 - \tau_C)$$

In the above equation, the Vierendeel action (Harding[48]) was ignored. It was assumed that edge girder flanges have insufficient flexural rigidity to resist diagonal tension, which is consequently reacted by the transverse stiffeners. As a result, the transverse stiffeners are subject to compressive loading.

The interaction coefficient φ proposed in the ABS *Buckling Guide* reflects the interaction between longitudinal stress and transverse stress (negative value is allowable). Based on the results of lab tests and numerical experiments, it is appropriate to take the following value:

$$\varphi = 1.0 - \beta/2$$

There are two extreme cases for the interaction coefficient. When the elastic configuration is dominant (large β), Von Mises yielding is relatively less significant. When $\varphi \to 2$ ($\beta \to 5$), the interaction equation becomes linear, which represents the most conservative interaction relationship between longitudinal and transverse stresses. As σ_e grows larger (occurring in inelastic configuration corresponding to small β), the von Mises yielding becomes dominant. When $\varphi \to 1$ ($\beta \to 0$), the interaction equation becomes Von Mises yield criteria if there is no shear stress.

Comparison Study – Ultimate Strength

Test Database

The plate test database consists of 206 sets of test results for plates under uniaxial compression along short edges and 15 tests for plates under uniaxial compression along long edges. The data were collected from numerous publications (Frieze[49]). No test data is related to plates under edge shear loading in the database.

FEM Simulation

A numerical analysis of the ultimate strength for the test plates was executed based on the general nonlinear finite element program, ANSYS. The finite element analysis uses the full Newton-Raphson equilibrium iteration scheme and arc-length method to include geometric and material nonlinearities and pass through the extreme points. The bisection and automatic time stepping features are activated to enhance the convergence. The material is idealized to be elastic-perfectly-plastic. The finite strain Shell 181 element type is used to discretize the model plates. This element type is appropriate for linear, large rotation and/or large strain nonlinear applications and supports both full and reduced integration schemes. Simply supported boundary conditions are applied, as shown in Section C3, Figure 11.

FIGURE 11
Boundary Conditions

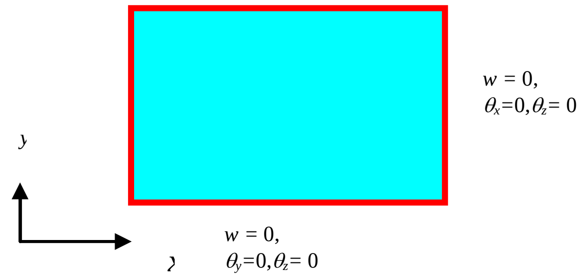

In the FEM analysis, initial imperfection is assumed to be of the form:

$$\frac{W_{p0}}{t} = [\delta_{10}\sin(\frac{\pi x}{\ell}) + \delta_{31}\sin(\frac{3\pi x}{\ell})]\sin(\frac{\pi y}{s})$$

where

α = Aspect ratio

δ_{10} = $\dfrac{2W^*}{3t}$

δ_{31} = $\dfrac{W^*}{3t}$

W^* = fabrication tolerance of plate panels

The first term represents the dominant initial imperfection mode and the second term is the buckling mode of long plates with the aspect ratio of 3 (Davidson et al[50]). The amplitude of the imperfection is selected based on statistics from ship plating by Smith et al[52].

Two kinds of in-plane boundary conditions are used:

i) *FEM1*. All edges move freely during loading. This boundary condition is applicable in the single plate test.

ii) *FEM2*. All edges remain straight during loading. The element types, Beam4 and Combin7, are used to simulate the in-plane boundary condition. The special geometrical property with very small sectional area and very large moment of inertia is assigned to the element BEAM4. This boundary condition is accepted in continuous plated structures as long as the stiffeners are strong enough so that they do not fail prior to buckling of plate.

Comparison Basis

Comparisons between the strength predictions of existing formulations and test data are generally conducted on the basis of utilization factors excluded (set to unity). When assessing accuracy in terms of 'Modeling Uncertainty' as defined in Section 1, the test or FEM result is then divided by the value from code formulations. The average of all of these modeling uncertainty values is calculated along with the standard deviation so that the COV (coefficient of variation) can be determined as the ratio of (standard deviation) ÷ (average). The average (or mean or bias as it is more usually referred to) and COV provide the statistics by which the accuracy of the formulation can be quantified.

Comparison Results

- *Long Plates*. Section C3, Figure 12 shows the ultimate strength, σ_U versus slenderness ratio, β, in which the predictions from the ABS *Buckling Guide*, DnV CN30.1 and API BULLETIN 2V, test results and FEA simulation with freely movable in-plane edges (FEM1) are compared. The modeling uncertainty is shown in Section C3, Figure 13. The mean and COV are given in Section C3, Table 4.

TABLE 4
Mean/COV of Modeling Uncertainty of Plates

	API Bulletin 2V & ABS Buckling Guide	*DnV CN30.1*	*FEM1*
Mean	0.9559	1.0744	1.0114
COV	14.81%	14.95%	15.98%

FIGURE 12
Ultimate Strength of Long Plates

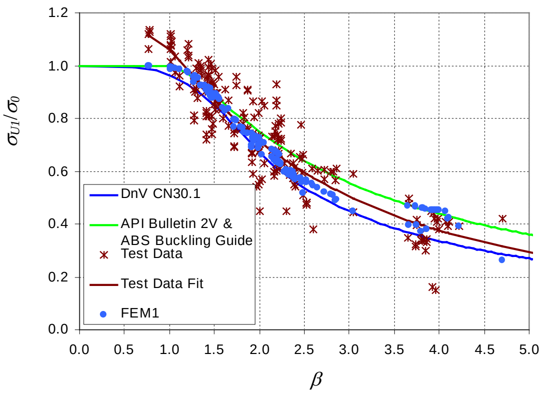

FIGURE 13
Modeling Uncertainty of Long Plates

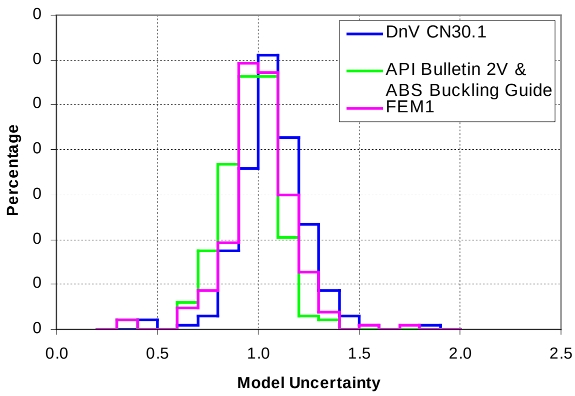

FEM1 provides the best match to the test data. The mean of the modeling uncertainty from API Bulletin 2V and the ABS *Buckling Guide* is less than 1 whereas the mean of the modeling uncertainty from FEM1 and DnV CN30.1 is slightly greater than 1. This implies that almost all test plates are for the boundary condition freely moving in-plane during loading. As indicated above, this type of boundary conditions may possibly be suitable for single plates; but it can't represent the real conditions of plate panels in continuous plate structure. Although the formula from DnV CN 30.1 seems to underestimates the ultimate strength of plates in the continuously plated structures, DnV MOU used a higher adjustment coefficient of 1.1 to modify the estimate. After this coefficient applies, the mean of modeling uncertainty reduces to 0.9767.

Section C3, Figure 14 shows a comparison of the ultimate strength, σ_{U1}, versus slenderness ratio, β, in which the boundary condition that retains straight edges during loading is applied for the FEA simulation (FEM2). The modeling uncertainty of the prediction based on FEM2 is shown in Section C3, Figure 15. The mean and COV are given in Section C3, Table 5.

TABLE 5
Mean/COV of the Modeling Uncertainty of FEM2/Predictions

	API Bulletin 2V & ABS Buckling Guide	*DnV CN 30.1*
Mean	1.0111	1.1433
COV	4.17%	11.34%

FIGURE 14
Ultimate Strength of Long Plates

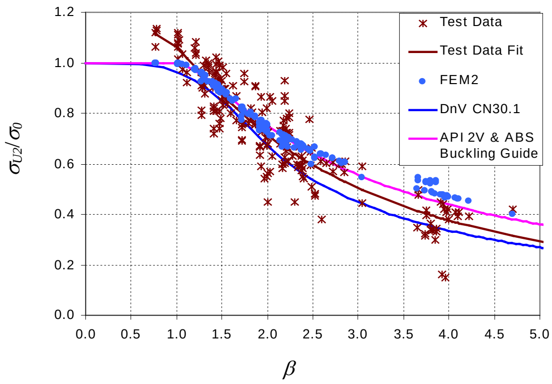

FIGURE 15
Modeling Uncertainty of Long Plates

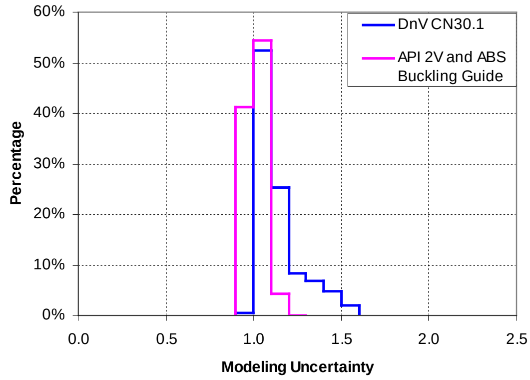

- *Wide Plates.* Section C3, Figure 16 shows a comparison of the ultimate strength, σ_{U2}, versus slenderness ratio, β, based on the formulae of DnV CN30.1, API BULLETIN 2V and the ABS *Buckling Guide*, test results and FEA simulation with the boundary conditions that remain straight edges during loading (FEM2). The mean and COV of modeling uncertainty with the base of FEM2 are given in Section C3, Table 6.

TABLE 6
Mean/COV of the Modeling Uncertainty of FEM2/Predictions

	DnV CN30.1	*API Bulletin 2V*	*ABS Buckling Guide*
Mean	1.0038	1.1250	0.9852
COV	11.95%	13.33%	6.62%

FIGURE 16
Ultimate Strength of Wide Plates

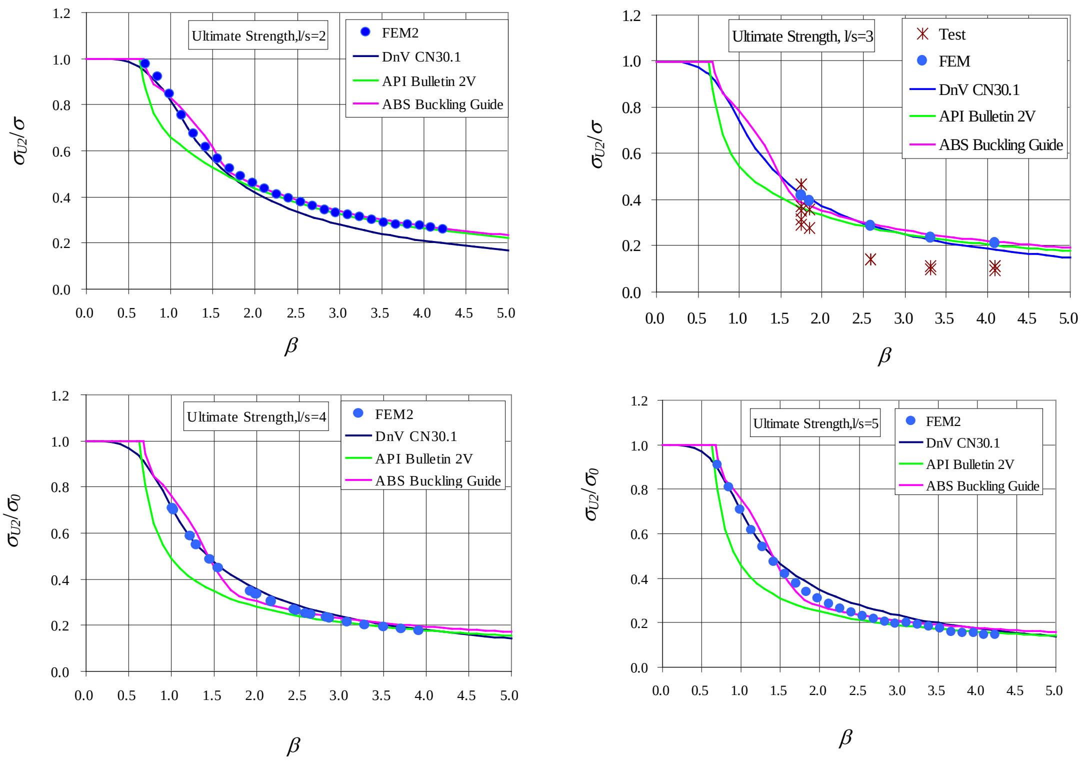

- *Edge Shear Loading.* Section C3, Figure 17 provides the comparison of the ultimate strength, τ_U, versus slenderness ratio, β, based on the formulae of DnV CN30.1, API BULLETIN 2V and the ABS *Buckling Guide* and FEM analysis. The results presented here are based on the strain control condition applied along the panel edges representing the presence of stiffeners and flanges. A limit of shear yield strain, γ_0, has been set when evaluating the ultimate strength from a design point of view in order to limit the overall panel shear deformation.

FIGURE 17
Ultimate Strength of Plates in Edge Shear Loading

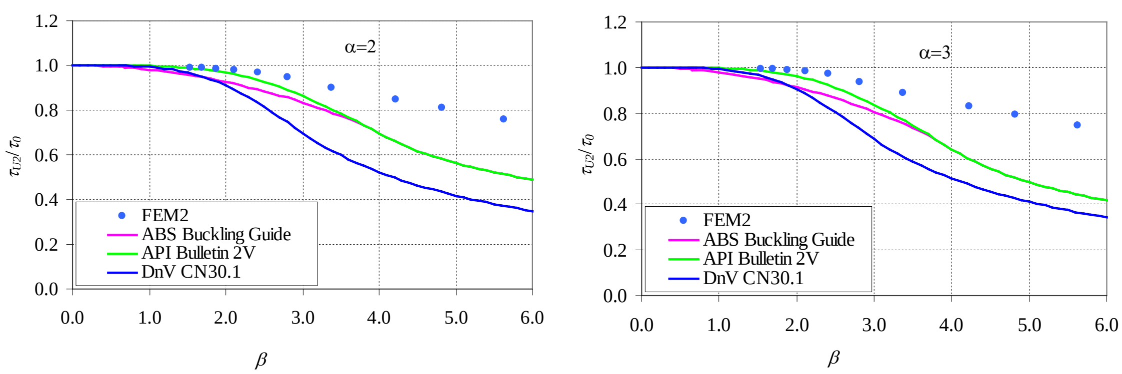

- *Combined In-plane Compression and Lateral Loads.* The influence of lateral pressure on the behavior of plates subjected to in-plane loads is a complex problem. Experiments on an isolated single plate without stiffeners and girders supported show that the lateral pressure has an inconsistent influence on in-plane compressive ultimate strength; e.g., the effect of lateral pressure generally increases the strength of long plates but decreases the strength of wide plates. In order to better see the influence of lateral pressure, an extensive FEM simulation for isolated plates has been carried out for the purpose of this comparison study.

  The ultimate strength due to lateral strength proposed in API Bulletin 2V Commentary (2000) is given by:

$$\frac{\sigma'_{Ui}}{\sigma_0} = \left(\frac{\sigma_{Ui}}{\sigma_0}\right)^{0.8Q^2+0.84Q+1}$$

  where

  Q = pE/σ_0^2

  p = applied pressure

Comparison Study

The data available consists of 56 test data sets and 173 results of non-linear FEA, in which 78 of them are for wide plates. The results, as shown in Section C3, Figure 18, are normalized by the ultimate strength from the ABS *Buckling Guide*.

FIGURE 18
Combined In-plane Compression and Lateral Pressure for Isolated Plates

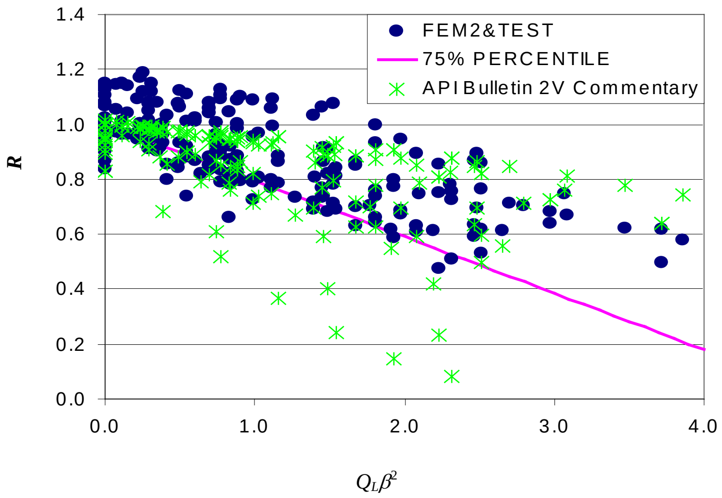

It can be seen that:

i) There is large spread of results;

ii) Regression analysis gives the reduction factor at the 75th percentile as:

$$R = 1 - 0.205Q_L\beta^2$$

where

Q_L = pE/σ_0^2

p = applied pressure

Yao et al[53-55] published a series papers to clarify the behaviors of buckling/plastic collapse and strength of ship bottom plates subjected to combined bi-axial thrust and lateral pressure. They considered a portion of continuously stiffened plates for the analysis taking into account symmetry conditions, and they performed a series of elastic-plastic FEM analysis to examine the influence of lateral pressure on the buckling/plastic collapse and strength for the continuously stiffened plates. They concluded:

i) The buckling strength increases with the increase of applied lateral pressure.

ii) The buckling strength is also increased by the stiffeners, which constrain the rotation of panel along its edge.

iii) With the increase of the applied lateral pressure, the boundary condition of the panel between stiffeners changes from simply supported condition to clamped condition. This change increases the buckling/plastic collapse strength of stiffened plates.

iv) With larger lateral pressure, yielding starts earlier. This reduces the buckling/plastic collapse strength of stiffened plates.

v) The formulae by classification societies give conservative buckling strength under bi-axial compression, and the bottom plating has much reserve strength when the lateral pressure is acting on it.

To verify the above conclusions, a FEM model for continuously stiffened plates similar to Yao et al is constructed. The plate length and width are taken as 2400 mm and 800 mm respectively. The plate thickness is changed systematically to cover the typical slenderness ratios of plates used in offshore structures. The numerical results of ultimate strength for the long plates and wide plates, normalized by the ultimate strength obtained from the ABS *Buckling Guide*, are given in Section C3, Figure 19, which are consistent with those by Yao et al[53-55]. The ultimate strength for the continuously stiffened plates from the FE analysis is always greater than that predicted by the formula in the ABS *Buckling Guide* even when very large lateral pressure is applied. Therefore, it is conservative to ignore the effect of lateral pressure on the in-plane compressive ultimate strength of plates in continuous plate structure.

FIGURE 19
Effect of Lateral Pressure to Ultimate Strength of Continuously Stiffened Plates

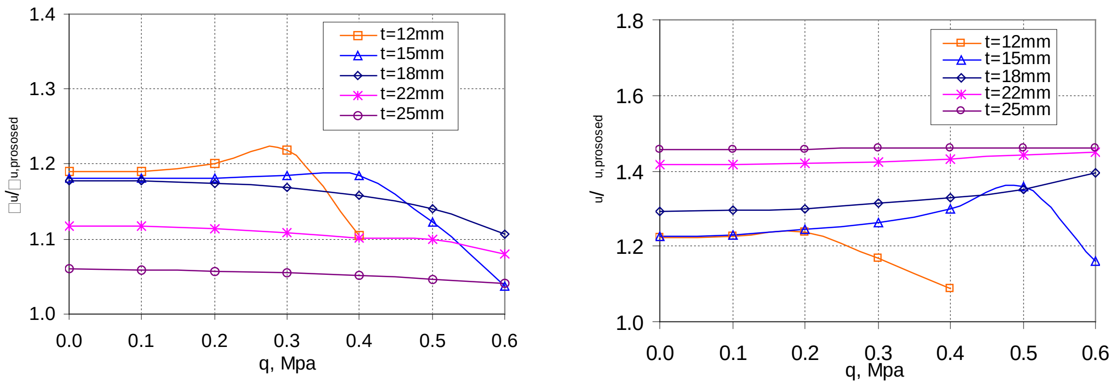

(a) Long Plates (b) Wide Plates

- *Combined In-plane Biaxial Compression and Shear.* A lot of comparisons have been performed of the interaction equations for buckling stress limit (BSL) and ultimate strength (US) among DnV CN30.1, API Bulletin 2V(2002), the ABS *Buckling Guide* and FEM simulation (FEM2) with the different aspect ratio, slenderness ratio and edge shear loading. Section C3, Figure 20 displays some typical comparison results.

FIGURE 20
Interaction Equations of Plate Panels

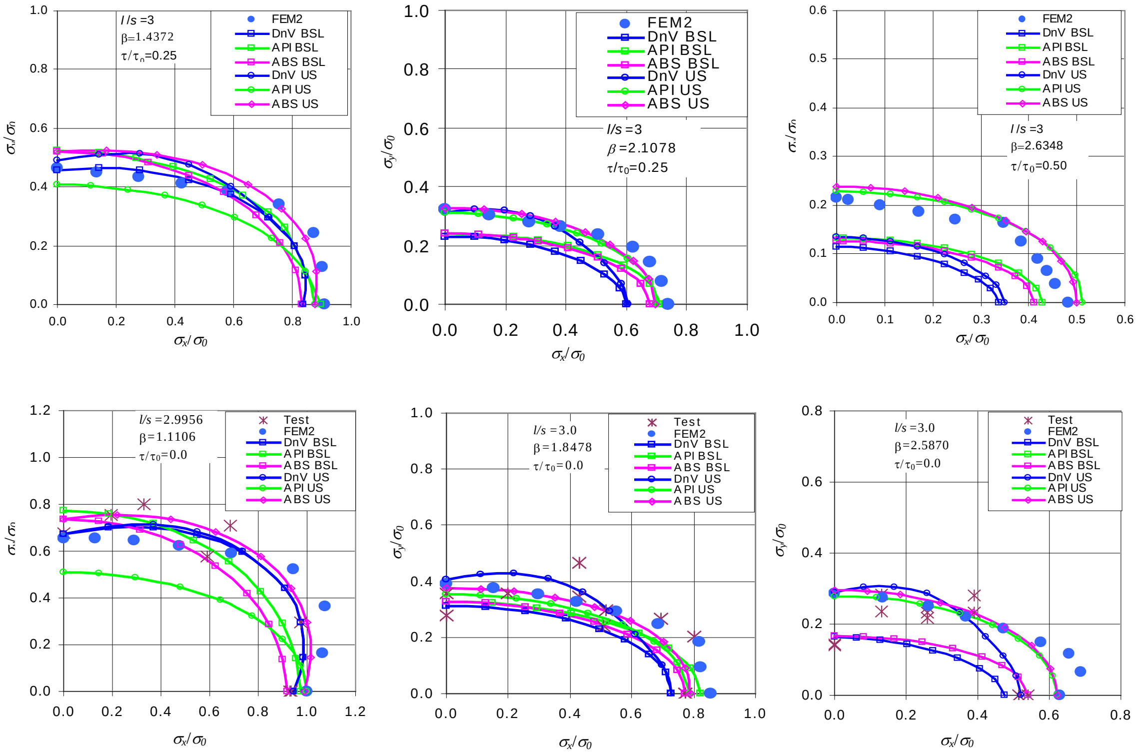

Based on the comparison results, it is concluded that the recommended criterion in the ABS *Buckling Guide* predicts the reasonable capacities and the case with difference from the nonlinear FEM are acceptable compared with the existing offshore codes.

C3.5 Uniform Lateral Pressure

There are many references on the ultimate strength of rectangular plates under uniform lateral pressure alone, or predominant lateral pressure combined with the in-plane stresses, such as Johns[56] among others. When considering rectangular plates supported by an orthogonal stiffening system, the plate edges have a certain degree of in-plane axial and rotational restraints. If there are axial in-plane restraints, the plate is able to resist lateral pressure by membrane action. This can provide very large reserve strength. The failure modes may include large inelastic deformation (permanent set) of the plate, tearing (tensile failure) of the plate material at the supports and transverse shear failure of the plate material at the supports.

In the ABS *Buckling Guide*, a panel between stiffeners subjected to uniform lateral pressure alone or combined with in-plane stress is to satisfy the following equation:

$$p_u = \eta 4.0\sigma_0\left(\frac{t}{s}\right)^2\left(1+\frac{1}{\alpha^2}\right)\sqrt{1-\left(\frac{\sigma_e}{\sigma_0}\right)^2}$$

where

t = plate thickness

α = aspect ratio, $\alpha = \dfrac{\ell}{s}$

σ_0 = yield stress of plate

σ_e = equivalent stress according to von Mises

$$= \sqrt{\sigma_1^2 - \sigma_1\sigma_2 + \sigma_2^{\;2} + 3\tau^2}$$

This equation was derived from the lower bound of the yield line theory associated with the effect of in-plane loadings.

Comparison Study

Section C3, Figure 21 shows the effect of the permanent set without in-plane stress applied. Increasing the amount of permissible permanent set always increases the ultimate strength of plates under lateral pressure. Section C3, Figure 22 shows ultimate strength as a function of the ratio of thickness to width without in-plane stress applied. The API formula is overly conservative for the plate subjected to lateral pressure alone.

FIGURE 21
Effect of Permanent Set

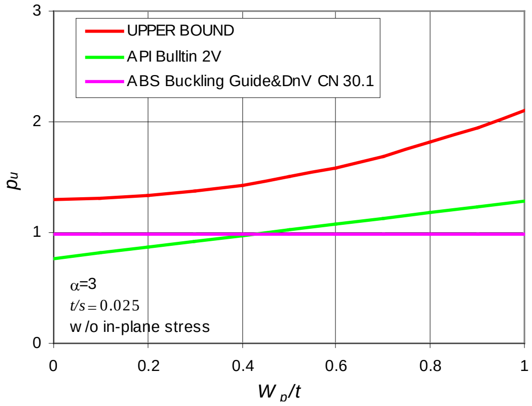

FIGURE 22
Ultimate Strength vs. *t/s*

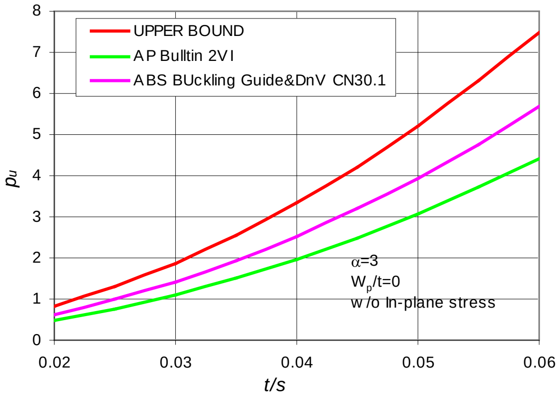

Monte Carlo Simulation Technique is used to compare ABS *Buckling Guide* formula with DnV CN30.1 formula for the plates subjected to combined lateral pressure and in-plane stresses. The range of sampling points of basic variables is given in Section C3, Table 7; 5000 simulations are carried out. The sampling sets are established from a generator of uniform random numbers. If the obtained equivalent stress is greater than the yield stress, then the sampling set is discarded. The comparison results are shown in Section C3, Figure 23. The mean and coefficient of variation (COV) of the ratio of the ABS *Buckling Guide* formula over DnV formula excluding the adjustment factor of 1.1 are 1.08 and 0.08, respectively. In general, the predictions from ABS *Buckling Guide* formula are in quite good agreement with those from the DnV CN30.1 formula.

TABLE 7
Basic Variables

Variables	*Range*	*Variables*	*Range*
t, mm	10~25	σ_0, MPa	240~480
s, mm	769	σ_x, MPa	0~σ_0
α	1~4	σ_y, MPa	0~σ_0
E, GPa	210	σ_{xy}, MPa	0~τ_0

FIGURE 23
Comparison of the ABS Buckling Guide with DnV CN30.1

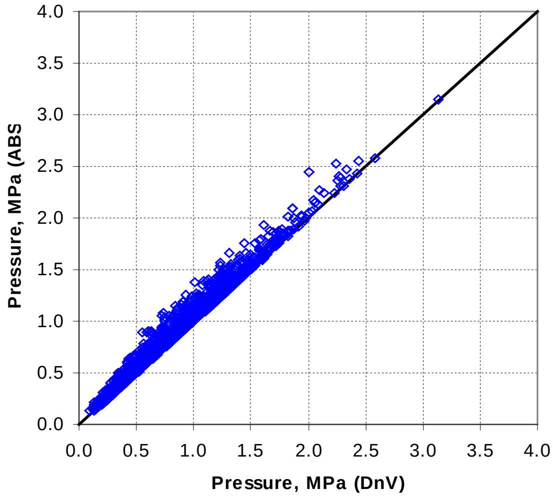

C5 Stiffened Panels

Stiffened panels are used extensively in offshore applications with emphasis on their stability as units, rather than on the stability of their individual elements. Thus local buckling of the stiffeners is suppressed by placing limitations on their geometry. It is important to prevent such forms of buckling because of their catastrophic consequences. However, plate elements between stiffeners can be allowed to buckle during the working life of the stiffened panel. Plate buckling produces a partial loss of the plate's effectiveness, and the effective plate width that is assumed to act as a flange of a stiffener is adopted in design recommendations.

The recommended method in the ABS *Buckling Guide* is based on the ABS *Steel Vessel Rules* as provided below.

C5.1 Beam-Column Buckling State Limit

The beam-column buckling state limit for a stiffened panel is assessed as follows:

$$\frac{\sigma_a}{\eta\sigma_{CA}(A_e / A)} + \frac{C_m\sigma_b}{\eta\sigma_0[1-\sigma_a/(\eta\sigma_{E(C)})} \le 1$$

where

σ_{CA}	=	critical buckling stress
$\sigma_{E(C)}$	=	Euler's buckling stress
A_e	=	effective sectional area.

This criterion is similar to ABS *Steel Vessel Rules* (2003). The difference is that the effects of transverse stress and shear stress on plating edge are taken into account. The effective width is written by:

$$s_e = C_x C_y C_{xy} s$$

where

C_x	=	reduction factor due to the plating subjected to longitudinal loading only

C_y = reduction factor due to transverse loading, which is derived from the ultimate strength interaction equation without shear loading in Section 3/3.3 of the ABS *Buckling Guide*. C_y is solvable under the condition that the plate panel subjected to in-plane loadings does not collapse.

$$= 0.5\varphi\left(\frac{\sigma_{y\max}}{\sigma_{Uy}}\right) + \sqrt{1-(1-0.25\varphi^2)\left(\frac{\sigma_{y\max}}{\sigma_{Uy}}\right)^2}$$

$$\sigma_{Uy} = \sigma_0\left[\frac{s}{\ell}C_x + 0.1\left(1-\frac{s}{\ell}\right)\left(1+\frac{1}{\beta^2}\right)^2\right]$$

φ = $1.0 - \beta/2$

C_{xy} = reduction factor due to shear stress

C5.3 Torsional/Flexural Buckling State Limit

A stiffener may buckle by twisting about its line of attachment to the plating (See Section C3, Figure 24). This is commonly referred to as tripping. The plate may rotate somewhat to accommodate the stiffener rotation, and the direction of rotation usually alternates because this involves less elastic strain energy in the plate. Tripping and plate buckling interact, but they can occur in either order, depending on stiffener and plate proportions. Tripping failure is regarded as collapse because once tripping occurs the plate is left with no stiffening and overall buckling follows immediately. Also elastic tripping failure is a sudden phenomenon, and therefore it is a most undesirable mode of collapse. Because the open sections that are commonly used as stiffeners in offshore panels have relatively low torsional rigidity, such panels may be susceptible to tripping, and so it is very important to consider this mode of buckling and to provide an adequate margin of safety.

FIGURE 24
Torsional/Flexural Buckling

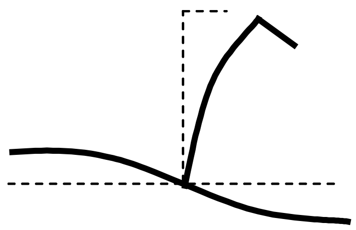

In the ABS *Buckling Guide,* the torsional-flexural buckling state limit of stiffeners is to satisfy the ultimate state limit given below:

$$\frac{\sigma_a}{\eta\sigma_{CT}} \le 1$$

where

σ_{CT} = critical torsional-flexural buckling stress with respect to the axial compression of a stiffener, including its associated plating, which is obtained from the following equations:

$$= \begin{cases} \sigma_{ET} & \text{if} \quad \sigma_{ET} \le P_r\sigma_o \\ \sigma_o\left[1-P_r(1-P_r)\dfrac{\sigma_o}{\sigma_{ET}}\right] & \text{if} \quad \sigma_{ET} > P_r\sigma_o \end{cases}$$

σ_{ET} = elastic torsional-flexural buckling stress with respect to the axial compression of a stiffener, including its associated plating with plate buckling considered.

Comparison Study

Test Database

The database consists of 359 test datasets of stiffened plates subjected to uniaxial in-plane compression and lateral pressure[49]. The compression flanges of box girders have also been included because of their close similarities to deck structures. A detailed set of assessments has been conducted using the formulae of API Bulletin 2V, DnV CN30.1 (1995) and the ABS *Buckling Guide*.

Section C3, Table 8 provides the mean and COV of modeling uncertainty of API Bulletin 2V (2000), DnV CN30.1 (1995) and the ABS *Buckling Guide* based on the test database before screening. Section C3, Figure 25 shows the distribution of modeling uncertainty after screening. The screening condition is that the stiffeners satisfy the stiffness requirement specified in 3/9.1 of the ABS *Buckling Guide*.

For all available data, the ABS *Buckling Guide* provides good predictions compared to the test database.

TABLE 8
Mean/COV of Modeling Uncertainty for Stiffened Panels Before Screening

Data Sources	*Test Number*	*API Bulletin 2V*		*DnV CN30.1*		*ABS Buckling Guide*	
		Mean	*COV*	*Mean*	*COV*	*Mean*	*COV*
Tanaka & Endo 1988	10	1.1862	0.0710	1.5923	0.2008	1.2308	0.0880
Horne et al, 1976,1977	33	1.0169	0.2024	1.1918	0.1354	0.9221	0.1226
Faulkner, 1977	43	0.9254	0.1871	1.1772	0.2489	0.8907	0.1253
Niho, 1978	7	1.0615	0.2781	1.4719	0.3358	1.0615	0.2781
Yao, 1980	7	1.0351	0.1657	1.4678	0.1943	1.0450	0.1537
Paik & Thayamballi, 1996	10	1.3527	0.3268	2.3176	0.4175	1.3527	0.3268
Carlsen, 1980	20	0.8959	0.2066	1.3137	0.2095	0.8362	0.1961
Kondo & Ostapenko, 1983	3	1.0797	0.2118	1.1633	0.2224	0.9146	0.1079
Horne and Narayanan, 1983	4	0.9318	0.0224	0.9999	0.0223	0.9163	0.0224
Murray, 1983	9	1.0145	0.0981	1.5233	0.2199	0.9877	0.1126
Fukumoto, 1983	27	1.0356	0.1505	1.3704	0.1470	0.9927	0.1414
J P KENNY,1983	8	1.0716	0.0666	1.1204	0.0598	1.0355	0.0487
Walker & El Sharkawi, 1983	15	0.8455	0.2287	1.0441	0.2146	0.8455	0.2287
Massonnet & Maquoi, 1973	3	1.3129	0.1241	1.7058	0.2640	1.2420	0.1734
Tromp 1976	9	1.2323	0.2156	1.4894	0.2337	1.0914	0.0999
Murray,1983	18	1.0685	0.0947	2.1875	0.1189	1.0576	0.0997
Bell et al, 1983	11	1.3420	0.1843	2.1442	0.2799	1.3549	0.1852
Ghavami, 1986,1987	6	0.9589	0.1576	1.0566	0.1628	0.9589	0.1576
Cho and Song	21	0.9744	0.1978	1.2220	0.2776	0.7326	0.2331
Dorman & Dwight	12	0.9760	0.1043	1.0381	0.0547	0.9291	0.0711
Walker & El Sharkawi	16	0.9220	0.2741	1.1522	0.2570	0.9220	0.2741
Ghavami, 1986-87	9	1.0266	0.0593	1.1979	0.0576	1.0266	0.0593
Kondo & Ostapenko, 1983	2	1.1433	0.0245	1.0197	0.0582	1.1433	0.0245
Smith 1976	11	1.1068	0.1252	1.2555	0.0930	1.0422	0.1495
Dean & Dowling	3	0.5675	0.2750	0.6206	0.2464	0.5675	0.2750
Dowling et al, 1973	8	1.2490	0.4024	1.7090	0.5980	1.1154	0.1986
Total		1.0260	0.2293	1.3532	0.3496	0.9721	0.2211

FIGURE 25
Modeling Uncertainty of Stiffened Panels (Test/Prediction) After Screening

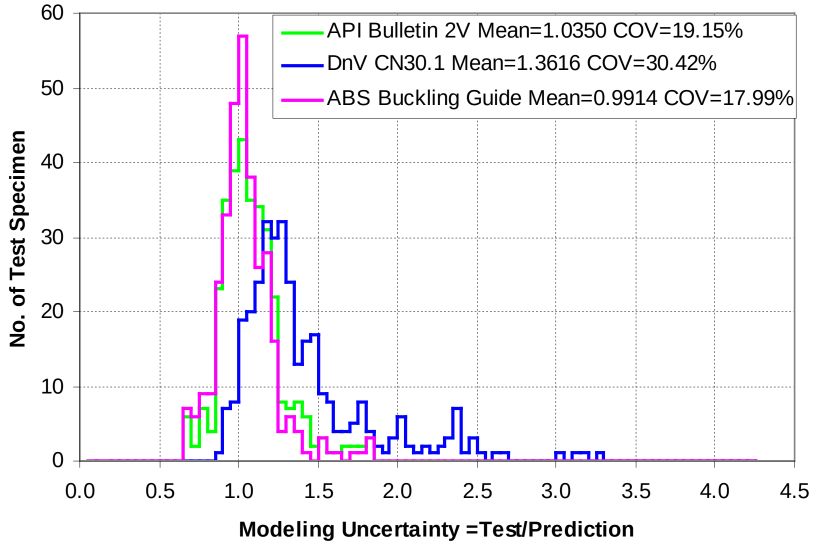

C5.5 Local Buckling of Web, Flange and Face Plate

<No Commentary>

C7 Girders and Webs

<No Commentary>

C9 Stiffness and Proportions

<No Commentary>

C11 Corrugated Panels

In the ABS *Steel Vessel Rules*, three levels of failures modes are given, namely flange/web plate level, unit corrugation level and entire corrugation level.

Corrugated panels are also used as the walls of living quarters in offshore structures. In this case, the shear stress due to wind or seismic forces is to be taken into account and the entire corrugation buckling criterion including shear stress should be applied to determine the buckling strength.

C11.1 Local Plate Panels

<No Commentary>

C11.3 Unit Corrugation

The pioneering work on the ultimate strength of corrugated panels subjected to lateral pressure was performed by Caldwell[57]. He carried out an extensive theoretical and experimental study to develop a rational design formula for steel and aluminum alloy corrugated panels and suggested the following formula for unit corrugations as:

$$\sigma_{E(B)} = k_c \frac{E}{12(1-\nu^2)}\left(\frac{t}{a}\right)^2$$

where

k_c = buckling coefficient, analytically expressed by:

= $[7.65 - 0.26(c/a)^2]^2$

a = width of the compressed flange

c = width of the web

The ABS *Buckling Guide* adopted this equation as the elastic bending buckling stress. The critical bending buckling stress is written as (Johnson-Ostenfeld plasticity correction):

$$\sigma_{CB} = \sigma_{E(B)} \qquad \text{for } \sigma_{E(B)} \le P_r\sigma_0$$

$$= \sigma_0[1 - P_r(1 - P_r)]\frac{\sigma_0}{\sigma_{E(B)}} \qquad \text{for } \sigma_{E(B)} > P_r\sigma_0$$

C11.5 Overall Buckling

Easley[58] discussed formulas for the elastic buckling loads of light-gauged corrugated metal shear diaphragms. The diaphragm is typically a rectangular assembly of corrugated metal sheets, fastened together and loaded uniformly along its edge by in-plane shear forces. He suggested the following formula to calculate the elastic buckling stress:

$$\tau_E = 3.65\pi^2(D_V^{3/4}D_H^{1/4})/tL^2$$

where

D_V, D_H = equivalent bending stiffness per unit length of the diaphragm

This formula is in fair agreement with experimental results and is recommended in the ABS *Buckling Guide* associated with the Johnson-Ostenfeld plasticity correction.

Comparison Study

Corrugated Panels in Axial Compression

Due to a lack of experimental data, numerical analysis of buckling strength for the 40 actual corrugated panels was performed using the finite element analysis method. Section C3, Figure 26 shows the comparison of ABS solutions for buckling strength with the finite element results. The mean and COV of modeling uncertainty are 1.11 and 8.35%. The local flange/web buckling failure mode controlled for all cases considered in both the FE analysis and the ABS *Buckling Guide*.

FIGURE 26
Corrugated Panels in Axial Compression

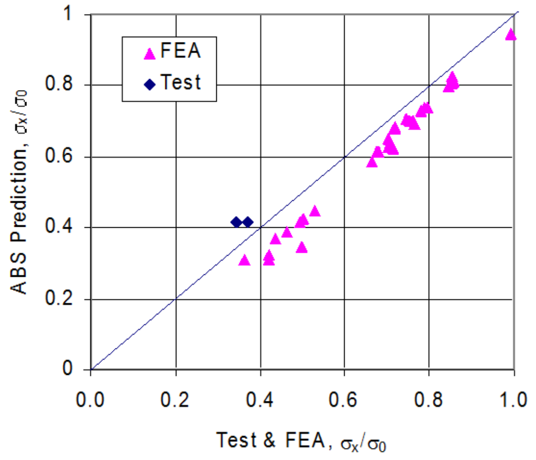

Corrugated Panels in Lateral Pressure

Section C3, Figure 27 compares the ABS solutions of buckling strength with the experimental results and FEA results available for 30 Caldwell's and Paik's models[57,59], and 18 FE models. The ABS recommended formula is conservative and the mean and COV of modeling uncertainty are 1.13 and 17.64% respectively. All cases exhibited the bending collapse due to local buckling of flange and web in the $^1/_3$ middle region of the corrugation span.

FIGURE 27
Corrugated Panels in Lateral Pressure

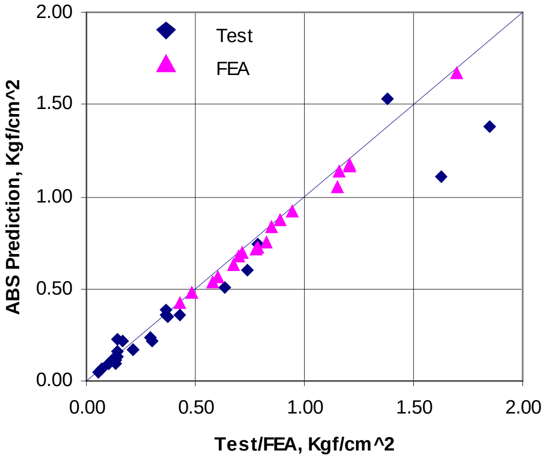

Corrugated Panels in Edge Shear

Section C3, Figure 28 presents the comparison of ABS solutions of buckling strength with the experimental results FEA results for Easley's models[58]. The FE models are created with overall length and width of the actual test specimens. The ABS recommended formula gave the mean and COV of modeling uncertainty as 1.10 and 12.62% respectively. All cases showed the overall shear buckling failure mode based on the model experiments, FEA and the ABS *Buckling Guide*.

FIGURE 28
Corrugated Panels in Edge Shear

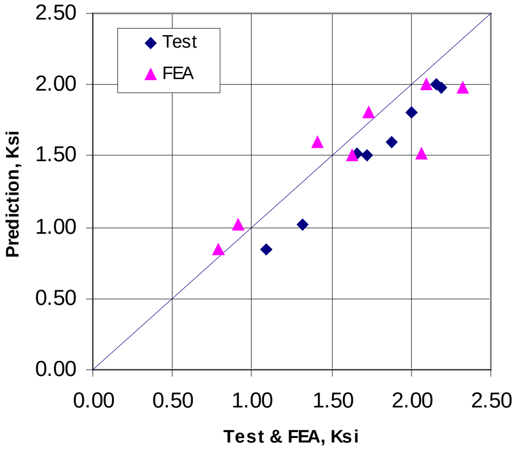

C13 Geometric Properties

<No Commentary>

SECTION C3 Appendix 1 – Examples of Buckling and Ultimate Strength Assessment of Plates and Stiffened Panels

An MS EXCEL application, entitled, *ABS-Plates and Stiffened Panels*, has been developed to facilitate the use of the ABS *Buckling Guide*. The calculation consists of three worksheets namely “Input Data”, “Output Data” and “Intermediate Results”. In the worksheet “Input data”, the input data including the Panel ID, Load case, Geometries, material parameters, Loadings and Basic factor corresponding to the specified load case are required. Once the input data are ready, a macro represented by a large button “Plates & Stiffened Panels” at the left-hand side corner is run. Buckling and ultimate strength assessment results and intermediate results can be seen in the worksheets “Output” and “Intermediate Results”. All symbols used in the spreadsheet are consistent with those in the ABS *Buckling Guide*.

Appendix C3A1, Table 1 shows several examples using Smith’s models of stiffened panels (Smith[66]).

TABLE 1
Examples of Buckling and Ultimate Strength Assessments of Stiffened Panels

	Panel ID		Smith Panels										
	Load Case		1a	1b	2a	2b	3a	3b	4a	4b	5	6	7
INPUT DATA													
General													
	Total length	L	6096	6096	6096	6096	6096	6096	1219.2	1219.2	6096	6096	6096
	Length between transverse frames	ℓ	1219.2	1219.2	1524	1524	1524	1524	1219.2	1219.2	1524	1219.2	1524
	Total Width	B	3048	3048	3048	3048	3048	3048	1016	1016	3048	3048	3048
	Width between longitudinals	s	609.6	609.6	304.8	304.8	304.8	304.8	254	254	609.6	609.6	609.6
	Plate thickness	t	8	7.87	7.72	7.37	6.38	6.4	6.43	6.4	6.43	6.32	6.3
	Length deduction to determine unsupported span	ℓ_d	0	0	0	0	0	0	0	0	0	0	0
	Specified minimum yield point of plates	σ_0	249.1	252.2	261.3	259.7	250.6	252.2	259.7	264.3	247.6	256.7	290.1
	Modulus of elasticity	E	2.06E+05	2.06E+05	2.06E+05	2.06E+05	2.06E+05	2.06E+05	2.06E+05	2.06E+05	2.06E+05	2.06E+05	2.06E+05
	Poisson's ratio	ν	0.3	0.3	0.3	0.3	0.3	0.3	0.3	0.3	0.3	0.3	0.3
Longitudinals and Stiffeners													
	Type (0= No Check, 1=Flat Bar, 2=T-bar, 3=Angle bar, 4=Bulb plate)		2	2	2	2	2	2	2	2	2	2	2
	Web height	d_w	153.67	152.4	115.57	114.3	77.72	77.22	76.71	76.96	116.08	76.2	115.06
	Web thickness	t_w	7.21	7.11	5.44	5.38	4.52	4.65	4.85	4.55	5.33	4.55	5.16
	Flange width	b_f	78.99	76.2	45.97	44.7	25.91	27.94	27.69	26.16	46.23	27.43	45.21
	Flange thickness	t_f	14.22	14.22	9.53	9.53	6.35	6.35	6.35	6.35	9.53	6.35	9.53
	Smaller outstanding dimension	b_1	39.5	38.1	22.99	22.35	12.96	13.97	13.85	13.08	23.12	13.72	22.61
	Specified minimum yield point	σ_0	253.7	252.3	253.1	263.3	246.8	247.3	252.5	257.3	244.9	255.2	303.3
Transverse Webs or Girders													
	Type (0= No Check, 1=Flat Bar, 2=T-bar, 3=Angle bar, 4=Bulb plate)		2	2	2	2	2	2	0	0	2	2	2
	Web height	d_w	257.56	254	204.98	203.71	156.21	153.92	0	0	154.18	114.55	153.92
	Web thickness	t_w	9.37	9.14	8.31	8.33	6.81	6.88	0	0	6.76	5.36	6.65
	Flange width	b_f	125.48	127	102.62	102.62	78.99	79.25	0	0	77.22	46.23	78.74
	Flange thickness	t_f	18.29	18.29	16.26	16.26	14.22	14.22	0	0	14.22	9.53	14.22
	Smaller outstanding dimension	b_1	62.74	63.5	51.31	51.31	39.495	39.625	0	0	38.61	23.115	39.37
	Specified minimum yield point	σ_0	249.1	252.2	261.3	259.7	250.6	252.2	0	0	247.6	256.7	290.1

TABLE 1 (continued)
Examples of Buckling and Ultimate Strength Assessments of Stiffened Panels

Loading												
Plating's maximum stress in longitudinal direction	σ_{xmax}	190.304	184.179	239.421	218.539	170.292	150.853	207.05	213.559	176.328	125.048	197.145
Plating's minimum stress in longitudinal direction	σ_{xmin}	190.304	184.179	239.421	218.539	170.292	150.853	207.05	213.559	176.328	125.048	197.145
Plating's maximum stress in transverse direction	σ_{ymax}	0	0	0	0	0	0	0	0	0	0	0
Plating's minimum stress in transverse direction	σ_{ymin}	0	0	0	0	0	0	0	0	0	0	0
Plating's Shear stress	τ	0	0	0	0	0	0	0	0	0	0	0
Lateral pressure on plating	q	0	0.103	0.048	0	0.021	0	0	0.055	0	0	0
Axial stress on stiffeners	σ_a	190.304	184.179	239.421	218.539	170.292	150.853	207.05	213.559	176.328	125.048	197.145
Lateral pressure on stiffeners	q_s	0	0.103	0.048	0	0.021	0	0	0.055	0	0	0
Maximum Allowable Utilization Factor	η	1	1	1	1	1	1	1	1	1	1	1
ASSESSMENT RESULTS												
Unity Check												
Plate's Buckling (3.2.1)		**1.35**	**1.35**	**1.04**	**0.97**	**0.82**	**0.72**	**0.9**	**0.92**	**1.94**	**1.42**	**2.26**
Plate's ultimate strength (3.2.2)		**1.25**	**1.21**	**1.00**	**0.94**	**0.81**	**0.71**	**0.87**	**0.89**	**1.38**	**0.97**	**1.43**
Lateral pressure (3.2.3)		**N/A**	**0.72**	**0.17**	**N/A**	**0.06**	**N/A**	**N/A**	**0.13**	**N/A**	**N/A**	**N/A**
Beam-column buckling of longitudinals (3.3.1)		**1.04**	**1.14**	**1.15**	**0.87**	**1.02**	**0.67**	**0.85**	**1.18**	**1.19**	**0.93**	**1.19**
Torsional flexible buckling of longitudinals (3.3.2)		**0.88**	**0.86**	**1.01**	**0.92**	**0.79**	**0.69**	**0.89**	**0.91**	**1.04**	**1.05**	**1.09**
Web local buckling of longitudinals (3.3.3)		**N/A**	**N/A**	**N/A**	**N/A**	**N/A**	**N/A**	**N/A**	**N/A**	**N/A**	**N/A**	**N/A**
Flange local buckling of longitudinals (3.3.3)		**N/A**	**N/A**	**N/A**	**N/A**	**N/A**	**N/A**	**N/A**	**N/A**	**N/A**	**N/A**	**N/A**
Stiffness and Proportion Checks												
Stiffness of longitudinals (3.5.1)		**Pass**	**Pass**	**Pass**	**Pass**	**Pass**	**Pass**	**Pass**	**Pass**	**Pass**	**Pass**	**Pass**
Stiffness of transverse girders (3.5.2)		**Pass**	**Pass**	**Pass**	**Pass**	**Fail**	**Fail**	**N/A**	**N/A**	**Pass**	**Pass**	**Pass**
Web proportion of longitudinal (3.5.4)		**Pass**	**Pass**	**Pass**	**Pass**	**Pass**	**Pass**	**Pass**	**Pass**	**Pass**	**Pass**	**Pass**
Flange proportion of longitudinal (3.5.3)		**Pass**	**Pass**	**Pass**	**Pass**	**Pass**	**Pass**	**Pass**	**Pass**	**Pass**	**Pass**	**Pass**
Web proportion of transverse frame (3.5.4)		**Pass**	**Pass**	**Pass**	**Pass**	**Pass**	**Pass**	**N/A**	**N/A**	**Pass**	**Pass**	**Pass**
Flange proportion of transverse frame (3.5.3)		**Pass**	**Pass**	**Pass**	**Pass**	**Pass**	**Pass**	**N/A**	**N/A**	**Pass**	**Pass**	**Pass**

TABLE 1 (continued)
Examples of Buckling and Ultimate Strength Assessments of Stiffened Panels

INTERMEDIATE RESULTS													
Plates													
	Aspect ratio	α	2	2	5	5	5	5	4.8	4.8	2.5	2	2.5
	Slenderness ratio	β	2.65	2.71	1.41	1.47	1.67	1.67	1.4	1.42	3.29	3.41	3.63
	Stress ratio in direction one	K_1	1	1	1	1	1	1	1	1	1	1	1
	Stress ratio in direction one	K_2	1	1	1	1	1	1	1	1	1	1	1
	Elastic shear buckling stress	τ_E	223.41	216.2	721.91	657.93	493.05	496.14	657.22	651.11	136.13	139.43	130.68
	Elastic buckling stress in direction one	σ_{E1}	140.95	136.41	525.02	478.5	358.58	360.83	524.48	519.6	91.06	87.97	87.41
	Elastic buckling stress in direction two	σ_{E2}	60.06	58.13	154.87	141.15	105.77	106.44	129.77	128.56	33.42	37.49	32.08
	Critical shear buckling stress	τ_C	121.6	122.07	143.3	141.74	134.49	135.35	141.73	144.01	106.92	110.4	115.97
	Critical buckling stress in direction one	σ_{C1}	140.95	136.41	230.09	225.87	208.57	209.89	228.84	232.03	91.06	87.97	87.41
	Critical buckling stress in direction two	σ_{C2}	60.06	58.13	154.87	141.15	105.77	106.44	129.77	128.56	33.42	37.49	32.08
	Effective width in direction one	s_e	373.15	366.72	279.31	273.72	255.99	255.99	233.02	231.61	314.38	305.37	289.41
	Effective width in direction two	ℓ_e	406.4	406.4	304.8	304.8	304.8	304.8	254	254	508	406.4	508
	Ultimate strength in shear	τ_U	128.87	129.78	144.47	143.01	136.08	136.95	143.05	145.39	116.92	122.77	130.26
	Ultimate strength in direction one	σ_{U1}	152.48	151.72	239.45	233.22	210.47	211.81	238.25	241	127.69	128.59	137.73
	Ultimate strength in direction two	σ_{U2}	92.49	92.13	154.87	141.15	105.77	106.44	129.77	128.56	68.81	79.44	75.23
	Coefficient in strength interaction eq.	φ	-0.33	-0.36	0.3	0.27	0.17	0.17	0.3	0.29	-0.64	-0.7	-0.82
	Von Mises equivalent stress	σ_e	190.3	184.18	239.42	218.54	170.29	150.85	207.05	213.56	176.33	125.05	197.15
	Ultimate strength under lateral pressure	q_u	N/A	0.14	0.28	N/A	0.34	N/A	N/A	0.41	N/A	N/A	N/A
STIFFENED PANELS													
Geometry													
	Unsupported spacing	ℓ_e	1219.2	1219.2	1524	1524	1524	1524	1219.2	1219.2	1524	1219.2	1524
	Effective width of attached plating	s_e	373.15	366.72	279.31	304.8	304.8	304.8	254	254	314.38	305.37	289.41
	Sectional area of longitudinals	A_s	2231.2	2167.13	1066.79	1040.93	515.82	536.49	547.88	516.28	1059.28	520.89	1024.56
	Sectional area of longitudinals with attached plating	$A = A_s + st$	7108	6964.68	3419.85	3287.3	2460.45	2487.21	2181.1	2141.88	4979.01	4373.56	4865.04
	Effective sectional area	A_e	5216.43	5053.21	3223.07	3287.3	2460.45	2487.21	2181.1	2141.88	3080.76	2450.8	2847.84
	Effective moment of inertia	I_e	2.55E+07	2.42E+07	7.17E+06	6.93E+06	1.64E+06	1.70E+06	1.63E+06	1.56E+06	7.03E+06	1.62E+06	6.58E+06
	Radius of gyration	r_e	69.91	69.27	47.16	45.91	25.78	26.11	27.35	27.02	47.76	25.68	48.08
	Effective breadth	s_w	353.57	353.57	269.63	269.63	269.63	269.63	220.58	220.58	353.57	353.57	353.57

TABLE 1 (continued)
Examples of Buckling and Ultimate Strength Assessments of Stiffened Panels

	Effective section modulus of the longitudinal at flange	SM_w	2.06E+05	1.98E+05	6.88E+04	6.61E+04	2.06E+04	2.16E+04	2.14E+04	2.03E+04	6.94E+04	2.11E+04	6.70E+04
	St Venant torsion constant	K	9.49E+04	9.13E+04	1.95E+04	1.88E+04	4.60E+03	4.97E+03	5.28E+03	4.65E+03	1.92E+04	4.73E+03	1.83E+04
	Horizontal distance	y_0	0	0	0	0	0	0	0	0	0	0	0
	Vertical distance	z_0	119.09	117.86	83.47	82.49	52.27	52.43	51.68	51.88	84.16	51.9	83.73
	Moment of inertia about y-axis	I_y	6.13E+06	5.88E+06	1.71E+06	1.64E+06	3.75E+05	3.86E+05	3.89E+05	3.69E+05	1.71E+06	3.66E+05	1.63E+06
	Moment of inertia about z-axis	I_z	5.89E+05	5.29E+05	7.87E+04	7.24E+04	9.80E+03	1.22E+04	1.20E+04	1.01E+04	7.99E+04	1.15E+04	7.47E+04
	Polar moment of inertia	I_0	3.84E+07	3.65E+07	9.22E+06	8.79E+06	1.79E+06	1.87E+06	1.86E+06	1.77E+06	9.30E+06	1.78E+06	8.88E+06
	Parameter	I_{zf}	5.84E+05	5.24E+05	7.71E+04	7.09E+04	9.20E+03	1.15E+04	1.12E+04	9.47E+03	7.85E+04	1.09E+04	7.34E+04
	Warping constant	Γ	1.38E+10	1.22E+10	1.04E+09	9.33E+08	5.68E+07	7.01E+07	6.75E+07	5.73E+07	1.06E+09	6.46E+07	9.77E+08
Beam-column buckling													
	Axial compression stress	σ_a	190.3	184.18	239.42	218.54	170.29	150.85	207.05	213.56	176.33	125.05	197.15
	Euler's elastic buckling stress	$\sigma_{E(C)}$	6677.96	6557.42	1944.72	1843.53	581.43	596.01	1021.84	997.34	1994.64	900.94	2021.86
	Critical buckling stress	σ_{CA}	248.29	249.9	250.48	251.98	224.05	225.75	242.27	246.02	239.68	238.99	282.7
	Bending moment	M	0.00E+00	7.78E+06	2.83E+06	0.00E+00	1.24E+06	0.00E+00	0.00E+00	1.73E+06	0.00E+00	0.00E+00	0.00E+00
	Bending stress	σ_b	0	39.33	41.15	0	60.07	0	0	85.3	0	0	0
	Moment adjustment coefficient	C_m	0.75	0.75	0.75	0.75	0.75	0.75	0.75	0.75	0.75	0.75	0.75
Torsional-flexible buckling													
	Elastic torsional-flexible buckling stress	σ_{ET}	4.29E+02	4.07E+02	7.36E+02	6.89E+02	4.30E+02	4.50E+02	6.28E+02	5.95E+02	1.91E+02	1.19E+02	1.84E+02
	Number of half-waves	n	1	1	2	2	3	3	3	3	1	2	1
	Critical torsional-flexible buckling stress	σ_{CT}	215.46	214.67	236.92	237.1496	214.96	217.47	232.48	234.79	170.25	118.59	180.98
Stiffness and proportions													
	Designed moment of inertia of longitudinals	I_w	2.50E+07	2.40E+07	7.10E+06	6.72E+06	1.60E+06	1.66E+06	1.58E+06	1.52E+06	7.24E+06	1.65E+06	6.93E+06
	Required moment of inertia of longitudinals	i_0	6.82E+05	6.47E+05	1.83E+06	1.61E+06	8.99E+05	9.15E+05	7.51E+05	7.30E+05	4.92E+05	2.63E+05	4.61E+05
	Designed moment of inertia of girders	I_G	8.41E+07	8.12E+07	3.28E+07	3.18E+07	1.40E+07	1.36E+07			1.83E+07	5.98E+06	1.82E+07
	Required moment of inertia of girders	I_s	1.07E+07	1.01E+07	2.93E+07	2.57E+07	1.44E+07	1.46E+07			3.93E+06	4.12E+06	3.69E+06

Units: Length – [mm], Area – [mm^2], Sectional Modulus – [mm^3], Sectional Moment of Inertia – [mm^4], St. Venant torsional constant – [mm^6], Force – [N], Bending Moment – [N-mm], Stress and Pressure – [N/mm^2]

SECTION C3 Appendix 2 – Design Code Examples and Comparisons

This Appendix contains two examples, one dealing with a Spar structure is next; comparisons of results using the ABS *Buckling Guide* and DnV CN 30.1 are presented. The other example is a converted FPSO in C3A2/3. In the latter example, comparsions between the ABS *Buckling Guide* and the SafeHull Criteria meant for ship structure are given.

1 Spar

Appendix C3A2, Figure 1 provides examples of buckling and ultimate strength assessments for plate panels and stiffened panels used in a Spar design. All plate panels satisfy the ultimate strength criterion. The results of ultimate strength assessment for plates from the ABS *Buckling Guide* and DnV CN30.1 are remarkably close.

FIGURE 1
Design Practice of Spar

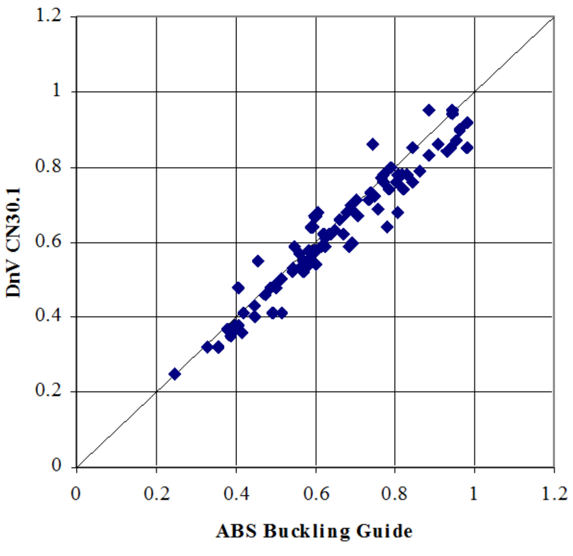

(a) Ultimate Strength of Plate Panels

FIGURE 1 (continued)
Design Practice of Spar

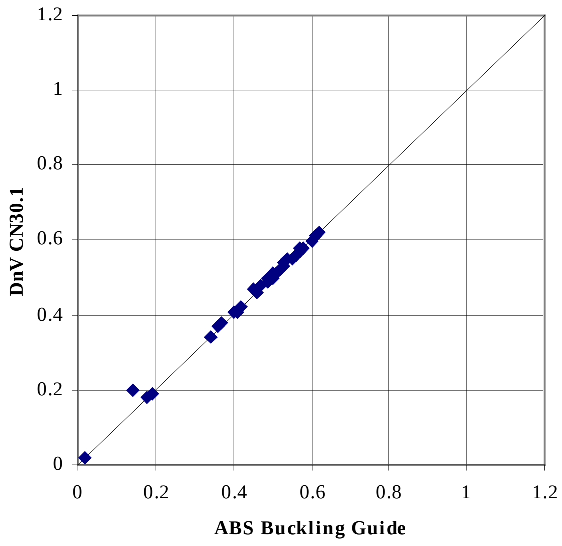

(b) Uniform Lateral Pressure of Plate Panels

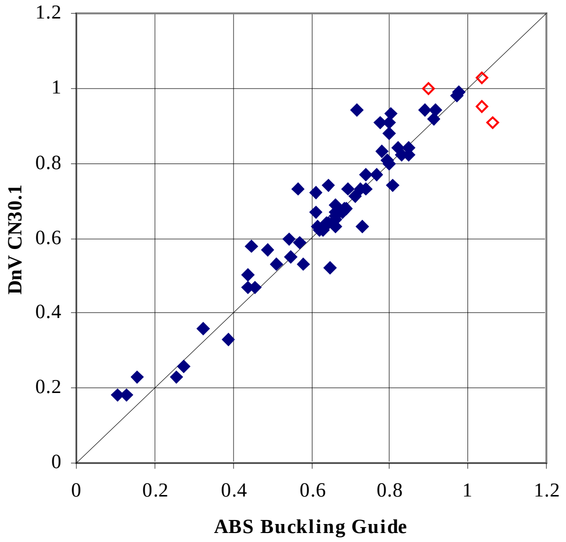

(c) Buckling Strength of Stiffened Panels

One stiffener does not satisfy the beam-column buckling requirement of the ABS *Buckling Guide*, whereas two stiffeners do not pass the beam-column buckling criteria of DnV CN 30.1. Because the stiffeners are very deep bulb plates, many stiffeners do not satisfy web proportion requirements. In this case, the local web buckling is to be assessed. It was found that there are two stiffeners that cannot pass the local web buckling requirement. But if the bulb plates are regarded as equivalent angle bars, as the designer did under DnV CN30.1, all stiffeners fulfill the web proportion requirement and no local web buckling check is necessary. As mentioned before, in order to avoid possible local web buckling, the application of bulb plates with deep webs should be very carefully considered.

3 Converted FPSO

In current industry practice, the buckling and ultimate strength assessment for primary hull structures of an FPSO system receives the ship approach and its topside structures should satisfy the requirements from the offshore approach (Valenzuela et al[72]). The main differences of the two approaches are illustrated in Appendix C3A2, Table 1.

TABLE 1
Main Differences between Ship Approach and Offshore Approach

	Ship Approach	*Offshore Approach*
Scantling	Net scantling Nominal design corrosion values should be deducted from the design/as-gauged thickness.	Gross Scantling No deduction due to corrosion damage is considered and the actual design/as-gauged thickness is used.
Allowable Utilization Factor	Allowable utilization factor = 1. The material reduction factor is to be considered according to steel grade.	Allowable utilization factor is always less than 1, depending on vessel loading patterns, loading types and failure consequence. For plates and stiffened panels, the allowable utilization factor is 0.6 for static or normal operation condition and 0.8 for combined or severe storm condition. The material reduction factor is not considered.
Design Loads	The design loads are based on 20-year return period. β-Factors are introduced to reflect the 100-years design load requirements for FPSOs.	The design loads are based on 100-years return period.

The comparison between the two approaches is carried out to exhibit the differences of each failure mode of stiffened panels in a converted FPSO based on ABS SafeHull and ABS *Buckling Guide*. The main principal particulars of the FPSO is given in Appendix C3A2, Table 2.

TABLE 2
Main Principal Particulars of the Converted FPSO

Length overall, L	334.0 m
Length between perpendiculars, L_{BP}	320.0 m
Breadth molded, B	54.5 m
Depth molded, D	27.0 m
Design draft, T	21.4 m
Block coefficient, C_B	0.83
Steel grade	Mild

To determine the global response of the hull structures, a 3-hold FE model of the hull structure within 0.4L was created. Net scantling that is the deduction of as-gauged thickness and nominal corrosion value was used in the model. The β-factors corresponding to 100-years return period at the intended service site were calculated and the total loads of the 18 SafeHull standard load cases were automatically applied to the 3-hold model by SafeHull system. The von Mises stress contour to Load Case No. 2 obtained from SafeHull system is illustrated graphically in Appendix C3A2, Figure 2. The summary of buckling and ultimate strength assessment for the FPSO is shown in Appendix C3A2, Figure 3.

FIGURE 2
Von Mises Stress Contour and Deflection of Load Case No.2

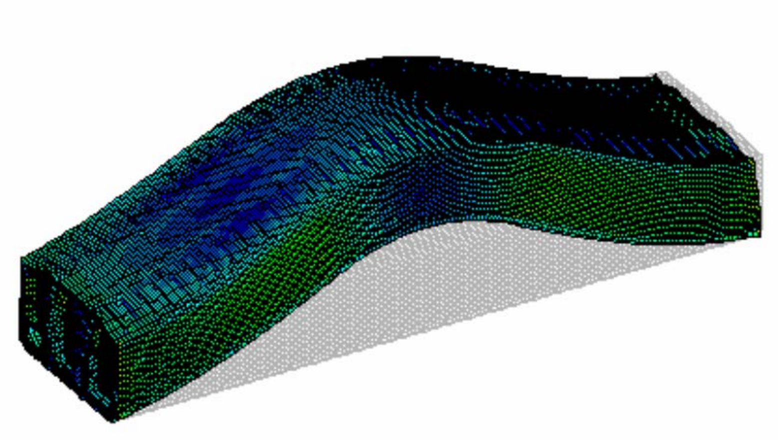

In order to transfer the global stress response from net scantling model to gross scantling model, it is assumed that the total internal forces and bending moment for each plate panel and stiffener are kept constant. Therefore, the transformed stresses can be approximately written by:

i) *For Plate Panels:*

$$\sigma_{xG} = \frac{\sigma_{xN} t_N}{t_G}$$

$$\sigma_{yG} = \frac{\sigma_{yN} t_N}{t_G}$$

$$\tau_{xyG} = \frac{\tau_{xyN} t_N}{t_G}$$

ii) *For Stiffeners:*

$$\sigma_{aG} = \frac{\sigma_{aN} A_N}{A_G}$$

where

σ_{xG}, σ_{yG}, τ_{xyG} = stresses on plate panels associated with gross thickness

σ_{xN}, σ_{yN}, τ_{xyN} = stresses on plate panels associated with net thickness

σ_{aG} = longitudinal stress on stiffener associated with gross thickness

σ_{aN} = longitudinal stress on stiffener associated with net thickness

t_N, A_N = net thickness of plate panels and net area of stiffeners

t_G, A_G = gross thickness of plate panels and gross area of stiffeners

FIGURE 3
Summary of Buckling and Ultimate Strength Assessment from SafeHull

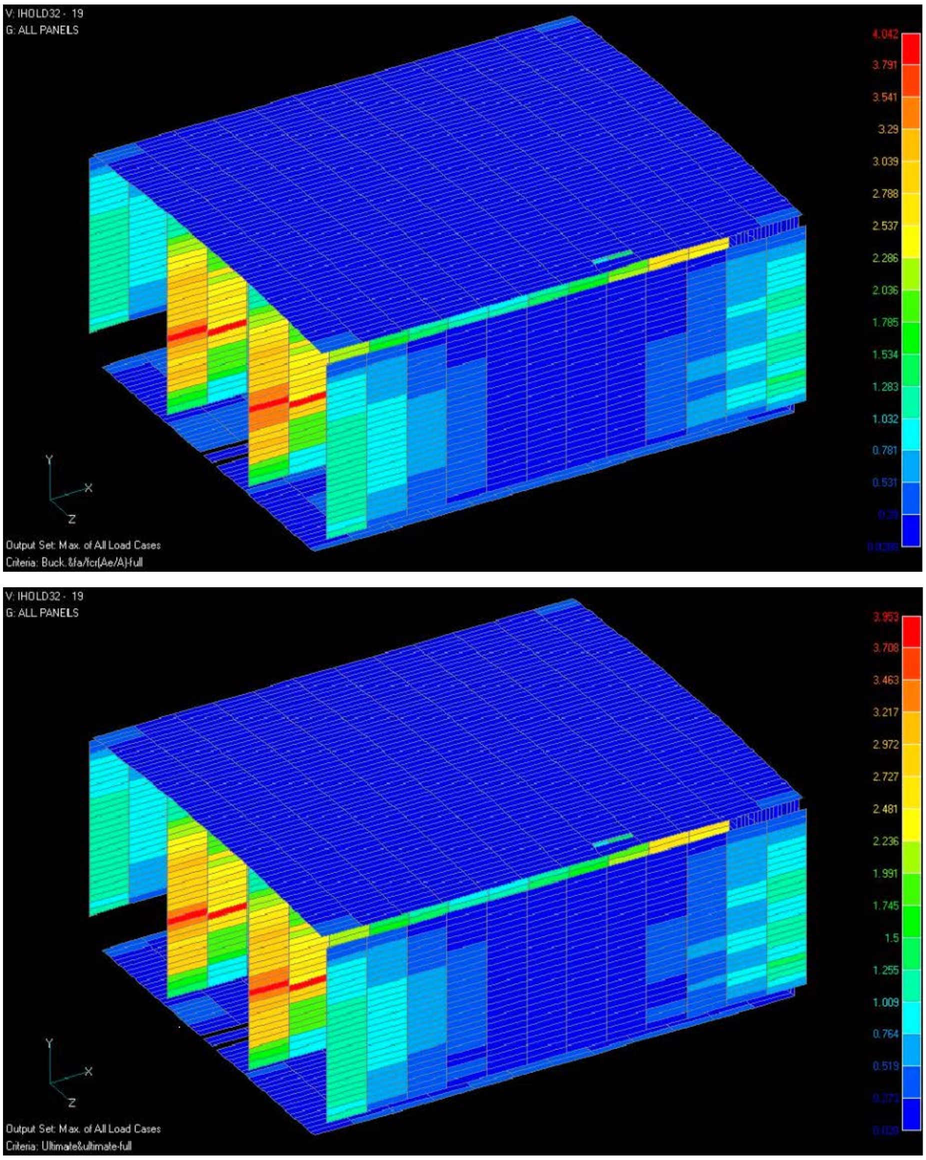

Appendix C3A2, Figures 4-7 provide the comparison of buckling and ultimate strength assessment based on the ABS SafeHull and ABS *Buckling Guide*. The horizontal axis is the ratio of corresponding unity check equation values from the ABS SafeHull and ABS *Buckling Guide*. The vertical axis represents the percentage of the buckling and ultimate strength assessment based on *Offshore Guide*. The allowable utilization factor is taken at 0.8 in compliance with 100-years return period of design loads.

FIGURE 4
Comparison between SafeHull Approach and the ABS Buckling Guide: Deck Panels

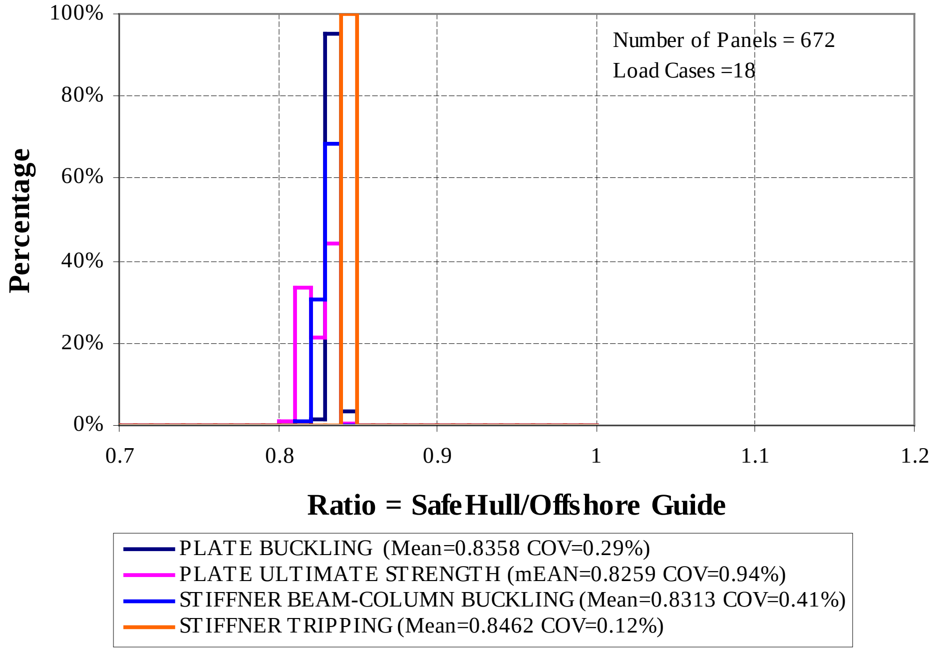

FIGURE 5
Comparison between SafeHull Approach and the ABS Buckling Guide: Bottom Panels

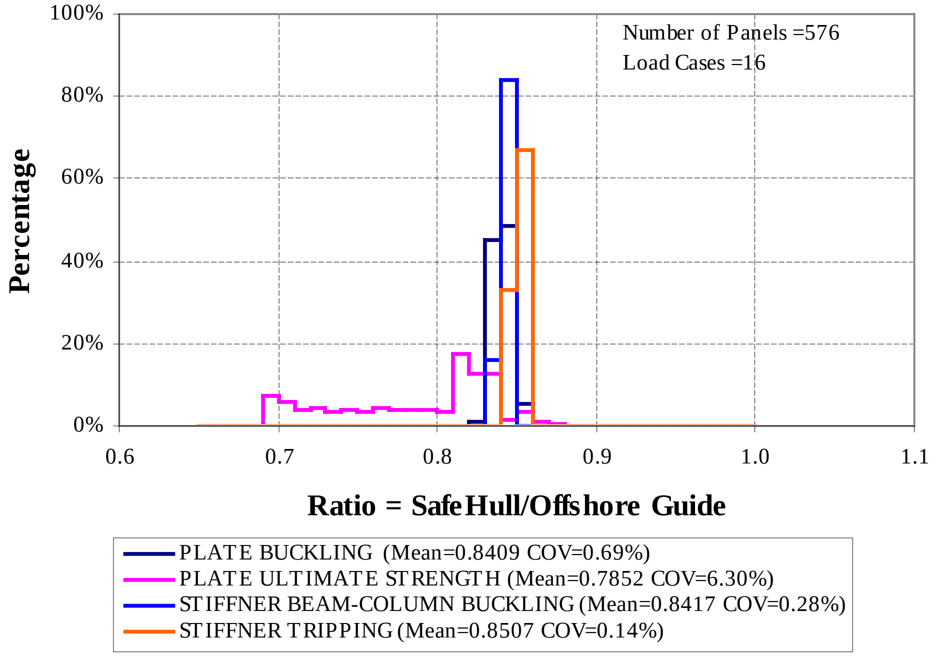

FIGURE 6
Comparison between SafeHull Approach and the ABS Buckling Guide: Longitudinal Bulkhead Panels

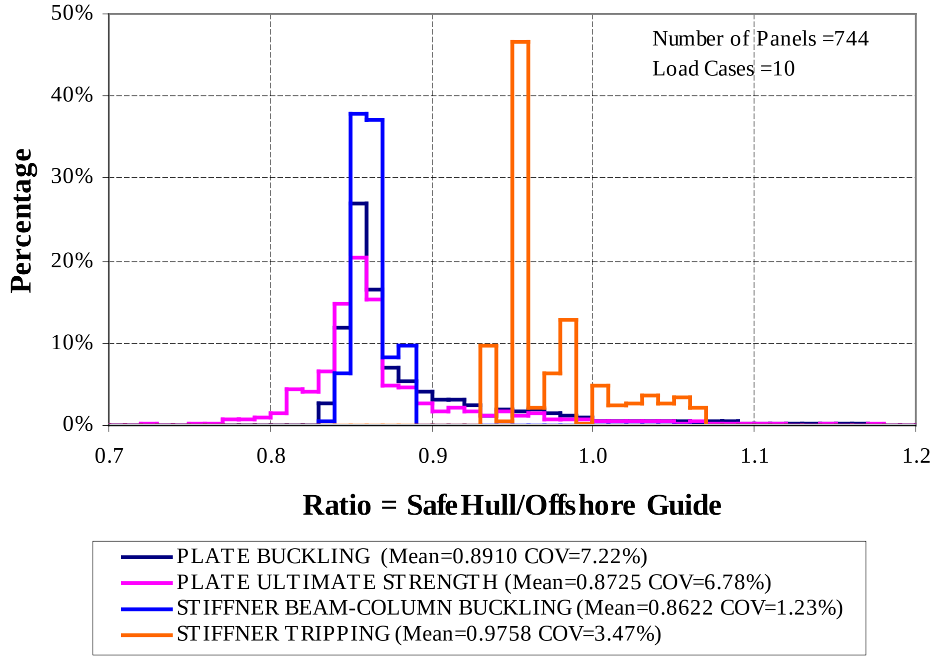

FIGURE 7
Comparison between SafeHull Approach and the ABS Buckling Guide: Side Shell Panels

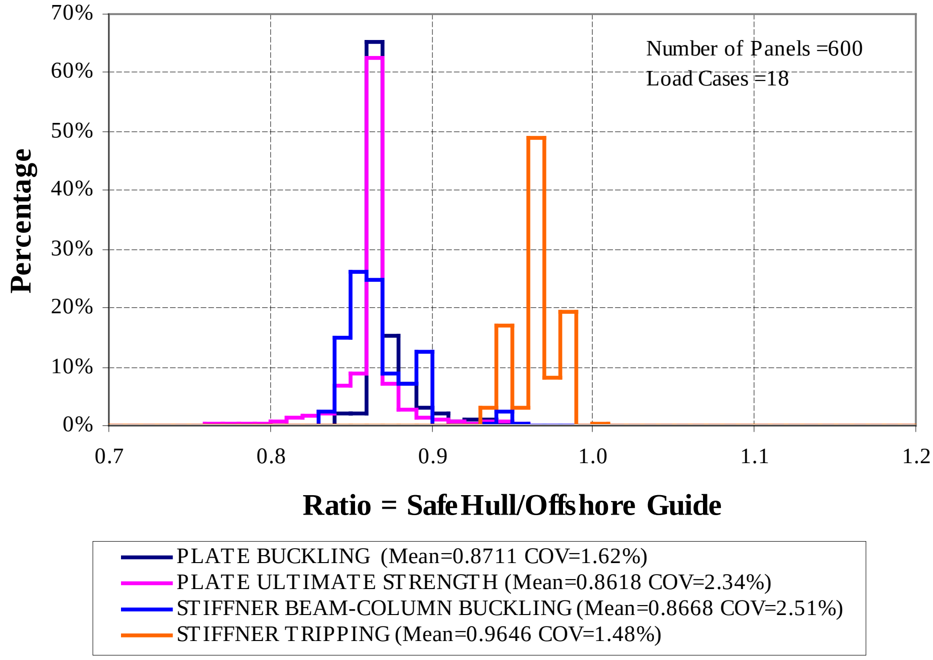

Some observations from the present comparison study are given below:

i) The ratio of plate buckling for the deck panels and bottom plates is very stable, lying between 0.83 and 0.85.

ii) The small slenderness ratio (β = 1.16) of bottom panels, and stress ratio entering into the shaded region on the panels cause the ratio of plate ultimate strength is relative small compared with others, as shown in Appendix C3A2, Figure 8.

FIGURE 8
Ultimate Strength Interaction Curves of Bottom Plate Panels

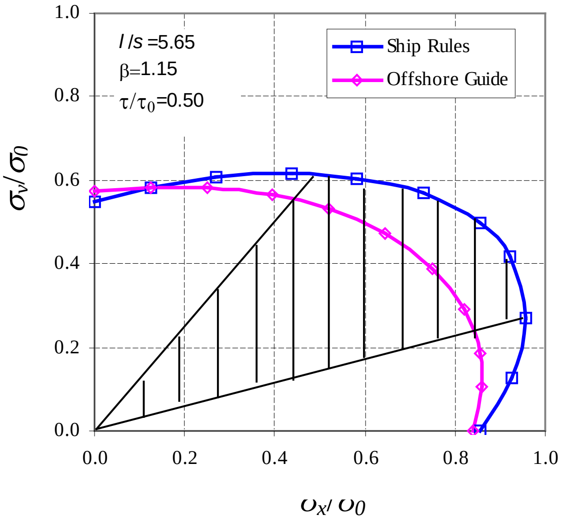

i) The buckling and ultimate strength ratios are significantly affected by the fraction of nominal design corrosion value to nominal design thickness. Therefore, they are distributed more widely for side structure panels and longitudinal panels because the plate thickness and stiffener types are changed frequently along vertical direction.

ii) The effect of nominal corrosion design values on tripping of angle-bars is more significant than flat bars and T-bars. This causes the tripping ratio of side shell and longitudinal bulkhead closer to 1.0.

iii) The ABS *Buckling Guide* is in general more conservative than SafeHull Approach for this converted FPSO when the SafeHull standard loads are applied.

SECTION C4 Cylindrical Shells

C1 General

A major type of compression element used in offshore structures is the fabricated steel cylindrical shell, which is stiffened against buckling by ring and/or stringer stiffeners. A very large number of theoretical and experimental studies have been performed on the buckling of cylindrical shells over many years. The increasing offshore application of stiffened cylindrical shells, especially in deep water, has raised new questions still needing to be resolved.

Ring stiffeners to strengthen a cylindrical shell are very effective against loading by external pressure. Stringer stiffeners are normally used to provide additional stiffness in axially compressed members. However, it is usual to restrain stringer-stiffened cylindrical shells circumferentially at regular intervals by use of ring stiffeners. Effectively the shell then becomes orthogonally stiffened. The shell segments between adjacent stringer stiffeners and ring stiffeners are effectively unstiffened curved panels that merit special attention. It is normal practice in offshore design to suppress buckling modes that involve buckling of the ring stiffeners, and therefore in such cases the capacities of stringer stiffeners and shell plates determine collapse.

In this section a considerable amount of experimental data on the buckling of ring and/or stringer stiffened cylindrical shells have been collected, processed and analyzed. The data have been obtained mainly from past and current offshore-related research, much of it funded at least in part by ABS. The data sources are given in Section C4, Tables 1 and 2. The diameter to thickness ratio of testing specimen is in the range of $E/(4.5\sigma_0)$ to 1000. The processed experimental data have formed the basis of extensive comparisons with the ABS *Buckling Guide* recommendations.

The buckling strength assessment procedures for unstiffened or ring stiffened cylindrical shells and ring and stringer stiffened cylindrical shells are shown in Section C4, Figures 1 and 2. The procedures have been incorporated into an MS EXCEL application developed by OTD, ABS Technology.

TABLE 1
Test Database for Ring-stiffened Cylindrical Shells (Das[38])

Sources	*Axial Compression*	*External Pressure*	*Combined Loadings*	*Total*
Dowling, P J & Harding, J E[73]	3			3
Sridharan, P. & Walker, A.C[74]	7			7
Odland, J[75]	9			9
Miller, C D[76]	4		23	27
Mitsubishi Heavy Industries, 1982	8			8
Miller, C D[77]	27			27
Kendrick, S B[78]		35		35
Miller, C D & Kinra, R K[79]		14		14
Miller, C D et al[80]			7	7
Total	58	49	30	137

TABLE 2
Test Database for Ring and Stringer Stiffened Cylindrical Shells (Das[38])

Sources	*Sponsor*	*Axial Compression*	*External Pressure*	*Combined Loadings*	*Total*
Imperial College/ University of Surrey	---	3	3	3	3
Imperial College	---	2	-	4	2
Shell Oil Co.	---	1	-	2	1
I Imperial College	UK Dept. of En.	6	-	-	6
University College	UK Dept. of En.	18	-	-	18
Glasgow University	UK Dept. of En.	3	-	-	3
C.B.I./G.U.-Phase I	Conoco/ABS	14	8	22	14
C.B.I.-Phase II	Conoco/ABS	1	1	4	1
Total		48	12	35	48

C1.1 Geometry of Cylindrical Shells

The criteria given in this section apply to equally spaced ring and/or stringer stiffened cylindrical shells with the diameter to thickness ratio in the range of $E/(4.5\sigma_0)$ to 1000. Stiffeners in a given direction are to be equally spaced, parallel and perpendicular to panel edges, and have identical material and geometric properties. General types of stiffener profiles, such as flat bar, T-bar, L-bar, and bulb plates, may be used. The material properties of the stiffeners may be different from those of the shell plating.

C1.3 Load Application

<No Commentary>

C1.5 Buckling Control Concepts

In the design of ring and/or stringer stiffened cylindrical shells, one should keep in mind that there are five failure modes including local shell plate buckling, local stiffener flexural-torsional buckling, bay or inter-ring buckling level, general instability, and beam-column buckling; the higher level of failure usually leads more severe consequence than the preceding level. Therefore suitable scantling proportions between shell plates, rings and stringers are necessary to better assure the safety of ring and/or stringer stiffened cylindrical shells.

Theoretically, the resistance of a cylindrical shell decreases after the bifurcation point is reached, so the buckling strength is equal to the ultimate strength of the cylindrical shell, as shown in Section C4, Figure 3. However, initial imperfections have a detrimental effect on load-carrying capacity due to the very unstable postbuckling behavior of cylindrical shells. Therefore initial imperfections should be monitored carefully during fabrication, assembly and installation.

FIGURE 1
Flowchart for Buckling Strength Assessment: Unstiffened or Ring Stiffened Cylindrical Shells

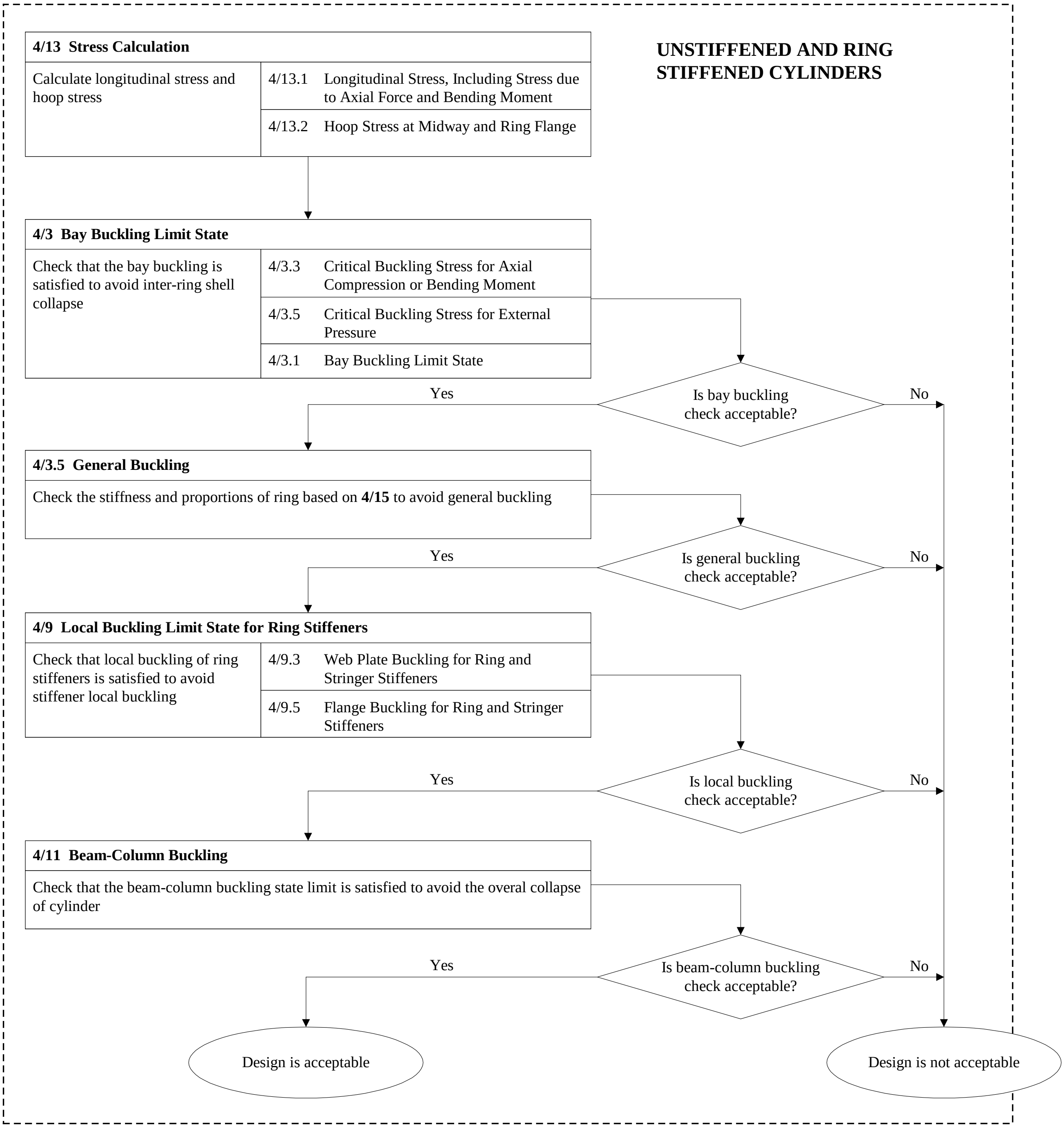

FIGURE 2
Flowchart for Buckling Strength Assessment: Ring and Stringer Stiffened Cylindrical Shells

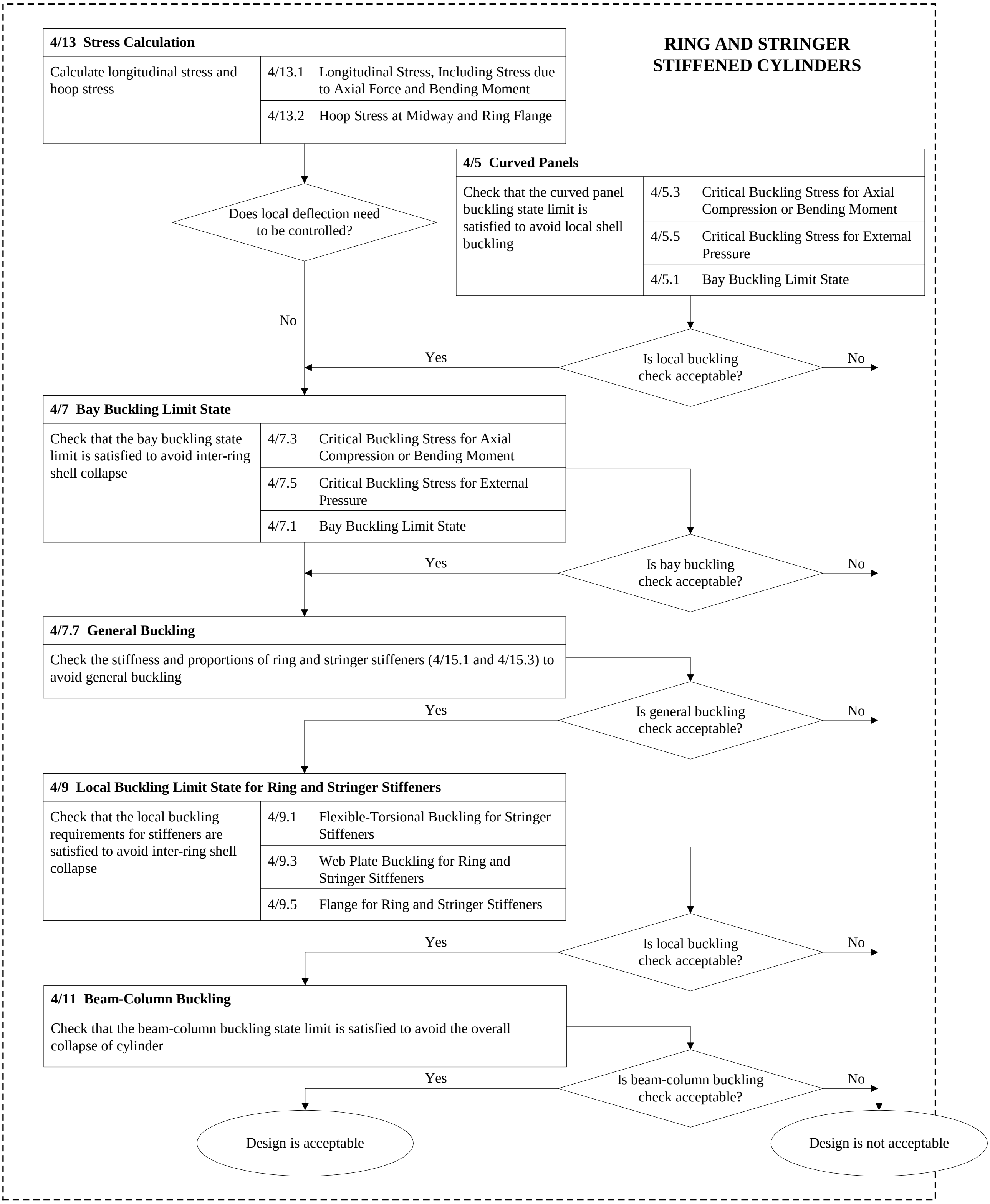

FIGURE 3
Buckling and Postbuckling Behavior of Cylindrical Shells

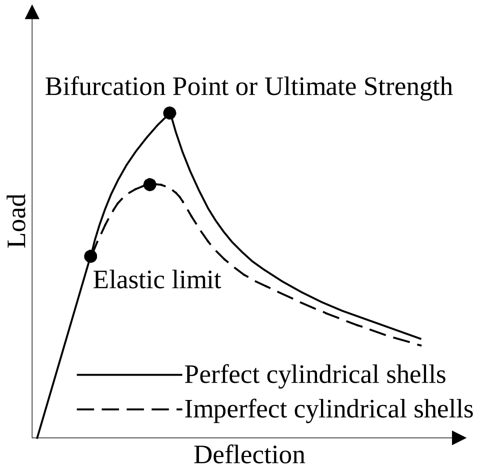

C1.7 Adjustment Factors

The adjustment factors for the allowable basic utilization factor in the existing offshore codes are provided in Section C4, Table 3.

TABLE 3
Adjustment Factors

	Local Shell Buckling	*Stringer Tripping*	*Inter-Ring or Bay Buckling*	*General Instability*	*Beam-Column Buckling*
ABS Buckling Guide	$\psi = 0.833$ if $\sigma_{Ci} \le 0.55\sigma_0$ $= 0.629 + 0.371\sigma_{Ci}/\sigma_0$ if $\sigma_{Ci} > 0.55\sigma_0$	$\psi = 1.0$	Taking the same form as local buckling	$\psi = 1.0$	$\psi = 0.87$ if $\sigma_{EA} \le P_r\sigma_0$ $= 1 - 0.13\sqrt{P_r\sigma_0 / \sigma_{EA}}$ if $\sigma_{EA} > P_r\sigma_0$
ABS MODU/ SPM Rules	N/A	$\psi = 1.0$	N/A	N/A	$\psi = 0.87$ if $\sigma_{EA} \le 0.5\sigma_0$ $= 1/(1 + 0.15\sqrt{0.5\sigma_0 / \sigma_{EA}})$ if $\sigma_{EA} > 0.5\sigma_0$
API RP 2A WSD/API Bulletin 2U	$\psi = 0.8333$ if $\sigma_{Ci} \le 0.55\sigma_0$ $= \dfrac{1}{1.444 - 0.444\left(\dfrac{\sigma_0}{\sigma_{Ci}}\right)}$ if $\sigma_{Ci} > 0.55\sigma_0$	$\psi = 1.0$	Taking the same form as local buckling	Taking the same form as local buckling	$\psi = 0.87$ if $\sigma_{EA} \le 0.5\sigma_0$ $= \dfrac{1}{1 + 0.1588\left(\dfrac{\sigma_0}{\sigma_{EA}}\right)^{0.5} - 0.0529\left(\dfrac{\sigma_0}{\sigma_{EA}}\right)^{1.5}}$ if $\sigma_{EA} > 0.5\sigma_0$
DnV MOU Rules	$\psi = 1.0$ if $\sigma_{EA} \ge 25\sigma_0$ $= 1.050 - 0.250\sqrt{\sigma_0 / \sigma_{EA}}$ if $\sigma_0 < \sigma_{EA} \le 25\sigma_0$ $= 0.8$ if $\sigma_{EA} \le \sigma_0$	$\psi = 1.0$	Taking the same form as local buckling	N/A	$\psi = 1.0$ if $\sigma_{EA} \ge 25\sigma_0$ $= 1.025 - 0.125\sqrt{\sigma_0 / \sigma_{EA}}$ if $\sigma_0 < \sigma_{EA} \le 25\sigma_0$ $= 0.9$ if $\sigma_{EA} \le \sigma_0$

C3 Unstiffened or Ring Stiffened Cylinders

A ring stiffened (and unstiffened) cylindrical shell is the most prevalent type of compression element used in steel jacket platforms. The recommended buckling criteria for ring stiffened cylindrical shells are described in this subsection along with some background and comparisons with other Design Codes.

C3.1 Bay Buckling State Limit

The intebraction equation for bay buckling of an unstiffened or ring stiffened cylindrical shell subjected to combined axial compression, bending and external pressure is in the form consistent with the ultimate strength interaction equation for plate panels in the ABS *Buckling Guide*. The equation is given by:

$$\left(\frac{\sigma_x}{\eta\sigma_{CxR}}\right)^2 - \varphi_R\left(\frac{\sigma_x}{\eta\sigma_{CxR}}\right)\left(\frac{\sigma_\theta}{\eta\sigma_{C\theta R}}\right) + \left(\frac{\sigma_\theta}{\eta\sigma_{C\theta R}}\right)^2 \le 1$$

where

σ_x = compressive stress in longitudinal direction

σ_θ = compressive stress in circumferential direction

φ_R = interaction coefficient, which is related to the critical buckling stresses in the two directions and specified minimum yield point and taken as the same as the one given in API Bulletin 2U[5].

Comparison Study

The database consists of 30 test datasets. Section C4, Table 4 provides the statistical characteristics of the modeling uncertainty and Section C4, Figure 4 shows the distribution of modeling uncertainty based on the formulae of API Bulletin 2U, DnV CN30.1 and the ABS *Buckling Guide*.

TABLE 4
Modeling Uncertainty of Bay Buckling: Combined Loading

	API Bulletin 2U	*DnV CN30.1*	*ABS Buckling Guide*
Mean	1.1074	1.4317	1.1362
COV	16.32%	19.52%	14.63%

FIGURE 4
Modeling Uncertainty of Bay Buckling: Combined Loading

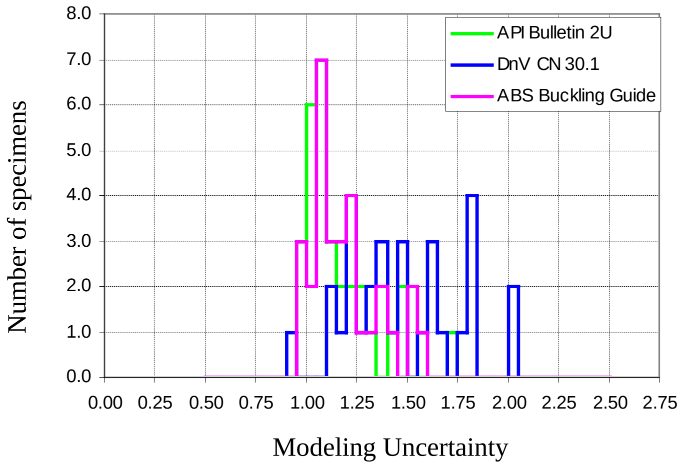

C3.3 Critical Buckling Stress for Axial Compression or Bending Moment

In the ABS *Buckling Guide*, the critical buckling stress formulation of ring stiffened cylindrical shells subjected to axial compression or bending moment is consistent with that in the ABS *Steel Vessel Rules* and Section 3 of the ABS *Buckling Guide* for flat plates; i.e.:

$$\sigma_{CxR} = \begin{cases} \sigma_{ExR} & for \quad \sigma_{ExR} \le P_r \sigma_0 \\ \sigma_0 \left[1 - P_r (1 - P_r) \dfrac{\sigma_0}{\sigma_{ExR}} \right] & for \quad \sigma_{ExR} > P_r \sigma_0 \end{cases}$$

where

P_r = material linear elastic proportional limit. The correction for plasticity is based on Johnson-Ostenfeld method.

σ_{ExR} = elastic buckling stress of cylindrical shells based on Faulkner et al[81], in which the effects of shell length and shape imperfections are taken into account.

Comparison Study

The database consists of 21 available test datasets. Section C4, Table 5 gives the statistical characteristics of the modeling uncertainty and Section C4, Figure 5 shows the distribution of modeling uncertainty based on API Bulletin 2U, DnV CN30.1 and the ABS *Buckling Guide*.

TABLE 5
Modeling Uncertainty of Bay Buckling: Axial Compression

	API Bulletin 2U	*DnV CN30.1*	*ABS Buckling Guide*
Mean	1.1074	1.4317	1.1362
COV	16.32%	19.52%	14.63%

FIGURE 5
Modeling Uncertainty of Bay Buckling: Axial Compression

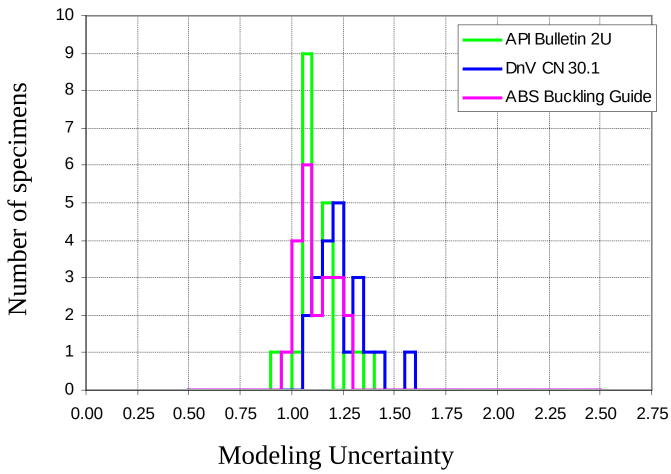

C3.5 Critical Buckling Stress for External Pressure

In the ABS *Buckling Guide*, the critical buckling stress of ring-stiffened cylindrical shell subjected to external pressure is similar to that in API Bulletin 2U and is taken as:

$$\sigma_{C\theta R} = \Phi \sigma_{E\theta R}$$

where

Φ = plasticity reduction factor obtained directly from test data for non stress relieved cylinders, and also adopted by API Bulletin 2U. Johnson-Ostenfeld or Merchant-Rankine correction for plasticity was tested, but the error from the correction was unacceptable compared to the test results

$\sigma_{E\theta R}$ = elastic buckling stress of a cylindrical shell, in which the effects of shape imperfections are taken into account and the corresponding knock-down factor is taken at 0.8 to meet the fabrication tolerance

Comparison Study

The database consists of 49 test datasets. Section C4, Table 6 gives the statistical characteristics of the modeling uncertainty, and Section C4, Figure 6 gives the distribution of modeling uncertainty based on API Bulletin 2U, DnV CN30.1 and the ABS *Buckling Guide*.

TABLE 6
Modeling Uncertainty of Bay Buckling: External Pressure

	API Bulletin 2U	*DnV CN30.1*	*ABS Buckling Guide*
Mean	1.0596	0.9839	1.0546
COV	9.65%	12.19%	9.28%

FIGURE 6
Modeling Uncertainty of Bay Buckling: External Pressure

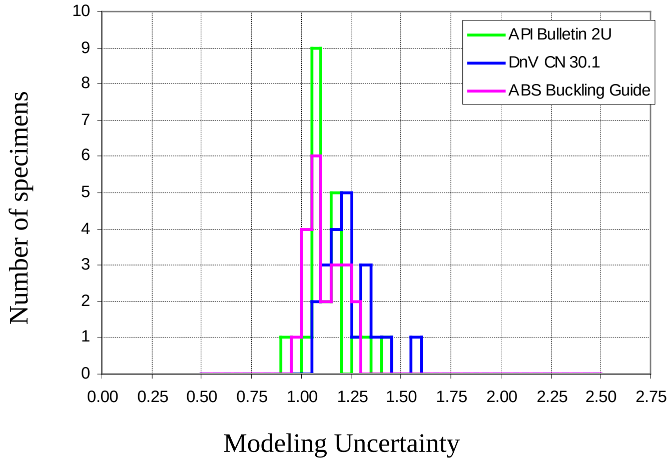

C3.7 General Buckling

The general buckling of a ring stiffened cylindrical shell involves the collapse of one or more ring stiffeners together with shell plating and should be avoided due to the catastrophic consequences. The ring stiffeners are to be proportioned in accordance with Subsection 4/15 of the ABS *Buckling Guide* to preclude the general buckling failure mode.

The stiffness requirement has been verified to be conservative (Ellinas, C P et al[62]).

ASME and API Bulletin 2U have recommended that the critical buckling stress of general buckling is to be greater than the critical inter-ring buckling stress multiplied by a factor of 1.2. This may not always lead to a safe design, as the factor may need to be higher to avoid possible interaction between inter-ring buckling and general instability (Ellinas, C P et al[62]).

C5 Curved Panels

This mode is characterized as shell plate buckling between adjacent stiffeners such that the shell plate/stiffener junctions remain straight. The stress at which the shell plate develops initial buckling is dependent on its slenderness ratio (s/t) and aspect ratio (ℓ/s) and therefore upon the number of ring and stringer stiffeners and shell thickness as well as the stiffness of the stiffeners. Generally for low slenderness ratios (many stringer stiffeners), the shell plate can be approximated as a flat plate and is expected to have stable initial postbuckling behavior. For a high slenderness ratio, the postbuckling behavior is unstable.

Local curved panel buckling in ring and stringer stiffened cylindrical shells will not necessarily lead to complete failure of the shell because stresses can be redistributed to the remaining effective section associated with the stringer stiffness. The knowledge of the local buckling behavior is necessary to control the local deflection for serviceability requirements, and to determine the sections to be considered effective in the buckling strength of the complete ring and stringer stiffened shells.

C5.1 Buckling State Limit

In the ABS *Buckling Guide*, the interaction equation for the buckling of curved panel between adjacent stiffeners of a ring and stringer stiffened cylindrical shell subjected to combined loading is consistent with the interaction equation for plate panels in Section 3 of the ABS *Buckling Guide*. It is also similar to the one given in API Bulletin 2U. The equation is written by:

$$\left(\frac{\sigma_x}{\eta\sigma_{CxP}}\right)^2 - \varphi_P\left(\frac{\sigma_x}{\eta\sigma_{CxP}}\right)\left(\frac{\sigma_\theta}{\eta\sigma_{C\theta P}}\right) + \left(\frac{\sigma_\theta}{\eta\sigma_{C\theta P}}\right)^2 \le 1$$

where

σ_x = compressive stress in longitudinal direction

σ_θ = compressive stress in circumferential direction

φ_P = interaction coefficient, which is related to the critical buckling stresses in the two directions and the specified minimum yield strength, and it is the same as given in API Bulletin 2U.

Comparison Study

The database consists of 35 test datasets. Section C4, Table 7 gives the statistical characteristics of the modeling uncertainty and Section C4, Figure 7 shows the distribution of modeling uncertainty based on API Bulletin 2U, DnV CN30.1 and the ABS *Buckling Guide*.

As stated earlier, local buckling of curved panels between adjacent stringers and ring stiffeners does not necessarily cause the complete failure of the stiffened shell. From the available test data for ring and stringer stiffened cylindrical shells under combined loadings, it is expected that all three methods predict local panel critical buckling stress less than the actual collapse stress, and there will be a large scatter of the modeling uncertainty.

TABLE 7
Modeling Uncertainty of Local Buckling: Combined Loadings

	API Bulletin 2U	*DnV CN30.1*	*ABS Buckling Guide*
Mean	1.8607	2.0570	1.5523
COV	45.18%	47.96%	35.15%

FIGURE 7
Modeling Uncertainty of Local Buckling: Combined Loading

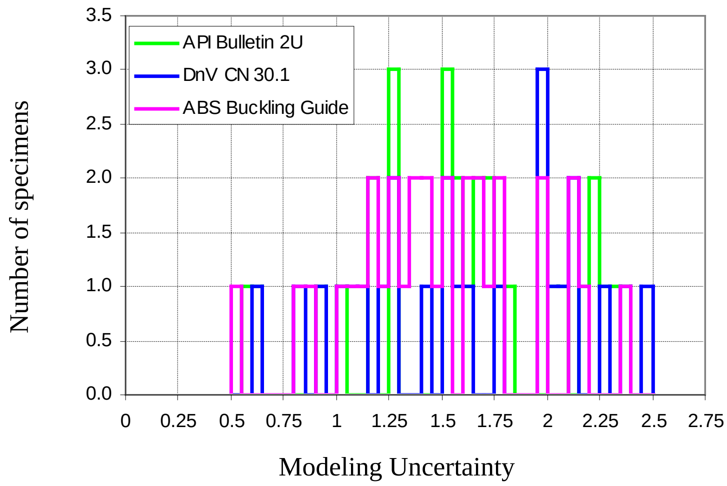

C5.3 Critical Buckling Stress for Axial Compression or Bending Moment

In the ABS *Buckling Guide*, the critical buckling stress formula for curved panels subjected to axial compression or bending moment is consistent with that for flat plates in the ABS *Steel Vessel Rules* and Section 3 of the ABS *Buckling Guide*, i.e.:

$$\sigma_{CxP} = \begin{cases} \sigma_{ExP} & for \quad \sigma_{ExP} \le P_r\sigma_0 \\ \sigma_0\left[1 - P_r(1-P_r)\dfrac{\sigma_0}{\sigma_{ExP}}\right] & for \quad \sigma_{ExP} > P_r\sigma_0 \end{cases}$$

where

P_r = material linear elastic proportional limit. The correction for plasticity is based on the Johnson-Ostenfeld method.

σ_{ExP} = elastic buckling stress of imperfect curved panel, in which model bias and the effect of shape imperfections are taken into account

= $B_{xP}\rho_{xP}\sigma_{CExP}$

σ_{CExP} = classical buckling stress for a perfect curved panel between adjacent stringer stiffeners

ρ_{xP} = nominal, or lower bound, knock-down factor to account for shape imperfections

Comparison Study

The database for ring and stringer stiffened shells subjected to axial compression contains 48 test datasets. Section C4, Table 8 gives the statistical characteristics of the modeling uncertainty, and Section C4, Figure 8 shows the distribution of modeling uncertainty.

TABLE 8
Modeling Uncertainty of Local Buckling: Axial Compression

	API Bulletin 2U	*DnV CN30.1*	*ABS Buckling Guide*
Mean	1.1452	1.2163	1.0823
COV	15.07%	27.60%	22.70%

FIGURE 8
Modeling Uncertainty of Local Buckling: Axial Compression

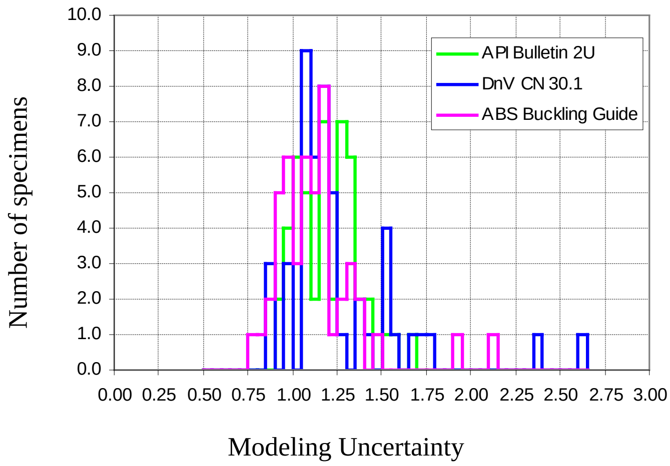

All three methods provide critical buckling stress less than the collapse stress, which is reasonable because local shell buckling doesn't lead to the complete collapse of the stiffened shells.

C5.5 Critical Buckling Stress under External Pressure

In the ABS *Buckling Guide*, the critical buckling stress of curved panels between adjacent stiffeners of ring and stringer stiffened cylindrical shell subjected to external pressure is taken as:

$$\sigma_{C\theta P} = \Phi \sigma_{E\theta P}$$

where

Φ = plasticity reduction factor

$\sigma_{E\theta P}$ = elastic buckling stress of imperfect curved panel

The local buckling pressure of a curved panel of ring and stringer stiffened cylinders can be obtained from the same equation as ring stiffened cylinders when the minimum number of buckling waves is not less the half number of stringers. The effect of fabrication imperfections is ignored due to the stable postbuckling characteristic of curved panels subjected to external pressure.

Comparison Study

The database for ring and stringer stiffened shells subjected to external pressure contains 12 test datasets. Section C4, Table 9 gives the statistical characteristics of the modeling uncertainty, and Section C4, Figure 9 shows the distribution of modeling uncertainty.

TABLE 9
Modeling Uncertainty of Local Buckling: External Pressure

	API Bulletin 2U	*DnV CN30.1*	*ABS Buckling Guide*
Mean	1.9103	2.1404	1.9174
COV	45.49%	57.05%	45.43%

FIGURE 9
Modeling Uncertainty of Local Buckling: External Pressure

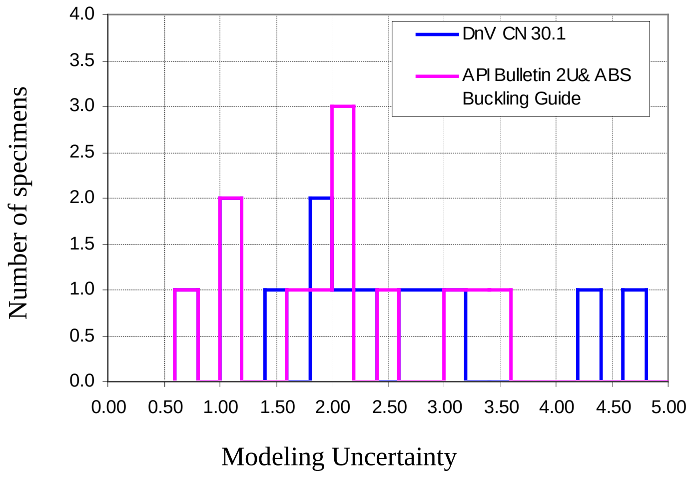

Test data demonstrate that most of the ring and stringer stiffened cylindrical shells, subjected to external pressure, continue to exhibit significant collapse resistance after local curve panels buckling. Three exceptions, whose modeling uncertainty is between 0.58 and 1.05, are cases where the ABS *Buckling Guide*'s proportioning ratio limits are not satisfied. In these cases buckling failure of the stiffener occurs prior to local curve panel buckling; thus emphasizing the importance of the proportioning criteria in the design of offshore structures.

C7 Ring and Stringer Stiffened Shells

Stringers together with ring stiffeners form the main stiffening elements of fabricated cylinders used as compression members in steel offshore structures. Bay buckling is characterized by the stringer stiffener/panel junction deflecting between the end supports or ring stiffeners. The positioning of stringer stiffeners has a significant influence on buckling behavior. Externally stiffened shells have higher buckling strength and increased imperfection sensitivity compared to their internally stiffened counterparts.

C7.1 Bay Buckling State Limit

In the ABS *Buckling Guide*, the interaction equation for the bay buckling of a ring and stringer stiffened cylindrical shell between adjacent ring stiffeners subjected to combined loading is consistent with the ultimate strength interaction equation for plate panels in Section 3 of the ABS *Buckling Guide*. It is also similar to the one in API Bulletin 2U. The equation is written as:

$$\left(\frac{\sigma_x}{\eta\sigma_{CxB}A_e/A}\right)^2 - \varphi_B\left(\frac{\sigma_x}{\eta\sigma_{CxB}A_e/A}\right)\left(\frac{\sigma_\theta}{\eta\sigma_{C\theta B}}\right) + \left(\frac{\sigma_\theta}{\eta\sigma_{C\theta B}}\right)^2 \leq 1$$

where

σ_x = compressive stress in longitudinal direction

σ_θ = compressive stress in circumferential direction

φ_B = interaction coefficient, which is related to the critical buckling stresses in the two directions and the specified minimum yield strength,

The database for ring and stringer stiffened shells subjected to combined loading contains 35 test datasets. Section C4, Table 10 gives the statistical characteristics of the modeling uncertainty, and Section C4, Figure 10 shows the distribution of modeling uncertainty.

TABLE 10
Modeling Uncertainty of Bay Buckling: Combined Loading

	API Bulletin 2U	*DnV CN30.1*	*ABS Buckling Guide*
Mean	1.2012	1.8385	1.1786
COV	0.2680	0.4132	0.1522

FIGURE 10
Modeling Uncertainty of Bay Buckling: Combined Loading

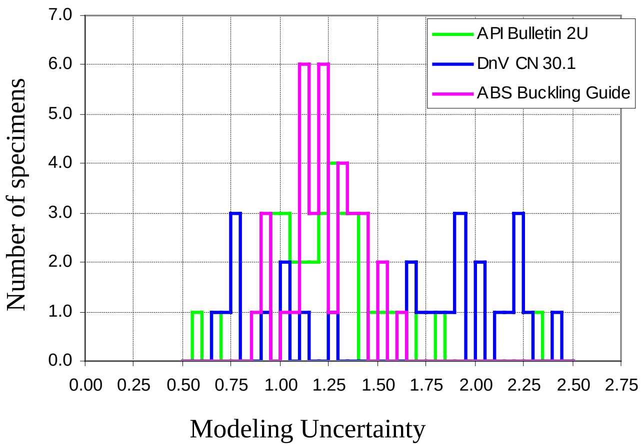

C7.3 Critical Buckling Stress for Axial Compression or Bending Moment

In the ABS *Buckling Guide*, the critical buckling stress of ring and stringer stiffened cylindrical shells subjected to axial compression or bending moment is obtained by following equation:

$$\sigma_{CxB} = \begin{cases} \sigma_{ExB} & for \quad \sigma_{ExB} \le P_r\sigma_0 \\ \sigma_0\left[1 - P_r(1 - P_r)\dfrac{\sigma_0}{\sigma_{exB}}\right] & for \quad \sigma_{ExB} > P_r\sigma_0 \end{cases}$$

where

P_r = material linear elastic proportional limit and may be taken as 0.6 for steel in accordance with ABS *Steel Vessel Rules*. The correction for plasticity is based on Johnson-Ostenfeld method. In API Bulletin 2U, the inelastic stress is calculated by the same formula and P_r is recommended to be 0.5 for non-stress relieved shells.

σ_{ExB} = elastic buckling stress of an imperfect stiffened shell, which is assumed to be the sum of the elastic buckling stress for an unstiffened shell and the elastic buckling stress of a column, in which a reduction factor of 0.75 is applied to the elastic buckling stress for unstiffened shell.

The elastic buckling stress of a column is calculated considering a column associated with the reduced effective width of shell plating, where stiffener eccentricity is negligible. The reduced effective width of shell plating is written as:

$$s_e = \frac{0.53}{\lambda_{xP}} s \qquad \text{for } \lambda_{xP} > 0.53$$

$$= s \qquad \text{for } \lambda_{xP} \le 0.53$$

where

s = shell plate width between adjacent stringers

λ_{xP} = reduced shell slenderness ratio

$$= \sqrt{\frac{\sigma_0}{\sigma_{ExP}}}$$

In API Bulletin 2U (2000), three kinds of effective width are defined, namely, reduced effective width, effective width and modified effective width. The first one is used for the calculation of an effective moment of inertia and the second is used for the effective area. In the ABS *Buckling Guide*, only the former is used to calculate both effective moment of inertia and effective area. Comparisons demonstrate that this change is reasonable. The modified effective width is the square root of the ratio of the bay's critical buckling stress to the elastic buckling stress of a curved panel, which is used to determine the final failure stress in API Bulletin 2U (2000) and the ABS *Buckling Guide*.

The database for ring and stringer stiffened shells subjected to axial compression contains 48 test datasets. Section C4, Table 11 gives the statistical characteristics of the modeling uncertainty, and Section C4, Figure 11 shows the distribution of modeling uncertainty.

TABLE 11
Modeling Uncertainty of Bay Buckling: Axial Compression

	API Bulletin 2U	*DnV CN30.1*	*ABS Buckling Guide*
Mean	1.0205	1.0127	1.0079
COV	15.22%	24.36%	15.73%

FIGURE 11
Modeling Uncertainty of Bay Buckling: Axial Compression

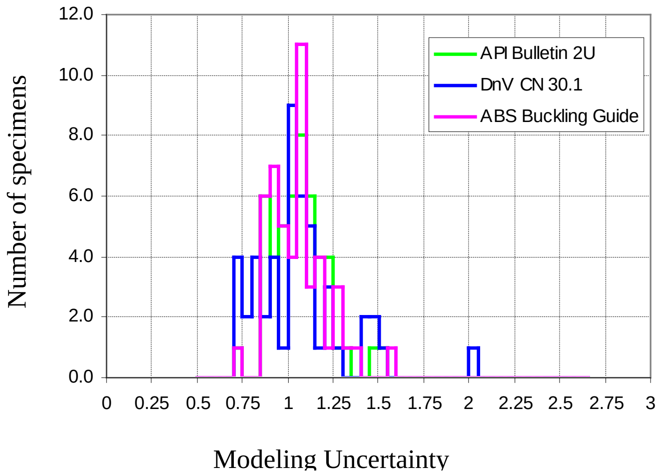

C7.5 Critical Buckling Stress for External Pressure

In the ABS *Buckling Guide*, the critical buckling stress of ring and stringer stiffened cylindrical shells subjected to external pressure is identical to that of API Bulletin 2U[5]. An improvement is that the critical buckling stress considering an unstiffened shell is used instead of its elastic buckling stress, as is done in API Bulletin 2U (2000). This replacement is reasonable; the critical stress is made up of two parts: inelastic buckling stress of an unstiffened shell and plastic collapse stress of the stringers acting compositely with effective shell plating. The sum is then modified by an effective correction factor. The formulation is written as:

$$\sigma_{C\theta B} = (\sigma_{C\theta R} + \sigma_{sp})K_p$$

where

$\sigma_{C\theta R}$ = critical buckling stress of an unstiffened shell

σ_{sp} = collapse circumferential stress of a stringer stiffener with its associated shell plating

K_p = coefficient to account for the strengthening effect of ring stiffener

The database for ring and stringer stiffened shells subjected to external pressure only contains 12 test datasets. Section C4, Table 12 gives the statistical characteristics of the modeling uncertainty, and Section C4, Figure 12 shows the distribution of modeling uncertainty.

TABLE 12
Modeling Uncertainty of Bay Buckling: External Pressure

	API Bulletin 2U	*DnV CN30.1*	*ABS Buckling Guide*
Mean	1.1781	1.4113	1.1900
COV	0.1584	0.3717	0.1745

FIGURE 12
Modeling Uncertainty Distribution of Bay Buckling: External Pressure

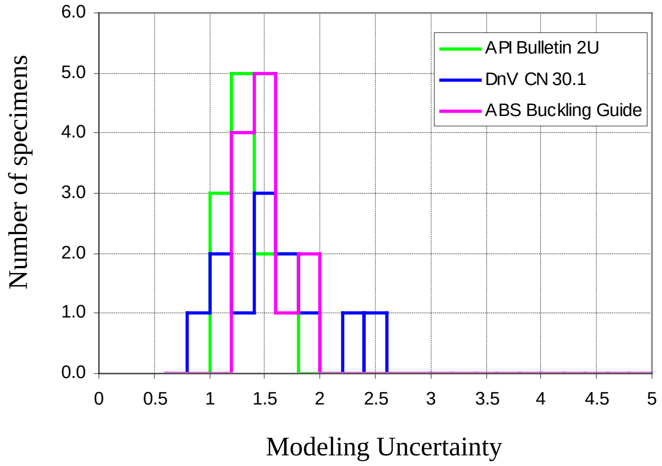

C7.7 General Buckling

The general buckling of ring and stringer stiffened cylindrical shell involves the collapse of one or more ring stiffeners together with shell plating plus stringer stiffeners. General buckling should be avoided due to catastrophic consequences. The ring and stringer stiffeners are to be proportioned in accordance with Subsection 4/15 of the ABS *Buckling Guide* to preclude the general buckling failure mode.

The stiffness requirement for a ring stiffener to prevent the general buckling failure mode is conservative (See Ellinas, C P et al[62]). ASME and API Bulletin 2U recommended that critical general buckling stress is to be greater than critical inter-ring buckling stress multiplied by a factor of 1.2. This recommendation may not always lead to a safe design, as the factor may need to be higher to avoid possible interaction between local and general stability.

The formula for the stiffness of a stringer stiffener is identical to that given in the ABS *Steel Vessel Rules*. The difference is that the stiffener spacing of stiffened panels is substituted by the shell width between adjacent stringers.

C9 Local Buckling State Limits for Ring and Stringer Stiffeners

C9.1 Torsional-Flexural Buckling

On the longitudinal axis of a stiffener around the circumference of a cylindrical shell, the torsional stiffness of a stiffener is low, but the slenderness ratio of the curved panels is relatively high. In this situation, the stiffeners can suffer torsional-flexural buckling (tripping) at a stress lower than that required for local or bay buckling. When a stiffener buckles, it loses a large part of its effectiveness to maintain the initial shape of the shell. The buckled stiffener sheds it applied load to the shell and therefore, stiffener tripping should be suppressed.

The torsional-flexural buckling state limit of stringer stiffeners is identical to that of stiffened panels in Section 3 of the ABS *Buckling Guide*. The difference is that the stiffener spacing of stiffened panel is replaced by the shell plate width between adjacent stringers. The torsional/flexural critical stress is not affected significantly by boundary conditions, but it is sensitive to the initial deflection in the form of straightness. The fabrication tolerances should be especially met in this case.

API Bulletin 2U (2000) doesn't provide this state limit. DnV CN30.1 provides a formulation similar to that used for stiffened panels with some modifications. Section C4, Figure 13 shows the comparison of modeling uncertainty for DnV CN30.1 and the ABS *Buckling Guide* with test results for ring and stringer stiffened shells subjected to axial compression.

FIGURE 13
Modeling Uncertainty of Stiffener Tripping

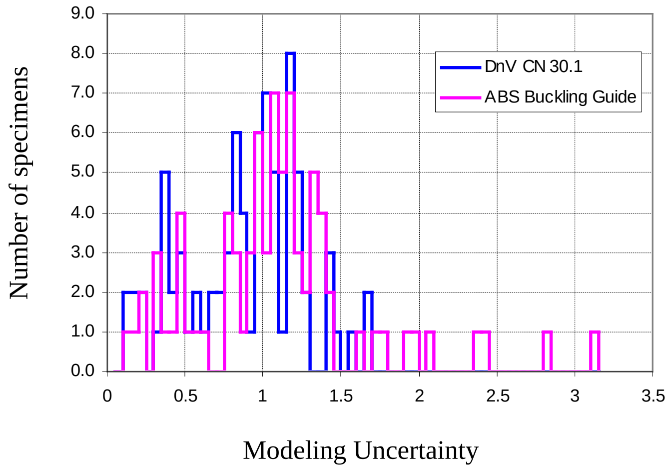

The modeling uncertainty greater than 1.5 predicted by the formula proposed in the ABS *Buckling Guide* is related to cylinders where the number of stringers is less than 24. In this case, the curved panel between adjacent stiffeners has a relatively high slenderness ratio, and the cylinder failure occurs due to the combination of local buckling of curved panels and tripping of stiffeners. The prediction is acceptable.

C9.3 Web Plate Buckling

<No Commentary>

C9.5 Faceplate and Flange Buckling

<No Commentary>

C11 Beam-Column Buckling

<No Commentary>

C13 Stress Calculations

Stiffened cylindrical shells, as main resistance components, are mainly subjected to axial compression, bending moment, external pressure and combinations of these loads. The stress due to bending moment is treated as an equivalent axial stress in the local and bay buckling assessments. The external pressure is simplified to be distributed uniformly between adjacent ring stiffeners or support ends, although it may vary in the longitudinal and circumferential directions.

C13.1 Longitudinal Stress

<No Commentary>

C13.3 Hoop Stress

The formula to evaluate the hoop stress in the ABS *Buckling Guide* is identical to that in ASME BPV[82] and BS5500[83], which is the analytical solution based on thin shell theory. It is written as:

- At midway on the shell between adjacent ring stiffeners:

$$\sigma_\theta = \frac{p(R + 0.5t)}{t} K_\theta$$

- At out edge of ring flange:

$$\sigma_{\theta R} = \frac{p(r + 0.5t)}{t} \frac{r_F}{r} K_{\theta R}$$

where K_θ and $K_{\theta R}$ are coefficients to account for the strengthening effect of ring stiffeners

The simplication of the above equation was made in API Bulletin 2U (2000) and comparison of the exact the simplified hoop stress factors was demonstrated.

DnV CN30.1 used a similar formula to evaluate the hoop stress, in which the effects of ring eccentricity and web thickness of ring are ignored. The exact solution will degenerate to the formula adopted in DnV CN30.1 when $r_R = r$ and $t_w = 0$.

C15 Stiffness and Proportions

To fully develop the intended buckling strength of the assemblies of stiffened cylindrical shells, ring and stringer stiffeners, the following criteria should be satisfied for stiffness and proportion in highly stressed regions.

C15.1 Stiffness of Ring Stiffeners

The moment of inertia of the ring stiffeners, i_r, with effective shell plating, ℓ_{eo}, is to be not less than that given by the following equation:

$$i_r = \frac{\sigma_x \delta t r_e^4}{500E\ell} + \frac{\sigma_\theta r_e^2 \ell t}{2EK_\theta}\left(1 + \frac{z_e}{100r}\frac{E}{\eta\sigma_0 - \sigma_{\theta R}}\right)$$

It has been verified that ring stiffener design based on the above formula is conservative (Ellinas, C P et al, 1984).

C15.3 Stiffness of Stringer Stiffeners

A formula identical to that given in the ABS *Steel Vessel Rules* (2003) for the stiffness check of longitudinal stiffeners is adopted in the ABS *Buckling Guide*. The moment of inertia of the stringer stiffeners, i_s, with an effective breadth of plating, s_{em}, should not be less than that given by the following equation:

$$i_o = \frac{st^3}{12(1 - \upsilon^2)}\gamma_o$$

C15.5 Proportions of Webs of Stiffeners

The ABS *Steel Vessel Rules* (2003) specified that the depth-thickness ratio of webs of stiffeners is to satisfy the limits:

$d_w/t_w \le 1.5(E/\sigma_0)^{1/2}$ for angles and tee bars

$d_w/t_w \le 0.85(E/\sigma_0)^{1/2}$ for bulb plates

$d_w/t_w \le 0.5(E/\sigma_0)^{1/2}$ for flat bars

These limits are adopted in the ABS *Buckling Guide*.

It can be seen that the ABS *Steel Vessel Rules* has less demanding for web proportion of angles and tee bars but are more demanding for bulb plates than DnV CN30.1 and API Bulletin 2U. This is reasonable because a bulb plate may be more likely to experience local buckling than a T or angle stiffener.

C15.7 Proportions of Flanges and Face Plates

The ABS *Steel Vessel Rules* (2003) specified that the breadth-thickness ratio of flanges and face plates of stiffeners should satisfy the limits:

$$b_2/t_f = 0.4(E/\sigma_0)^{1/2}$$

where b_2 is the larger outstanding dimension of flange.

This equation is adopted in the ABS *Buckling Guide*.

SECTION C4 Appendix 1 – Examples of Buckling Assessment of Stiffened Cylindrical Shells

An MS EXCEL application, entitled, *ABS-Cylindrical Shells*, has been developed to facilitate the use of the ABS *Buckling Guide*. The calculation consists of four worksheets namely "Input Data", "Output Data", "Intermediate Results-Ring" and "Intermediate Results-Stringer". In the worksheet "Input data", the input data including Cylinder ID, Load case, Geometries, material parameters, Effective length factors, Loadings and Basic utilization factor corresponding to the specified load case are required. Once the input data are ready, a macro represented by a large button "Stiffened Cylindrical Shells" at the left-hand side corner is run. Buckling strength assessment results and intermediate results can be seen in the worksheets "Output" and "Intermediate Results-Ring" for ring stiffened cylinders and "Intermediate Results-Stringer" for ring and stringer stiffened cylinders. All symbols used in the spreadsheet are consistent with those in the ABS *Buckling Guide*. Appendix C4A1, Tables 1 and 2 show several examples of tested cylinders.

TABLE 1
Examples Containing Detailed Information for Ring Stiffened Cylinders

Test Name			IC-1	1	6.1
Shell Geometry					
	Total Length(Assumed)	L	2239.50	2438.49	2522.10
	Length between ring stiffeners	ℓ	746.50	812.83	840.70
	Mean radius	r	749.70	197.20	3175.00
	Thickness	t	3.52	12.57	6.35
	Specified minimum yield stress	σ_0	281.00	301.00	276.00
	Modulus of elasticity	E	2.05E+05	2.04E+05	1.99E+05
	Poisson's ratio	ν	0.30	0.30	0.30
Ring stiffeners					
	Type of ring stiffener(0=Flat Bar, 1=Angle bar, 2=T-bar, 3=Bulb bar)		1	1	2
	Height of ring stiffener web	d_w	48.00	-78.70	95.20
	Thickness ring of stiffener web	t_w	3.52	13.28	6.35
	Width of ring stiffener flange	b_f	0.00	0.00	76.20
	Thickness ring of stiffener flange	t_f	0.00	0.00	6.35
	Smaller outstanding dimension	b_1	1.76	6.64	3.18
Stringer stiffeners					
	No. of stringer stiffeners	N_s	0	0	0
	Type of ring stiffener(0=Flat Bar, 1=Angle bar, 2=T-bar, 3=Bulb bar)		1	1	1
	Height of stringer stiffener web	d_w	0.00	0.00	0.00
	Thickness of stringer stiffener web	t_w	0.00	0.00	0.00
	Width of stringer stiffener flange	b_f	0.00	0.00	0.00
	Thickness of stringer stiffener flange	t_f	0.00	0.00	0.00
	Smaller outstanding dimension	b_1	0.00	0.00	0.00
Loading					
	Axial force	F_x	2.94E+06	0.00E+00	2.04E+05
	Bending moment	M	0.00		
	External pressure	p	0.00	15.20	0.12
	Type of pressure(1=Radial, 2=Hydrostatic)			2	1
Maximum Allowable Utilization Factor		η	1.00	1.00	1.00

Test Name			**IC-1**	**1**	**6.1**
Utilization Factors					
	Buckling of curved panels		**N/A**	**N/A**	**N/A**
	Bay buckling		**1.01**	**1.05**	**1.01**
	General buckling		**Pass**	**Pass**	**Fail**
	Torsional flexible buckling		**N/A**	**N/A**	**N/A**
	Column buckling		**N/A**	**N/A**	**N/A**
Stiffness and Proportion Checks					
	Web plate of ring stiffener		**Fail**	**Pass**	**Pass**
	Flange of ring stiffener		**N/A**	**N/A**	**Fail**
	Web plate of stringer stiffener		**N/A**	**N/A**	**N/A**
	Flange of stringer stiffener		**N/A**	**N/A**	**N/A**
Intermediate Results					
Geometry	Sectional Area	A	1.66E+04	1.56E+04	1.27E+05
	Moment of Inertia	I	4.66E+09	3.03E+08	6.38E+11
	Ring area	A_R	168.96	1045.14	1088.39
	Radius to ring flange	r_F	696.42	295.47	3070.28
	Ring space upon mean radius ratio	ℓ/r	1.00	4.12	0.26
	Mean radius upon shell thickness ratio	r/t	212.98	15.68	500.00
	Batdorf parameter	Z	201.44	254.20	33.44
Stress	Normal stress due to axial force	σ_a	177.31	0.00	1.61
	Normal stress due to bending moment	σ_b	0.00	0.00	0.00
	Stress Coefficient	K_θ	1.00	1.00	1.03
	Stress Coefficient	$K_{\theta R}$	0.62	0.53	0.56
	Modified Area of Ring	A_{RB}	181.20	689.22	1140.48
	Hoop stress at midway	σ_θ	0.00	246.01	63.79
	Hoop stress at ring flange	$\sigma_{\theta R}$	0.00	130.47	34.69
Bay Buckling					
Axial Compression	Length dependent factor	C	1.00	1.00	1.00
	Knock-down factor	ρ_{xR}	0.31	0.35	0.25
	Classical buckling stress	σ_{cexR}	582.32	7868.96	240.79
	Elastic buckling stress	σ_{exR}	179.01	2729.45	60.20
	Critical buckling stress	σ_{cxR}	175.14	293.03	60.20
External Pressure	Parameter	A_L	13.36	15.69	4.75
	Parameter	C_p	0.06	1.00	0.01
	Knock-down factor	$\rho_{\theta R}$	0.80	0.80	0.80
	Elastic buckling pressure	$p_{ce\theta R}$	0.31	44.19	0.15
	Elastic buckling hoop stress	$\sigma_{e\theta R}$	53.15	572.17	63.43
	Stress Ratio	Δ	0.19	1.90	0.23
	Critical buckling stress	$\sigma_{c\theta R}$	53.15	235.26	63.43
Combined Loading	Interaction coefficient	φ	-0.19	0.76	-0.55
General Buckling					
	Effective length	ℓ_{eo}	80.14	77.68	221.50
	Radius to centriod	r_e	740.05	220.79	3143.00
	Distance from out edge of ring to centroid of ring	z_e	40.11	61.40	72.73
	Moment of inertia of ring stiffener required	i_r	2446.65	1.42E+06	9.79E+06

TABLE 2
Examples Containing Detail Information for Ring and Stringer Stiffened Cylinders

Model Name			**IC6**	**2-1C**	**2-1B**
Shell Geometry					
	Total length(Assumed)	L	2847.36	9909.97	9919.09
	Length between ring stiffeners	ℓ	180.00	228.60	228.60
	Mean radius	r	160.00	571.40	571.10
	Thickness	t	0.84	1.96	1.97
	Specified minimum yield stress	σ_0	348.00	393.20	395.70
	Modulus of elasticity	E	2.01E+05	2.16E+05	2.18E+05
	Poisson's ratio	ν	0.30	0.30	0.30
	Effective Length Factor	K	0.30	0	0
Ring stiffeners					
	Type of ring stiffener(0=Flat Bar, 1=Angle bar, 2=T-bar, 3=Bulb bar)		1.00	1	1
	Height of ring stiffener web	d_w	26.80	60.96	60.96
	Thickness ring of stiffener web	t_w	0.84	1.91	1.96
	Width of ring stiffener flange	b_f	0.00	0.00	0.00
	Thickness ring of stiffener flange	t_f	0.00	0.00	0.00
	Smaller outstanding dimension	b_1	0.42	0.96	0.98
Stringer stiffeners					
	No. of stringer stiffeners	N_s	40.00	36	36
	Type of ring stiffener(0=Flat Bar, 1=Angle bar, 2=T-bar, 3=Bulb bar)		1.00	1	1
	Height of stringer stiffener web	d_w	13.40	30.48	30.48
	Thickness of stringer stiffener web	t_w	0.84	1.91	1.96
	Width of stringer stiffener flange	b_f	0.00	0.00	0.00
	Thickness of stringer stiffener flange	t_f	0.00	0.00	0.00
	Smaller outstanding dimension	b_1	0.42	0.96	0.98
Loading					
	Axial force	F_x	4.61E+05	0.00E+00	7.56E+05
	Bending moment	M			
	External pressure	p	0.00	0.79	0.74
	Type of pressure(1=Radial, 2=Hydrostatic)		0.00	1.00	1.00
Maximum Allowable Utilization Factor		η	1.00	1.00	1.00
Utilization Factors					
	Buckling of curved panels		**1.13**	**1.87**	**1.78**
	Bay buckling		**1.11**	**1.19**	**1.08**
	General buckling		**Pass**	**Fail**	**Fail**
	Torsional flexible buckling		**1.22**	**0.00**	**0.28**
	Column buckling		**N/A**	**N/A**	**N/A**
Stiffness and Proportion Checks					
	Web plate of ring stiffener		**Pass**	**Pass**	**Pass**
	Flange of ring stiffener		**Fail**	**Fail**	**Fail**
	Web plate of stringer stiffener		**N/A**	**N/A**	**N/A**
	Flange of stringer stiffener		**Fail**	**Fail**	**Fail**
Intermediate Results					
Geometry	Sectional Area	A	1294.70	9118.26	9205.32
	Moment of Inertia	I	1.66E+07	1.49E+09	1.50E+09
	Ring area	A_R	22.51	116.43	119.48
	Radius to ring flange	r_F	132.78	509.46	509.16
	Stringer area	A_s	11.26	58.22	59.74
	Distance from centerline of shell to the centroid of stringer	z_{st}	6.70	15.24	15.24
	Moment of Inertia of stringer stiffeners	I_{st}	1.68E+02	4.51E+03	4.63E+03
	Ring space upon mean radius ratio	ℓ/r	1.13	0.40	0.40
	Mean radius upon shell thickness ratio	r/t	190.48	292.13	290.49

Model Name			**IC6**	**2-1C**	**2-1B**
	Batdorf parameter	Z	229.97	44.60	44.40
	Stringer spacing	s	25.13	99.73	99.68
	Curvature parameter	Zs	4.48	8.49	8.44
	Parameter	g	340.12	117.81	117.81
Stress	Normal stress due to axial force	σ_a	356.00	0.00	82.11
	Normal stress due to bending moment	σ_b	0.00	0.00	0.00
	Stress Coefficient	K_θ	1.00	1.00	1.00
	Stress Coefficient	$K_{\theta R}$	0.37	0.45	0.44
	Modified Area of Ring	A_{RB}	26.97	130.40	133.82
	Hoop stress at midway	σ_θ	0.00	230.30	214.17
	Hoop stress at ring flange	$\sigma_{\theta R}$	0.00	115.67	106.53
Curved Panel Buckling					
Axial Compression	Parameter	K_{xP}	4.62	6.22	6.19
	Knock-down factor	ρ_{xP}	0.88	0.73	0.73
	Classical buckling stress	σ_{CExP}	937.36	466.41	474.16
	Slenderness ratio for compensation	λ_{xmP}	0.62	1.01	1.00
	Bias factor	B_{xP}	1.10	1.15	1.15
	Elastic buckling stress	σ_{ExP}	315.89	297.81	300.94
External Pressure	Elastic buckling pressure	$P_{CE\theta P}$	1.11	0.42	0.43
	Buckling wave number	n	20.00	18.00	18.00
	Elastic buckling stress	$\sigma_{E\theta P}$	211.15	123.32	125.61
	Critical buckling stress	$\sigma_{C\theta P}$	194.61	123.32	125.61
Combined Loading	Interaction coefficient	φ_P	-0.21	-0.37	-0.37
Bay Buckling					
Axial Compression	Knock-down factor	ρ_{xB}	0.75	0.75	0.75
	Elastic buckling stress for shell	σ_c	1088.47	3621.55	3677.73
	Reduced slenderness ratio	λ_{xP}	0.62	1.01	1.00
	Reduced effective with of shell	s_e	21.48	52.57	52.89
	Moment of Inertia of stringer stiffeners with effective width	I_{se}	5.21E+02	1.43E+04	1.46E+04
	Elastic buckling stress for column	σ_s	416.41	344.04	347.47
	Elastic buckling stress for stiffened shell	σ_{exB}	1400.77	3879.58	3938.33
	Critical buckling stress for stiffened shell	σ_{cxB}	327.25	383.64	386.16
	Modified effective width	s_{em}	24.42	77.13	77.40
	Effective cross sectional area	σ_{cxBm}	321.23	316.68	320.02
External Pressure	Parameter	AL	14.36	5.67	5.65
	Parameter	Cp	0.08	0.02	0.02
	Elastic buckling pressure	$P_{ce\theta R}$	0.36	0.41	0.42
	Elastic buckling stress	$\sigma_{e\theta R}$	54.24	96.05	97.75
	Critical buckling stress for shell	$\sigma_{c\theta R}$	54.24	96.05	97.75
	Collapse pressure of stringer stiffener associated with shell plating width	p_s	0.55	1.14	1.18
	Collapse stress of stringer stiffener associated with shell plating width	σ_s	104.65	333.52	342.78
	Effective pressure correction	Kp	0.83	0.45	0.45
	Critical buckling stress for stiffened shell	$\sigma_{c\theta B}$	131.60	193.42	198.36
Combined Loading	Interactive coefficient	φ_B	-0.02	0.20	0.22

Model Name			IC6	2-1C	2-1B
General Buckling					
Ring	Effective length	ℓ_{eo}	18.09	52.15	52.27
	Radius to centroid	r_e	151.75	554.63	554.19
	Distance from out edge of ring to centroid of ring	z_e	18.97	45.17	45.03
	Moment of inertia of ring stiffeners required	i_r	1.34E+01	1.19E+05	1.09E+05
	Moment of inertia of ring stiffener including effective length used	i_e	3.08E+03	8.99E+04	9.17E+04
Stringer	Parameter	δ	7.16	2.29	2.29
	Parameter	γ_0	296.24	28.37	28.54
	Moment of inertia of stringer required	i_o	6.74E+02	1.80E+04	1.85E+04
	Moment of inertia of stringer including effective width used	i_e	5.38E+02	1.56E+04	1.59E+04
Column Buckling					
	Slenderness Ratio	λ_{xE}	2.00	2.00	2.00
	Classical elastic buckling stress of column	$\sigma_{E(c)}$	N/A	N/A	N/A
	Critical axial or bending stress of bay	σ_{Cx}	N/A	N/A	N/A
	Reduced slenderness ratio	λ_C	N/A	N/A	N/A
	Critical buckling stress	σ_{Ca}	N/A	N/A	N/A
	Amplification factor	m	N/A	N/A	N/A
			113.14	404.04	403.83
Tripping					
	St Venant torsion constant	K	2.65	70.79	76.50
	Unsymmetrical factor	u	0.00	0.00	0.00
	parameter	m	1.00	1.00	1.00
	Horizontal distance	y_0	0.00	0.00	0.00
	Vertical distance	z_0	6.70	15.24	15.24
	Polar moment of inertia	I_0	6.74E+02	1.80E+04	1.85E+04
	Moment of inertia	I_{zf}	0.00E+00	0.00E+00	0.00E+00
	Warping constant	Γ	3.96E+01	5.48E+03	5.92E+03
	Aspect ratio	ℓ/s	7.16	2.29	2.29
	Critical buckling stress for associated plating	σ_{cL}	837.44	305.59	311.96
	Parameter	C_0	1580.06	5395.33	5532.20
	Ideal elastic buckling stress	σ_E	515.19	335.81	350.11
	Buckling wave number	n	6	2	2
	Critical buckling stress	σ_{ct}	291.58	282.70	288.37

Units: Length – [mm], Area – [mm^2], Moment of Inertia – [mm^4], force – [N], Bending Moment – [N-mm], Stress and Pressure – [N/mm^2]

SECTION C4 Appendix 2 – Design Code Examples and Comparisons

This Appendix provides two examples of buckling strength assessment for stiffened cylindrical shells.

1 Ring Stiffened Cylindrical Shell of a Spar

The cylindrical shell was originally designed based on the criteria of API Bulletin 2U (2000). Appendix C4A2, Table 1 provides the comparison of results obtained from the ABS *Buckling Guide* with API Bulletin 2U (2000).

TABLE 1
Design Example of a Ring Stiffened Cylindrical Shell

Shell				
	Total length	L	6.00E+02	
	Length between ring stiffeners	ℓ	120.00	
	Mean radius	r	119.00	
	Thickness	t	1.00	
	Specified minimum yield stress	σ_0	50.00	
	Modulus of elasticity	E	2.90E+04	
	Poisson's ratio	ν	0.30	
Ring stiffeners				
	Type of ring stiffener		2	
	Height of ring stiffener web	d_w	8.43	
	Thickness ring of stiffener web	t_w	0.43	
	Width of ring stiffener flange	b_f	11.04	
	Thickness ring of stiffener flange	t_f	0.68	
	Smaller outstanding dimension	b_1	5.31	
Loading				
	Axial force	F_x	1.35E+04	
	External pressure	p	0.02	
			API Bulletin 2U	**ABS Buckling Guide**
Maximum Allowable Utilization Factor				
	Basic factor	η	0.80	0.80
	Reduction factor for bay buckling in compression	ψ_{xB}	0.92	0.91
	Reduction factor for bay buckling in external pressure	$\psi_{\theta B}$	0.83	0.83
Stresses				
	Axial stress due to axial force	σ_a	18.01	18.01
	Hoop stress at midway	σ_θ	2.42	2.41
Critical Buckling Stresses				
	Axial compression stress		40.81	37.52
	Hoop stress		18.29	18.30

Unity Check					
	Bay buckling	**Axial Stress**		**0.61**	**–**
		Hoop Stress		**0.67**	**–**
		Bay		**–**	**0.74**
	General buckling			**Pass**	**Pass**
	Column buckling			**N/A**	**N/A**
Stiffness and Proportion Checks					
	Web plate of ring stiffener			**Pass**	**Pass**
	Flange of ring stiffener			**Pass**	**Pass**

Units: Length – [in.], force – [kips], Stress and Pressure – [ksi]

The buckling assessment results from API Bulletin 2U and the ABS *Buckling Guide* are very consistent. In the ABS *Buckling Guide*, the unity check is done by calculating the ratio of the distance from the origin to the design load point over the distance from the origin to the point on interaction curve. In API Bulletin 2U, the unity check is given by the ratio of the component stress to its allowable stress which is calculated by the critical stress divided by the factor of safety. Therefore there are two different values to represent the final results of buckling assessment in API Bulletin 2U. The ABS *Buckling Guide* result is more conservative because a smaller permissible utilization factor is used in the interaction equation in the ABS *Buckling Guide* (see Appendix C4A2, Figure 1).

FIGURE 1
Interaction Curves of API Bulletin 2U and the ABS Buckling Guide

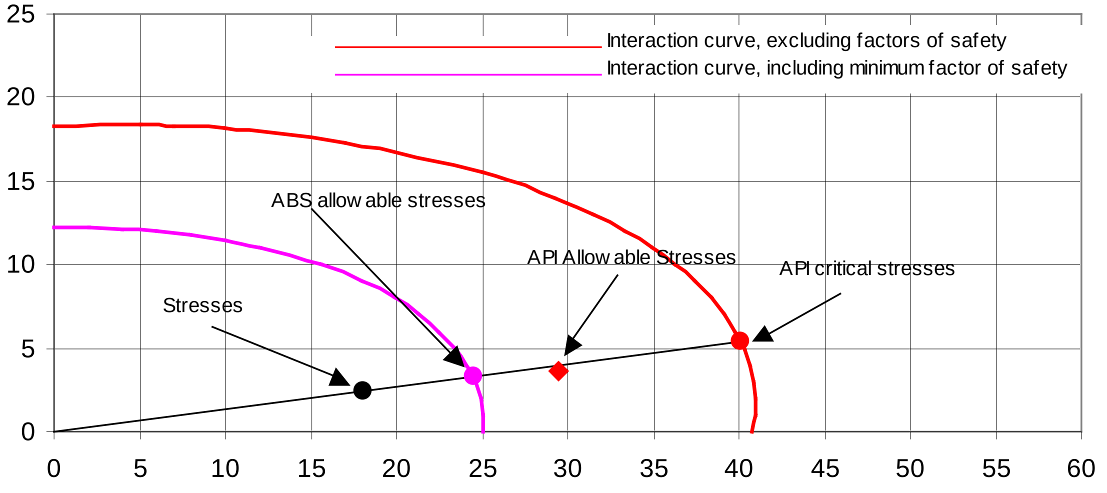

3 Examples of New API Bulletin 2U[84]

API published the Third Edition of Bulletin 2U in 2004 for the purposes of:

i) Providing buckling equations that are easier to comprehend and implement

ii) Taking advantage of more test data to develop less conservative buckling stresses closer to test data

iii) Providing sample calculations to illustrate application of equations and the sensitivity of key variables.

The examples provided in the Bulletin are used to verify the consistency between the ABS *Buckling Guide* and API Bulletin 2U (2004), which are given in Appendix C4A2, Tables 2 and 3

For the ring-stiffened cylindrical shell, the assessment results from the ABS *Buckling Guide* and API Bulletin 2U (2004) are remarkably consistent. However, bay buckling precedes local buckling for ring and stringer stiffened cylindrical shell according to API Bulletin 2U (2004). This seems unreasonable because the bay should not collapse before local panel buckling if the stiffness and proportioning requirements for the ring and stringer stiffeners have been satisfied.

TABLE 2
API Bulletin 2U (2004) Example I: Ring Stiffened Cylindrical Shell

Description				ABS Buckling Guide	API Bulletin 2U (2004)
	Normal stress due to axial force, ksi		σ_a	6.37	6.37
	Hoop stress at midway, ksi		s_q	10.68	10.67
	Hoop stress at ring flange, ksi		s_{qR}	5.31	6.13
Critical Buckling Stresses					
	Axial Critical buckling stress, ksi		σ_{CxR}	14.20	16.07
	Critical buckling stress, ksi		σ_{CqR}	18.89	19.80
Combined Loading	Interaction coefficient		j_R	-0.34	-0.28
Adjustment Factor					
	Axial compression for bay buckling		ψ_{xB}	**0.83**	**0.83**
	External pressure for bay buckling		ψ_{qB}	**0.83**	**0.83**
Unity Checks					
	Bay buckling	**Axial compression**			**1.07**
		External pressure			**1.07**
		Bay		**1.17**	
	General buckling	**Axial compression**			**0.34**
		External pressure			**0.59**
		Bay		**Pass**	
	Column buckling			**N/A**	**N/A**
Stiffness and Proportion Checks					
	Web plate of ring stiffener			**Pass**	**Pass**
	Flange of ring stiffener			**Pass**	**Pass**

TABLE 3
API Bulletin 2U (2004) Example II:
Ring and Stringer Stiffened Cylindrical Shell

Description				ABS Buckling Guide	API Bulletin 2U (2004)
Stresses	Normal stress due to axial force, ksi		σ_a	5.20	5.19
	Hoop stress at midway, ksi		σ_q	10.68	8.24
	Hoop stress at ring flange, ksi		σ_{qR}	5.31	7.48
Critical Buckling Stresses					
Curved Panels	Axial Critical buckling stress, ksi		σ_{CxP}	42.15	37.93
	Critical buckling stress, ksi		σ_{CqP}	27.30	26.2
	Interaction Coefficient			-0.24	-0.29
Bay	Axial Critical buckling stress, ksi		σ_{CxB}	48.67	47.9
	Critical buckling stress, ksi		σ_{CqB}	34.76	24.2
			φ_B	0.50	0.16
Unity Checks					
	Local Buckling	**Axial compression**			**0.46**
		External pressure			**0.73**
		Panel		**0.64**	
	Bay buckling	**Axial compression**			**0.66**
		External pressure			**0.52**
		Bay		**0.42**	
	General buckling	**Axial compression**			**0.25**
		External pressure			**0.23**
		General		**Pass**	
	Column buckling			**N/A**	**N/A**
	Flexural-torsional buckling			**0.15**	**N/A**
Stiffness and Proportion Checks					
	Stiffness of stringer			**Pass**	**Pass**
	Web plate of ring stiffener			**Pass**	**Pass**
	Flange of ring stiffener			**Pass**	**Pass**
	Web plate of stringer stiffener			**Pass**	**Pass**
	Flange of stringer stiffener			**Pass**	**Pass**

SECTION C5 Tubular Joints

C1 General

While tube-to-tube connections are not as common in floating platforms as they are in fixed steel platforms, they do represent an important structural element in jack-up legs, in particular. There are many joint configurations (e.g., T, X and K) throughout jack-up platform legs, with the most common connection type being a two brace K-joint, as illustrated in Section C5, Figure 1. It is common for these joints to have braces in two brace-chord planes (usually at 90° to each other). Additionally, for joints onto a vertical member, the leg chord is stiffened by the inclusion of a rack-plate. However, unlike fixed steel platforms, it is rare for jack-up platforms to have joints with a grouted chord member, overlapping braces, or cast joints rather than welded ones. Consequently, most tubular joints on mobile offshore platforms may be considered to be simple rather than complex configurations.

For this Section, much of the published experimental data on the ultimate strength of tubular joints has been collected, processed and analyzed. The data have been obtained mainly from past and current offshore-related research, some of it funded by ABS. The amount of test data considered to have passed the screening criteria is given in Section C5, Table 1, along with the total number of joints in parentheses. The screening criteria adopted in this study are summarized as follows:

- Minimum chord diameter $D \geq 100$mm
- Chord and brace thickness T and $t \geq 2.0$ mm
- Member thickness ratio $\tau \leq 1.20$
- Member diameter ratio no limits on β
- Chord slenderness ratio no limits on γ
- Chord length parameter no limit on α
- Gaps in K joints $g > t$

The processed experimental evidence has formed the basis of extensive comparisons with the Guide recommendations.

The flowchart for the strength assessment of tubular joints is shown in Section C5, Figure 2.

FIGURE 1
Examples of Jack-up Leg Tube-to-Tube Joints

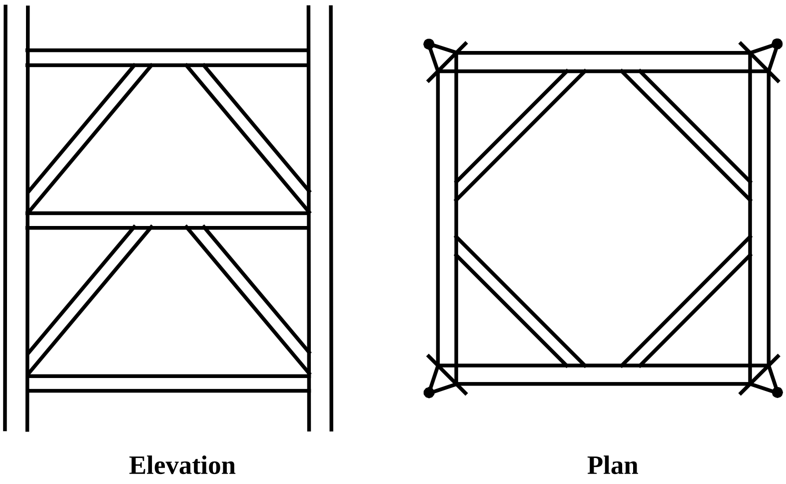

TABLE 1
Summary of Test Data (Frieze[49])

	K Joints	*T/Y Joints*	*X Joints*	*TOTAL*
Axial Compression	(207) 126	(150) 110	(89) 78	(446) 314
Axial Tension	(0) 0	(43) 14	(48) 32	(91) 46
In-plane Bending	(6) 6	(68) 15	(18) 7	(92) 28
Out-of-plane Bending	(10) 8	(23) 20	(5) 5	(38) 33
Chord Stress			(21) 21	(21) 21
Combined Loading			(39) 39	(39) 39
TOTAL	(223) 140	(284) 159	(181) 143	(727) 481

FIGURE 2
Flowchart of Tubular Joint Strength Assessment

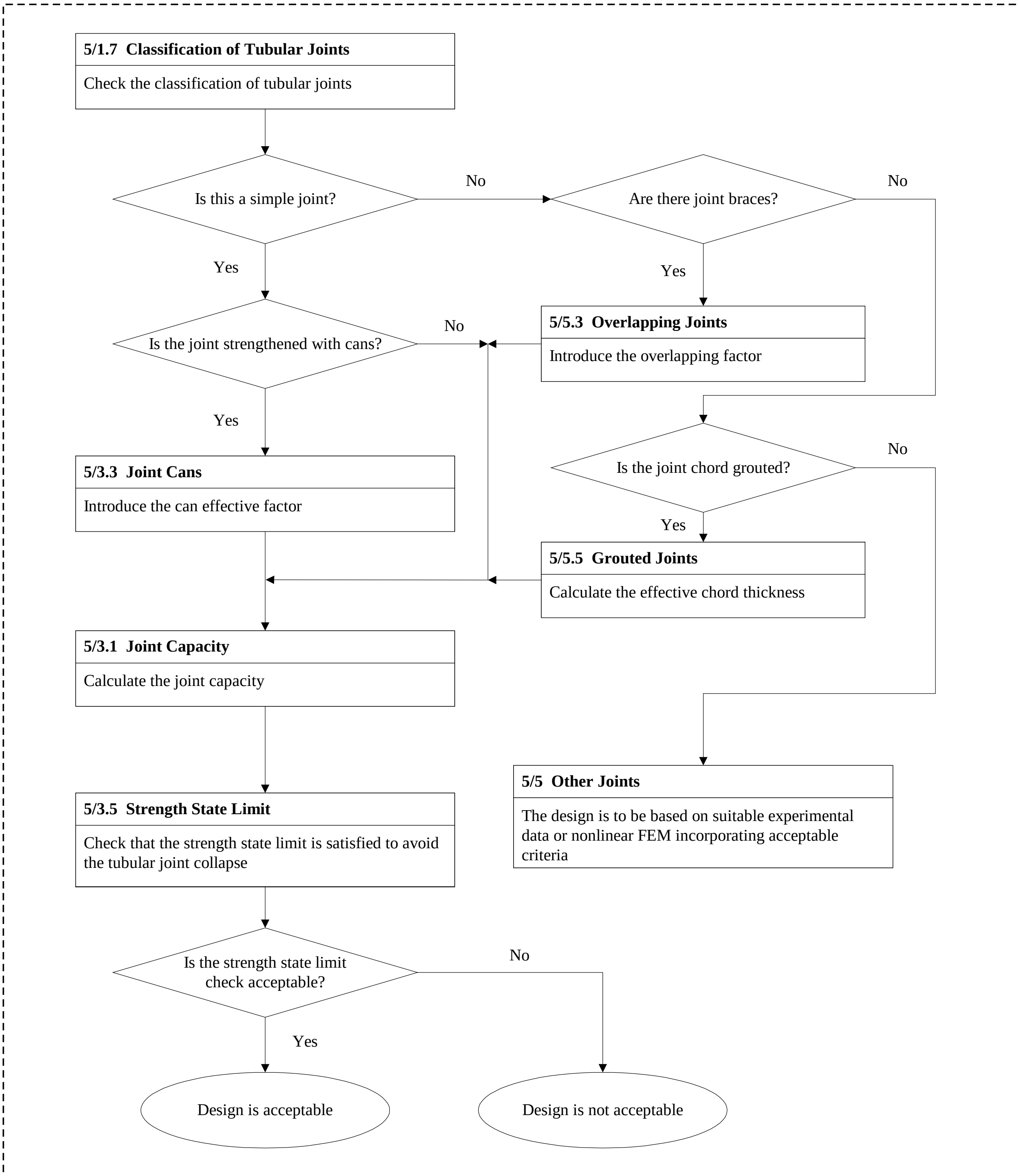

C1.1 Geometry of Tubular Joints

<No Commentary>

C1.3 Loading Application

<No Commentary>

C1.5 Failure Modes

The failure mode of a tubular joint depends upon the joint configuration, joint geometry and loading condition. These modes include:

i) Local failure of the chord:

- Plastic failure of the chord wall in the vicinity of the brace.
- Cracking leading to rupture of the brace from the chord.
- Local buckling in compression areas of the chord.

ii) Global failure of the chord:

- Ovalization of the chord cross-section.
- Beam bending failure.
- Beam shear failure between adjacent braces.

In addition, the joint can fail away from the brace-chord intersection from chord or brace overloading. These latter failure modes can be determined following the approach described in Section C2 of this Commentary for tubular members.

The failure of typical joints often involves a combination of these individual failure modes, especially the three local modes along with global chord ovalization.

In tension loaded joints, the chord wall around the brace can undergo large plastic deformation and the chord section distorts. As the load increases, a crack may initiate in the hot-spot region. The joint will continue to carry higher loads until the cracking becomes excessive, leading to gross separation of the brace from the chord. Failure in compression loaded joints is usually associated with buckling and/or plastic deformation of the chord wall. Joints made of relatively thin walled sections are particularly susceptible to local buckling.

For in-plane moment loaded joints, failure typically occurs due to fracture through the chord wall on the tension side of the brace, and plastic bending and buckling of the chord wall on the compression side. For out-of-plane moment loaded joints, local buckling of the chord wall near the brace saddle occurs, reducing stiffness. Failure is usually associated with fracture on the tension side of the brace after excessive plastic deformation.

Possible failure criteria that may be used to define the static strength of a tubular joint are:

i) *Ultimate or peak load limit.* The most universally accepted and used criterion to account for reserve strength and to define failure is based on ultimate or peak load. However, in some cases, e.g., in tensile loaded joints, crack initiation may precede and possibly influence the ultimate load. In moment loaded joints, an ultimate load may be reached only after excessive deformation or it may not be reached at all within the limits of the test rig. Accordingly, it is often felt that crack initiation and deformation limit criteria may be valid alternatives to the ultimate load criterion.

ii) *Crack initiation limit.* This failure criterion applies primarily to tension tests where joints continue to carry loads after cracks have initiated, and ultimately fail at higher loads than those corresponding to first evidence of cracking. This suggests that a conservative approach to estimating the static strength of tension loaded joints is desirable until the effects of cracking on ultimate strength have been evaluated more rigorously.

iii) *Deformation limit.* Benefits of employing a deformation limit include the possible absence of a clearly defined peak load and possible conservatism in isolated (test) joints as opposed to joints in a framed structure. The main argument against using a deformation limit is that it might be regarded as a serviceability criterion, which is not generally acceptable within an ultimate limit state concept.

iv) *Elastic limit.* The elastic limit criterion is clearly inappropriate for defining failure, because tubular joints have substantial reserve capacity beyond the associated limit load.

Based on the above discussion, the ultimate load definition of failure has been adopted in the ABS *Buckling Guide*, except for axial tension load where first crack is a more suitable and conservative definition.

C1.7 Classfication of Tubular Joints

Most codes provide guidance on joint classification for use in connection with design for static strength. Simple joints may be classified as T/Y, DT/X or YT/K joints on the basis of both joint configuration and joint loading. Section C5, Figure 3, similar to API RP 2A WSD, shows typical examples of joint classifications.

Each joint should be considered as a number of independent chord/brace intersections and the capacity of each intersection should be checked against the design requirement. Each plane of a multiplanar joint should be subjected to separate consideration and classification.

FIGURE 3
Examples of Tubular Joint Categoriztion

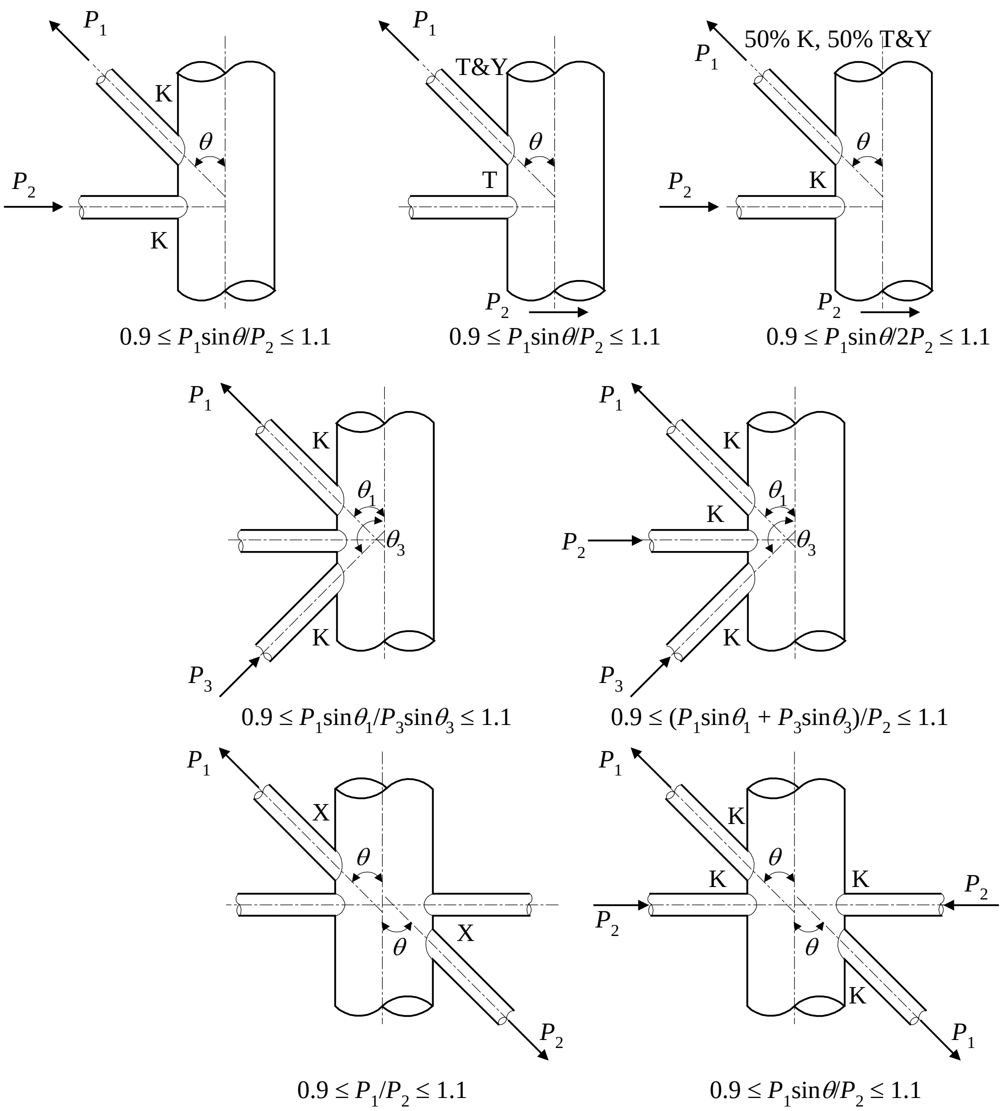

The examples of joint classification shown in Section C5, Figure 3 should be used with the following guidelines:

- For two or three brace joints on one side of the chord, the classification is dependent on the equilibrium of the axial load component in the brace members. If the resultant shear on the chord member is essentially zero, the joint should be allocated a K classification. If this criterion is not met, the joint can be downgraded to a Y classification as shown in Section C5, Figure 3. However, for braces that carry part of their load as K joints and part as Y or X joints, interpolation based on the portion of each in total may be valid. The procedure for interpolation in these cases should be agreed with the certifying authority.
- For multibrace joints with braces on either side of the chord as shown in the example K-K joint in Section C5, Figure 3, care should be taken in allocating the appropriate classification. For example, a K classification would be valid if the net shear across the chord is essentially zero. In contrast, if the loads in all the braces are tensile (e.g., at a skirt pile connection), even an X classification may be unsafe due to the increased ovalization effect. Classification for these cases should be agreed with the certifying authority.

C1.9 Adjustment Factor

In WSD Codes, the allowable joint strength incorporates an allowable utilization factor. This factor is applied in addition to the use of lower bound or a characteristic representation of relevant data (i.e., in the Q_u and Q_f term). The adjustment factor in API RP 2A WSD[3], AWS[126], HSE[127] and ABS *Buckling Guide* is summarized in Section C5, Table 2.

TABLE 2
Adjustment Factor in the Existing Offshore Structure Codes

	API RP 2A WSD	*AWS*	*HSE*	*ABS Buckling Guide*
Adjustment Factor	0.98	0.93	0.98	1.0

C3 Simple Tubular Joints

C3.1 Joint Capacity

In general, the following variables affect the strength of a tubular joint:

D	Chord outside diameter
T	Chord wall thickness
d	Brace outside diameter
g	Gap between in-plane braces
θ	Included angle between chord and brace
σ_0	Chord material yield strength

The dimensional parameters are generally expressed in terms on non-dimensional geometric ratios as follows:

$\beta = d/D$ $\gamma = D/2T$ $\zeta = g/D$

The calculation of joint strength is usually based on consideration of axial and moment load components perpendicular to the chord axis as follows:

$$P_u = \frac{\sigma_{oc} T^2}{\sin\theta} Q_u Q_f \text{ and } M_u = \frac{\sigma_{oc} T^2 d}{\sin\theta} Q_u Q_f$$

where

Q_u = geometric factor that is a function of member diameter, thickness and brace separation (β, γ and ζ)

Q_f = chord load factor that is a function of axial and moment loads, and material strength

The Q_u parameter was optimized using the solver minimization tool in association with an examination of the data. The objective of the equation fitting exercise was to minimize the goodness of fit of the strength formulae. However, it was recognized that the expressions should be kept reasonably simple, as with the existing API RP 2A WSD code, and that potentially small parameter effects (e.g., $\gamma^{0.1}$) should be ignored as these may really be a function of experimental inconsistencies.

For In-plane Bending Moment (IPB), in particular, the joint configuration would not be expected to have a significant effect. Similarly, it would be expected that T/Y joints would have the same strength as *K* joints with large brace separation. Consequently, several of the equations recommended in the following section could be individually improved, but then they may not correctly express the limiting conditions.

The expression for Q_u (and Q_f) has a characteristic or lower-bound format. Since a lower bound fit is largely dependent on the size of the database, a characteristic expression based on two standard deviations from the mean (i.e., ≈2.5% probability of overestimating strength) is proposed. This may be adjusted to give different characteristic formulae in association with the allowable utilization factor.

i) *Axial Compression.* Comparisons of the results from API RP 2A WSD, and the recommended Guide, equations for axial compression loading are given in Section C5, Table 3 and Section C5, Figure 4. It can be seen that the API RP 2A WSD formulations are based on a Q_u format $(a + b\beta)$, where a and b are coefficients. For the *K* configuration a simple gap term is applied, while for *X* joints, there is an additional β term (Q_β) in excess of 1.0 for $\beta > 0.6$. The formulae for *T* and *K* joints are the same at large gaps, while the *X* joint equation has coefficients that suggest a lower strength at low β values than for the equivalent *T* or *K* joint.

In this study, the best-fit equation for *T* and *K* joints includes a small but significant term in γ. Applying this term reduced the scatter in the data, but removed the need to also have a γ term in the gap parameter for the *K* joint equation. The proposed ABS gap term is a simple exponential that is 1.85 at $g/D = 0.0$ and has less than 5% effect at $g/D > 0.7$. Taking a γ value of 20 in the proposed formula for *T* and *K* joints yields a formula $(0.91 + 21.8\beta)Q_\beta^{0.5}$, and for *X* joints, $(3.0 + 14.5\beta)Q_\beta$.Therefore, apart from the inclusion of a γ value for *T* and *K* joints and the removal of the γ value for X joints, the ABS equation is very similar to that used in API RP 2A WSD.

FIGURE 4
Modeling Uncertainty for Axial Compression

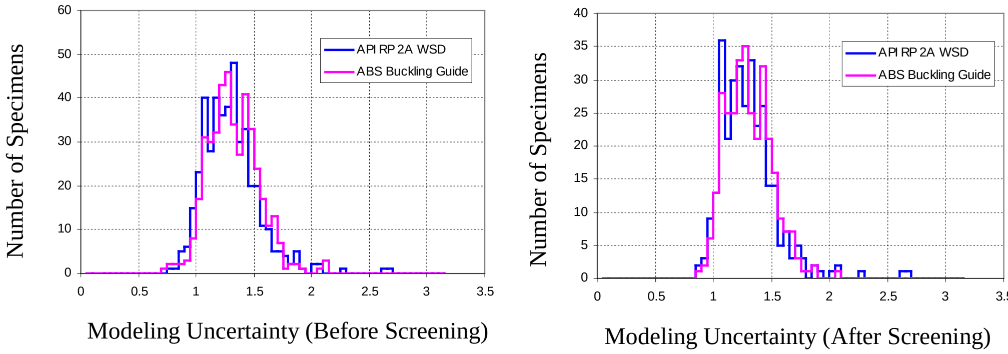

TABLE 3
Q_u in API RP 2A WSD and the ABS Buckling Guide for Axial Compression Loading

	API RP 2A WSD	*ABS Buckling Guide*
K	$(3.4 + 19\beta)\ Q_g$	$(0.5 + 12\beta)\ \gamma^{0.2}\ Q_\beta^{0.5}\ Q_g$
T/Y	$(3.4 + 19\beta)$	$(0.5 + 12\beta)\ \gamma^{0.2}\ Q_\beta^{0.5}$
DT/X	$(3.4 + 13\beta)\ Q_\beta$	$(3.0 + 14.5\beta)\ Q_\beta$

$Q_\beta = 0.3/[\beta(1 - 0.833\beta)]$ $\beta > 0.6$

$Q_\beta = 1.0$ $\beta \leq 0.6$

API RP 2A WSD

$Q_g = 1.8 - 0.1g/T$ $\gamma \leq 20$ $Q_g \geq 1$ in all cases

$Q_g = 1.8 - 4g/D$ $\gamma > 20$

The ABS Buckling Guide

$Q_g = 1 + 0.85\exp(-4g/D)$ $g/D \geq 0.0$

	No. of Data	*API RP 2A WSD*		*ABS Buckling Guide*	
		Mean	*COV*	*Mean*	*COV*
Screened Data – Axial Compression					
K	126	1.35	13.7%	1.31	14.6%
T/Y	110	1.21	25.9%	1.29	14.5%
X	78	1.14	9.6%	1.10	8.9%
All Data – Axial Compression					
K	207	1.31	15.8%	1.30	15.7%
T/Y	150	1.21	25.0%	1.32	17.4%
X	89	1.15	11.6%	1.11	11.1%

ii) *Axial Tension.* API RP 2A WSD and the ABS *Buckling Guide* equations for axial tension loading are given in Section C5, Table 4 and Section C5, Figure 5. This load case is complicated by the preference in the API RP 2A WSD code to base the design expression on the first crack definition of joint failure, while much of the test data only reports ultimate tensile strength.

The API RP 2A WSD equations are identical to those in compression with the exception of the removal of the Q_β term for X joints. This implies a lower strength under tensile loading than compressive loading for this joint configuration. Compared to the first crack database, the API RP 2A WSD equations underestimate the strength by more than 50%, while the ultimate strength is underestimated by more than 100%, on average. Therefore, the use of the axial compression equations for tensile axial load is very conservative, irrespective of the failure definition applied.

The best-fit equations have been derived using the ultimate strength database. It can be seen that these equations give a good fit to the ultimate strength data (COV = 12% to 20%). Characteristic expressions for ultimate tensile strength can be derived by reducing the coefficients in these expressions. However, the definition of tensile failure is based on first crack rather than ultimate tensile strength.

For first crack, there is insufficient quality data to derive meaningful parametric expressions. Consequently, the axial compression formulae are recommended. Since these are very conservative for tension load, the mean axial compression formulae are recommended for characteristic tensile first crack.

FIGURE 5
Modeling Uncertainty for Axial Tension

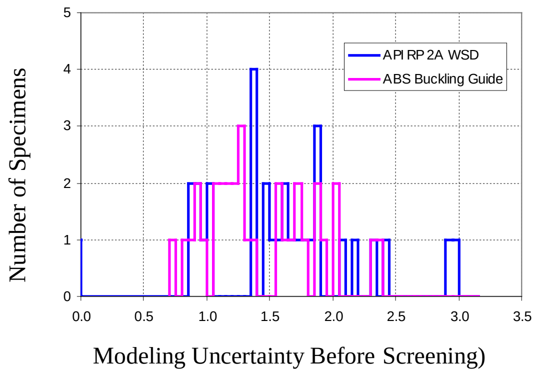

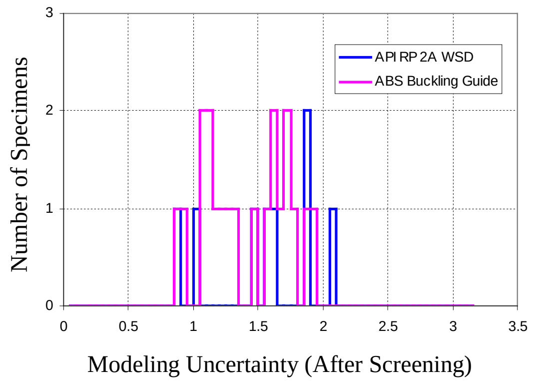

TABLE 4
Q_u in API RP 2A WSD and the ABS Buckling Guide for Axial Tension Loading

	API RP 2A WSD	*ABS Buckling Guide*
K	$(3.4 + 19\beta)\ Q_g$	$(0.65 + 15.5\beta)\ \gamma^{0.2}\ Q_\beta^{0.5}\ Q_g$
T/Y	$(3.4 + 19\beta)$	$(0.65 + 15.5\beta)\ \gamma^{0.2}\ Q_\beta^{0.5}$
X	$(3.4 + 13\beta)$	$(3.3 + 16\beta)\ Q_\beta$

Q_β and Q_g are as defined for compression loaded joints.

	No. of Data	*API RP 2A WSD*		*ABS Buckling Guide*	
		Mean	*COV*	*Mean*	*COV*
Screened Data – Axial Tension – 1st Crack					
K	0	-	-	-	-
T/Y	8	1.49	28.0%	1.27	29.1%
X	12	2.03	47.9%	1.42	20.5%
All Data – Axial Tension – 1st Crack					
K	0	-	-	-	-
T/Y	23	1.51	35.6%	1.24	36.0%
X	17	2.16	46.7%	1.51	24.5%
Screened Data – Axial Tension – Ultimate Strength					
K	0	-	-	-	-
T/Y	14	2.40	24.1%	1.97	19.0%
X	32	2.22	46.7%	2.14	23.7%
All Data – Axial Tension – Ultimate Strength					
K	0	-	-	-	-
T/Y	43	2.53	30.7%	2.05	28.0%
X	48	2.08	52.4%	2.00	28.1%

iii) *In-Plane Bending.* API RP 2A WSD and the ABS *Buckling Guide* equations for in-plane loading are given in Section C5, Table 5 and Section C5, Figure 6.

The API RP 2A WSD equations are similar to the T and K joint expressions for compression. The database of screened data is relatively small, but suggests a poor fit to T joints relative to the K and X joint databases.

The overall best-fit formula in the ABS *Buckling Guide* was recommended. Investigation of the database, both screened and unscreened, highlighted that the relatively poor fit of T joints to the test database is due to tests on inclined braces ($\theta < 90°$). Applying a factor of $\sin^{-1}(\theta)$ more than halved the scatter (COV = 10.1% from 20.6%), however such a factor was detrimental to the K joint database, where all braces were inclined at 45°.

It is believed that the K joints were tested with the loads separating the braces, i.e., leading to tension in the brace toe and compression in the brace heel. However, it is reported that the Y joints were tested in the opposite direction with compression in the brace toe and tension in the brace heel. There is a suggestion that the capacity of inclined braces under in-plane loading is higher when loaded towards the vertical, so that the measured strength of the two Y joints is optimistic. This phenomenon requires further investigation.

FIGURE 6
Modeling Uncertainty for In-Plane Bending

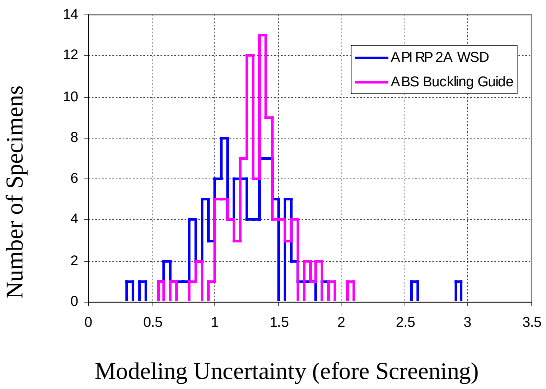

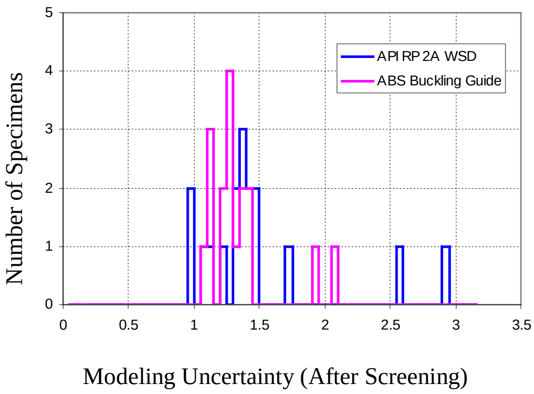

TABLE 5
Q_u in API RP 2A WSD and the ABS Buckling Guide for In-Plane Bending

	API RP 2A WSD	*ABS Buckling Guide*
K	$(3.4 + 19\beta)$	$4.5\beta\gamma^{0.5}$
T/Y	$(3.4 + 19\beta)$	$4.5\beta\gamma^{0.5}$
X	$(3.4 + 19\beta)$	$5.0\beta\gamma^{0.5}$

	No. of Data	*API RP 2A WSD*		*ABS Buckling Guide*	
		Mean	*COV*	*Mean*	*COV*
Screened Data – In-plane Bending					
K	6	1.29	9.5%	1.24	10.5%
T/Y	15	1.43	36.5%	1.22	9.7%
X	7	1.29	15.6%	1.09	4.5%
All Data – In-plane Bending					
K	6	1.29	9.5%	1.24	10.5%
T/Y	68	1.16	35.8%	1.28	21.3%
X	18	1.15	23.6%	1.27	14.4%

Note: No inclined T/Y joints passed the revised screening criteria.

iv) *Out-of-Plane Bending.* The results from API RP 2A WSD, and the ABS *Buckling Guide*, equations for out-of-plane loading are given in Section C5, Table 6 and Section C5, Figure 7.

The API RP 2A WSD equation is similar to the axial compression formula with a smaller β effect, Q_u = (3.4 + 7β)Q_β, for all joint configurations. The database of screened data is fairly small, but suggests a poor fit to *T* joints relative to the K and X joint databases.

The overall best-fit equation was recommended in the ABS *Buckling Guide*. The mean fits for each joint configuration yielded different coefficients, however, given the relative COVs for each expression it was considered acceptable to propose a single expression for all joint configurations.

FIGURE 7
Modeling Uncertainty for Out-of-Plane Bending

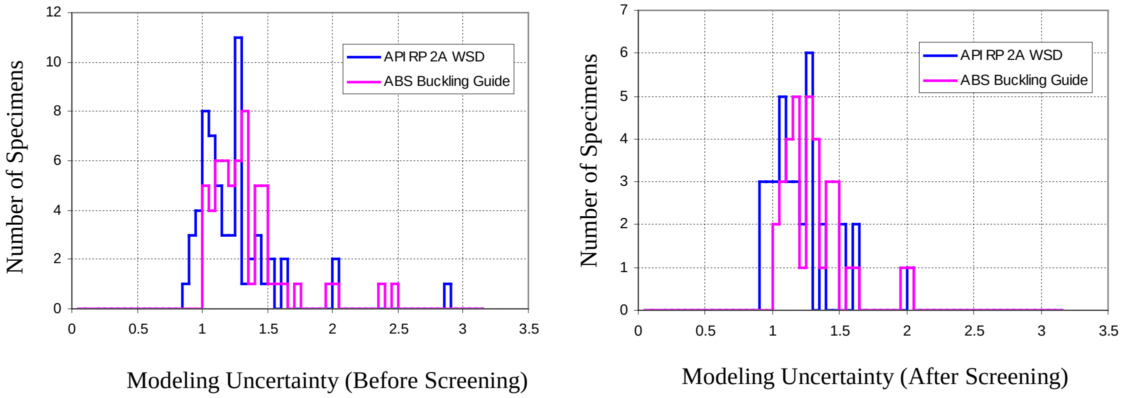

TABLE 6
Q_u in API RP 2A WSD and the ABS Buckling Guide for Out-of-Plane Bending

	API RP 2A WSD	*ABS Buckling Guide*
K	$(3.4 + 7\beta)\ Q_\beta$	$3.2\gamma^{(0.5\beta^2)}$
T/Y	$(3.4 + 7\beta)\ Q_\beta$	$3.2\gamma^{(0.5\beta^2)}$
X	$(3.4 + 7\beta)\ Q_\beta$	$3.2\gamma^{(0.5\beta^2)}$

$Q_\beta = 0.3/[\beta(1 - 0.833\beta)]$ $\quad\beta > 0.6$

$Q_\beta = 1.0$ $\quad\beta \le 0.6$

	No. of Data	*API RP 2A WSD*		*ABS Buckling Guide*	
		Mean	*COV*	*Mean*	*COV*
Screened Data – Out-of-plane Bending					
K	8	1.08	11.5 %	1.19	16.2 %
T/Y	20	1.20	23.8 %	1.34	18.9 %
X	5	1.08	12.0 %	1.10	5.6 %
All Data – Out-of-plane Bending					
K	10	1.11	12.2 %	1.17	15.2 %
T/Y	23	1.25	30.7 %	1.36	24.3 %
X	5	1.08	12.0 %	1.10	5.6 %

v) *Effect of Chord Stresses.* The effect of chord axial and bending stresses on the ultimate strength of tubular joints was considered in the reports by Hoadley and Yura[129] and Weinstein and Yura[130]. The static strength reduction factor was given by:

$$Q_f = 1 - \lambda\gamma A^2$$

where

λ	=	chord slenderness parameter	
	=	0.030	for brace axial load
	=	0.045	for brace in-plane bending moment
	=	0.021	for brace out-of-plane bending moment
A	=	chord utilization ratio	

$$= \frac{\sqrt{\sigma_{AC}^2 + \sigma_{IPC}^2 + \sigma_{OPC}^2}}{\eta\sigma_{oc}}$$

This reduction factor was adopted by API RP 2A WSD (2000) and is also recommended in the ABS *Buckling Guide*.

The values of modeling uncertainty for the ABS *Buckling Guide* and API RP 2A WSD equations are given in Section C5, Table 7 and Section C5, Figure 8.

FIGURE 8
Modeling Uncertainty for the Effect of Chord Stresses

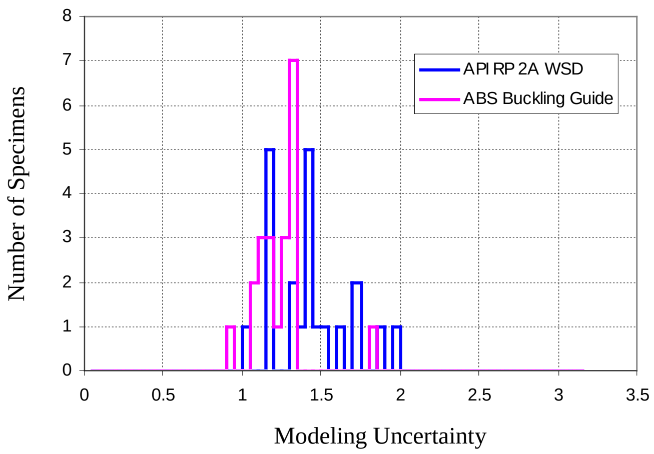

TABLE 7
Modeling Uncertainty for the Effect of Chord Stresses

TEST	*API RP 2A WSD*	*ABS Buckling Guide*
A21	1.25	1.15
AP25	1.95	1.78
A41	1.29	1.21
A46	1.12	1.04
AM47	1.14	1.07
I24	1.66	1.17
I29	1.80	1.27
IM30	1.45	1.03
O23	0.97	0.89
OP27	1.36	1.26
A1	1.39	1.28
AP2-1	1.35	1.24
AP2-2	1.38	1.27
AP5	1.39	1.28
AM6	1.39	1.28
I7	1.69	1.29
IM11	1.42	1.08
IP12	1.59	1.21
O8	1.14	1.13
OP9	1.11	1.09
OM10	1.14	1.12
Mean	1.38	1.20
COV	18.03%	14.28%

C3.3 Joint Cans

<No Commentary>

C3.5 Strength State Limit

Several interaction equations have been suggested for use in the design of tubular joints. The 21st Ed. of API RP 2A WSD recommendations used the arcsine equation, which is based on the plastic section strength of the branch member, given by:

$$\left|\frac{P}{P_u}\right| + \frac{2}{\pi}\arcsin\sqrt{\left(\frac{M}{M_u}\right)_{IPB}^2 + \left(\frac{M}{M_u}\right)_{OPB}^2} = 1$$

The ABS *Buckling Guide* interaction equation used the same form as the Hoadley's equation but with integer exponents, which is written as:

$$\left|\frac{P_D}{P_u}\right| + \left(\frac{M}{M_u}\right)_{IPB}^2 + \left|\frac{M}{M_u}\right|_{OPB} = 1$$

This equation was also adopted in the HSE code (1990).

Section C5, Table 8 contains the values of P_u and M_u computed for the University of Texas specimens along with the experimental values (Swensson, K and Yura[132]) for comparison.

The modeling uncertainties for the ABS *Buckling Guide* and API RP 2A WSD interaction equations are given in Section C5, Table 9 and shown graphically in Section C5, Figure 9.

The interaction equation adopted in the ABS *Buckling Guide* follows the trends of the test data better than the API RP 2A WSD equation. In addition, there is a reasonable amount of conservatism resulting from the ABS *Buckling Guide* equation.

FIGURE 9
Modeling Uncertainty for Combined Loadings

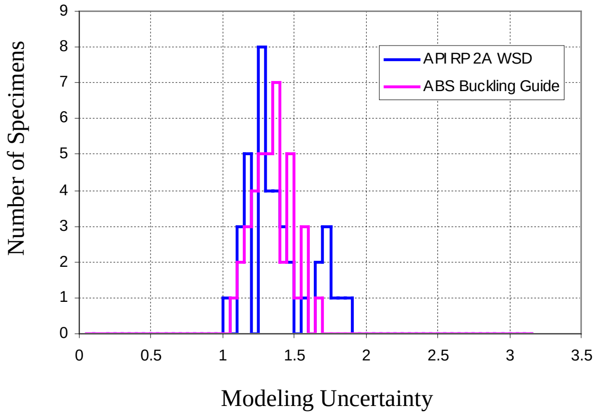

TABLE 8
Value of P_u and M_u

Load Type	*Test and Code Value*	*Ratio of brace diameter to chord diameter, β*		
		1.00	*0.67*	*0.35*
Axial(Kips)	Test	162.1	73.9	44.1
	API RP 2A WSD	141.1	57.1	38.1
	ABS Buckling Guide	150.0	61.5	42.6
OPB (Kips-in)	Test	1389	440	118
	API RP 2A WSD	1148	330	126
	ABS Buckling Guide	1234	341	105
IPB (Kips-in)	Test	2265	1056	257
	API RP 2A WSD	1373	650	216
	ABS Buckling Guide	1928	871	238

TABLE 9
Modeling Uncertainty for Combined Loadings

β	*TEST*	*API RP 2A WSD*	*ABS Buckling Guide*
0.35	A40	1.10	1.09
	A40	1.21	1.11
	O42	0.95	1.21
	I43	1.21	1.14
	AO44	1.10	1.51
	AO45	1.20	1.51
	AI46	1.20	1.16
	AI47	1.43	1.32
	IO48	1.21	1.55
	IO49	1.30	1.63
0.67	A1	1.38	1.28
	A51	1.24	1.15
	O8	1.21	1.23
	I7	1.63	1.29
	AO04	1.10	1.26
	AO13	1.27	1.37
	AI20	1.51	1.24
	AI17	1.65	1.33
	IO15	1.27	1.32
	IO14	1.29	1.33
	AIO16	1.25	1.41
	AIO18	1.39	1.41
	AIO19	1.32	1.34
1.00	A21	1.22	1.15
	A22	1.07	1.01
	O23	1.14	1.15
	O28	1.30	1.28
	I24	1.66	1.24
	AO31	1.06	1.18
	AO32	1.10	1.23
	AO33	1.05	1.10
	AI34	1.62	1.26
	AI35	1.81	1.44
	AI36	1.78	1.41
	AI50	1.73	1.37
	IO37	1.32	1.32
	IO38	1.41	1.40
	IO39	1.69	1.45
	IO26	1.36	1.30
Mean		1.33	1.29
COV		16.87%	10.60%

C5 Other Joints

C5.1 Multiplanar Joints

<No Commentary>

C5.3 Overlapping Joints

Guidance on the capacity of overlapping joints is given in API RP 2A WSD and other references. However, the guidance does not address the effects from the moments or out-of-plane overlap. A relatively complete summary of the limitations with existing guidance and background data can be found in Dexter and Lee[133] and Gazolla, F et al[134].

The ABS *Buckling Guid*e has been based on the ABS report (2001). The designer is encouraged to employ pertinent test evidence of calibrated FE results to specific cases.

C5.5 Grouted Joints

Grouted joints are becoming more common in new steel jacket structures and joint grouting is generally a cost-effective means of strengthening older structures. API and other offshore practices have historically said little about how to establish grouted joint capacity. Industry practice is based upon engineering approximations and some experimental evidence. The experimental evidence is primarily from double skin joints subjected to axial brace forces. The results of a joint industry project provide additional data for fully grouted joints. The ABS *Buckling Guide* recommends no benefit for grouting without first performing an independent assessment of any grouted joints. The exception to this recommendation is for members which are subjected to an axial compression loading where the joint capacity (excluding chord end load effects) can include a modified thickness.

C5.7 Ring-Stiffened Joints

Some reports from studies on strength are given in Sawada, Y et al[135] and Murtby et al [136]. Since effective codified practices are not yet available, ring-stiffened joints require more engineering attention than many of simpler joint types. For the same reason these joint designs are often more conservative than indicated from applicable evidence or calibrated FE analysis results.

C5.9 Cast Joints

<No Commentary>

SECTION C5 Appendix 1 – Examples of Strength Assessment of Simple Tubular Joints

An MS EXCEL application, entitled, *ABS-Tubular Joints*, has been developed to facilitate the use of the ABS *Buckling Guide*. The calculation consists of three worksheets namely “Input Data”, “Output Data” and “Intermediate Results”. In the worksheet “Input data”, the input data including Tubular joint ID, Load case, Geometries, Material parameters, Joint type, Loadings and Basic utilization factor corresponding to the specified load case are required. Once the input data are ready, a macro represented by a large button “Tubular Joints” at the left-hand side corner is run. Ultimate strength assessment results and intermediate results can be seen in the worksheets “Output” and “Intermediate Results”. All symbols used in the spreadsheet are consistent with those in the ABS *Buckling Guide*.

The table below shows several example calculations applied to tested tubular joints.

Name of Tubular Joints			University of Texas at Austin			
Location of Tubular Joints			A40	I43	O23	AO31
Geometry						
	Chord outer diameter	D	16.00	16.00	16.00	16.00
	Chord thickness	T	0.31	0.31	0.31	0.31
	Brace outer diameter	d	5.63	5.63	16.00	16.00
	Brace thickness	t	0.25	0.25	0.31	0.31
	Brace angle (Measured from chord)	θ	90.00	90.00	90.00	90.00
	Gap	g	0.00	0.00	0.00	0.00
	Specified minimum yield stress of chord	σ_{0c}	48.90	48.90	48.90	48.90
	Type of tubular joint		3	3	3	3
Loading						
Brace	Axial force	P_B	-4.20E+01	-4.80E+00	-1.35E+01	-4.44E+01
	In-plane bending moment	M_{IPB}	0.00E+00	2.57E+02	0.00E+00	1.00E+00
	Out-of-plane bending moment	M_{OPB}	0.00E+00	0.00E+00	1.30E+03	1.09E+03
Chord	Axial force	P_c	0.00E+00	0.00E+00	0.00E+00	0.00E+00
	In-plane bending moment	M_{IPC}	0.00E+00	0.00E+00	0.00E+00	0.00E+00
	Out-of-plane bending moment	M_{OPC}	0.00E+00	0.00E+00	0.00E+00	0.00E+00
Maximum Allowable Utilization Factor						
	Basic factor	η	1	1	1	1
Unity Check						
	Tubular joints		**1.09**	**1.14**	**1.15**	**1.18**
Intermediate Results						
Geometry	Chord sectional area	A_c	1.54E+01	1.54E+01	1.54E+01	1.54E+01
	Chord moment of inertia	I_c	4.73E+02	4.73E+02	4.73E+02	4.73E+02
	Chord sectional modulus	SM_c	5.91E+01	5.91E+01	5.91E+01	5.91E+01
	Parameters	β	0.35	0.35	1.00	1.00
		γ	2.56E+01	25.64	25.64	25.64
		τ	8.01E-01	0.80	1.00	1.00
Stress						
	Chord axial stress	σ_{ac}	0.00	0.00	0.00	0.00
	Chord in-plane bending stress	σ_{IPC}	0.00	0.00	0.00	0.00
	Chord out-of-plane stress	σ_{OPC}	0.00	0.00	0.00	0.00

Coefficients						
	Chord affecting coefficient	A	0.00	0.00	0.00	0.00
	Chord load factor-axial loading	Q_{fP}	1.00E+00	1.00	1.00	1.00
	Chord load factor-inplane bending	Q_{fMIP}	1.00E+00	1.00	1.00	1.00
	Chord load factor-out-of-plane bending	Q_{fMOP}	1.00E+00	1.00	1.00	1.00
	factor	$Q_{\square}$	1.00E+00	1.00	1.80	1.80
	Strength factor -axial loading	Q_{uP}	8.10E+00	8.10	31.44	31.44
	Strength factor -inplane bending	Q_{uMIP}	8.90E+00	8.90	25.32	25.32
	Strength factor -out-of-plane bending	Q_{uMOP}	3.91E+00	3.91	16.20	16.20
Ultimate Strength						
	Axial loading	P_u	3.85E+01	3.85E+01	1.50E+02	1.50E+02
	Inplane bending	M_{uip}	2.38E+02	2.38E+02	1.93E+03	1.93E+03
	Out-of-plane bending	M_{uop}	1.05E+02	1.05E+02	1.23E+03	1.23E+03

Units: Length – [in.], force – [kips], Stress and Pressure – [ksi]

APPENDIX C1 Review of Buckling Analysis by Finite Element Method (FEM)

C1 General

Finite element analysis (FEA) is the most common structural analysis tool in use today. Great strides have been made in theoretical and computational aspects of FEA. In offshore industries, the use of this technique is becoming more widespread in the design, reliability and risk analysis and performance evaluation of offshore structures.

Buckling analysis is a technique used to determine buckling loads – critical loads at which a structure becomes unstable – and buckled mode shapes – the characteristic shape associated with a structure's buckled response. This Section summarizes the fundamental principles and technical background related to buckling analysis by finite element method (FEM). The detailed information can be found in ANSYS Program Release 8.1 Documentation Preview for performing the buckling analysis[138].

Examples for perforated plate panels are illustrated to demonstrate the FEM application to the eigenvalue buckling and nonlinear buckling analysis.

C3 Engineering Model

Offshore structures are usually complex in nature, and can only be analyzed after idealization of the structure. Several simplifying assumptions are to be made in the idealization process. The elements that need to be considered in this idealization process are the character of loading, the primary loading paths, and the parts of the structure that participate in a FEA.

The analysts should describe and justify the extent of the model. The justification statement should include a discussion of:

- All significant structural action captured by the model.
- Requirement to accurately predict stresses and/or deflections.
- Region of structure of particular interest, whether St. Venant’s Principle is satisfied.
- Obvious changes in structural stiffness that suggest a model boundary
- Very local application of the load to a large uniform structure

The most common engineering materials used in the construction of offshore structures are metallic and exhibit a linear stress-strain relationship up to a stress level known as the proportional limit. If a material displays nonlinear or rate-dependent stress-strain behavior, the nonlinear material property should be defined. The bilinear isotropic and kinematic hardening models are most commonly used in plastic analysis. The former uses the von Mises yield criteria coupled with an isotropic work hardening assumption and the latter assumes the total stress range is equal to twice the yield stress, so that the Bauschinger effect is included.

Other kinds of nonlinear behavior might also occur along with plasticity. In particular, large deflection and/or large strain will often be associated with plastic material response. If large deformations are expected, these effects should be taken into account.

As described in the former sections, the buckling and ultimate strength of structural components are highly dependent on the amplitude and shape of the imperfections introduced during manufacture, storage, transportation, installation and on-site service. The imperfections should be described in order to keep the imperfect components within the acceptable safety level.

All loads and load combinations that need to be considered should be described. The loads typically applied in offshore units include permanent loads, variable functional loads, environmental loads, accidental loads etc.

The boundary conditions applied to the model should be described and suitably reflect the constraint relationship between the structural component and its surroundings. The description should include the assessment of influence on results of assumptions made concerning boundary conditions and.

The detailed information can be found in SSC-387[137] for assessing the engineering model.

C5 FEM Analysis Model

Before modeling a structural problem, it is useful to have a general idea of the anticipated behavior of the structure. This knowledge serves as a useful guide in several modeling decisions that need to be made in building the FE model.

To some extent all finite element types are specialized and can only simulate a limited number of types of response. An important step in the finite element modeling procedure is choosing the appropriate element types, which should best suit to the particular problem. The physics of the problem should be understood well enough to make an intelligent choice of element type.

Mesh design, the discretization of a structure into a number of finite elements, is one of the most critical tasks in finite element modeling and often a difficult one. The following parameters need to be considered in designing the layout of elements: mesh density, mesh transitions and the stiffness ratio of adjacent elements. As a general rule, a finer mesh is required in areas of high stress gradient. The performance of elements degrades as they become more skewed. If the mesh is graded, rather than uniform, as is usually the case, the grading should be done in a way that minimizes the difference in size between adjacent elements.

In modern FEA installations most analysts rely on preprocessors to develop the finite element mesh. Automatic mesh generators yield adequate meshes. However, in very demanding configurations the mesh generator may produce a poor mesh. In such situations the mesh should be manually improved to meet the guidelines.

In modeling complex structural assemblies there is a possibility of constructing models where adjacent structural elements have very different stiffness. To prevent large numerical errors, a conservative stiffness ratio of the order of 10^4 or more between members making up a model should be avoided.

Improper connections between elements of different types can cause errors. Solid elements types, for example, have only translation nodal degrees of freedom. If solid elements are interconnected with beam or plate/shell type elements, which have rotational degrees of freedom, in addition to translation ones, care must be taken to allow for the transfer of moments if that is what is intended.

There is a big challenge task in the selection of boundary conditions. Generally, the support condition assumed for the degree of freedom concerned is idealized as completely rigid or completely free. In reality the support condition is usually somewhere in between.

Several techniques are used to minimize the impact on the analysis of the assumptions made in boundary conditions. The most popular is to develop models large enough such that the area of interest is sufficiently remote from the boundary. It is also the practice to make conservative assumptions so that the results will represent upper bound solutions.

Loading in finite element modeling may be applied in a variety of ways. Typical structural loads in finite element models are forces, pressure load, gravity, body forces and temperatures applied or transferred at nodes and on elements of the model. The load may be applied or transferred to:

- Nodes (e.g., nodal forces and body forces)
- Element edges or faces (e.g., distributed line loads, pressure)
- Entire model (e.g., gravity loads)

The detailed information can be found in SSC-387[137] for assessing the FEM analysis model.

C7 Solution Procedure

Two techniques are available for predicting the buckling load and buckling mode shape of a structure: nonlinear buckling analysis, and eigenvalue (or linear) buckling analysis. Since these two methods frequently yield quite different results, the differences between them need to be examined before discussing the details of their implementation.

Eigenvalue buckling analysis predicts the theoretical buckling strength (the bifurcation point) of an ideal linear elastic structure. This method corresponds to the textbook approach to elastic buckling analysis: for instance, an eigenvalue buckling analysis of a column matches the classical Euler solution. However, imperfections and nonlinearities prevent most real-world structures from achieving their theoretical elastic buckling strength. Thus, eigenvalue buckling analysis often yields unconservative results, and should generally not be used in actual day-to-day engineering analyses.

Buckling is formulated as an eigenvalue problem:

$$([K] + \lambda_i[S]\{\psi_i\}) = 0$$

where

$[K]$ = stiffness matrix

$[S]$ = stress stiffness matrix

λ_i = i^{th} eigenvalue (used to multiply the loads which generated $[S]$)

ψ_i = i^{th} eigenvector of displacements

The eigenproblem is solved as discussed in Eigenvalue and Eigenvector Extraction. The eigenvectors are normalized so that the largest value is 1.0. Thus, the stresses (when output) may only be interpreted as a relative distribution of stresses.

Eigenvalue buckling analysis generally yields unconservative results, and usually should not be used for the design of actual structures. Eigenvalue buckling analysis follows the following procedure:

- *Create the analysis model.*

  It should be kept in mind that only linear behavior is valid. Nonlinear elements, if any, are treated as linear. Young's modulus must be defined. Material properties may be linear, isotropic or orthotropic, and constant or temperature-dependent. Nonlinear properties, if any, are ignored.

  i) *Obtain the static solution.* The procedure to obtain a static solution is the same as structural static analysis with the following exceptions:

  - Prestress effects must be activated. Eigenvalue buckling analysis requires the stress stiffness matrix to be calculated.
  - Unit loads are usually sufficient (that is, actual load values need not be specified). The eigenvalues calculated by the buckling analysis represent buckling load factors. Therefore, if a unit load is specified, the load factors represent the buckling loads. *All* loads are scaled.

  Note that eigenvalues represent scaling factors for *all* loads. If certain loads are constant (for example, self-weight gravity loads) while other loads are variable (for example, externally applied loads), one needs to ensure that the stress stiffness matrix from the constant loads is not factored by the eigenvalue solution.

  ii) *Obtain the eigenvalue buckling solution.* The procedure to obtain a static solution is the same as structural static analysis with the following exceptions:

  - Prestress effects must be activated. Eigenvalue buckling analysis requires the stress stiffness matrix to be calculated.
  - Unit loads are usually sufficient (that is, actual load values need not be specified). The eigenvalues calculated by the buckling analysis represent buckling load factors. Therefore, if a unit load is specified, the load factors represent the buckling loads. *All* loads are scaled.

Note that eigenvalues represent scaling factors for *all* loads. If certain loads are constant (for example, self-weight gravity loads) while other loads are variable (for example, externally applied loads), one needs to ensure that the stress stiffness matrix from the constant loads is not factored by the eigenvalue solution.

iii) *Expand the solution.* If the buckled mode shape(s) is to be reviewed, the solution should be expanded regardless of which eigenvalue extraction method is used.

iv) *Solve the eigenvalue problem.* Follow the steps to obtain the eigenvalue buckling solution.

- Select solution method. There are two methods to perform the eigenvalue buckling analysis: Subspace method and Block Lanczos method.
- Specify the number of eigenvalues to be extracted.

v) *Review the results.* Eigenvalue buckling results consisting of buckling load factors, buckling mode shapes, and relative stress distributions can be reviewed in the general postprocessor.

Nonlinear buckling analysis is usually the more accurate approach and is therefore recommended for design or evaluation of actual structures. This technique employs a nonlinear static analysis with gradually increasing loads to seek the load level at which the structure becomes unstable.

In the nonlinear technique, features such as initial imperfections, plastic behavior, gaps, and large-deflection response can be included. In addition, using deflection-controlled loading, the post-buckled performance of the analyzed structure can also be tracked.

Two approaches, namely the total Lagrange formulation and the updated Lagrangian formulation, are widely used to calculate the nonlinear finite element stiffness matrix. The latter is usually used in the nonlinear buckling analysis.

By applying the principle of virtual work, the following equation should be satisfied:

$$\{L\} + \{\Delta R\} = [K]^E\{\Delta U\}$$

where

$\{L\}$ = unbalance force caused by the difference between the total external forces, $\{R\}$ and total internal forces, $\{r\}$

$\{\Delta R\}$ = nodal force increment

$\{\Delta U\}$ = displacement increment

$[K]^E$ = elastic tangent stiffness matrix

This incremental equation can be solved by (modified) Newton-Raphson Method. To solve the unstable post-collapse behavior, the arc-length method is typically useful. This method is iteratively executed until the unbalanced force vector converges to zero within the specified tolerance limit.

It should be noted that an unconverged solution does not necessarily mean that the structure has reached its maximum load. It could also be caused by numerical instability, which might be corrected by refining the modeling technique.

The load-deflection history of the structure's response is to be tracked to decide whether an unconverged load step represents actual structural buckling, or whether it reflects some other problem. In the preliminary analysis, the arc-length method to predict an approximate value of buckling load should be applied. The approximate value is needed to compare to the more precise value calculated using bisection to help determine if the structure has indeed reached its maximum load.

The following points should be kept in mind:

i) If the loading on the structure is perfectly in-plane (that is, membrane or axial stresses only), the out-of-plane deflections necessary to initiate buckling will not develop, and the analysis will fail to predict buckling behavior. To overcome this problem, apply a small out-of-plane perturbation, such as a fabrication tolerance, to initiate the buckling response. (A preliminary eigenvalue buckling analysis of the structure may be useful as a predictor of the buckling mode shape, allowing the analyst to choose appropriate locations to apply perturbations to stimulate the desired buckling response). The failure load is in general very sensitive to these parameters.

ii) In a large-deflection analysis, forces (and displacements) will maintain their original orientation, but surface loads will "follow" the changing geometry of the structure as it deflects. Therefore, it is important to apply the proper type of loads.

iii) Stability analysis should be carried through to the point of identifying the critical load in order to calculate the structure's factor of safety with respect to nonlinear buckling.

iv) The arc-length method is to be activated so that the analysis can be extended into the post-buckled range to trace the load-deflection curve through regions of "snap-through" and "snap-back" response.

C9 Verification and Validation

The results obtained from a finite element analysis (FEA) should always be verified and validated. To make sure that the results are devoid of any errors in modeling or analysis, it is necessary to perform the general solution and postprocessing checks.

General solution checks can be performed using the graphical display features available with most FEA software systems. Where such features are not available, these checks will have to be performed by examining printed output results.

i) *Errors and warnings.* Well established finite element software systems generally have several built in checks to identify poor modeling and analysis practices. A warning or an error message is issued when built in criteria are violated. The correct practice is to resolve any such messages and take the appropriate remedial action. If the warning/error message is not applicable to the analysis, proper justification should be provided.

ii) *Mass and centre of gravity.* It is good practice to verify the mass of the model and the location of the model's centre of gravity. Several programs provide the mass without the need for a full analysis. If this option is unavailable, the analysis could be run with a 1 g (acceleration of gravity) loading (with no other applied loads).

iii) *Self-consistency.* The results should be checked for 'self-consistency', For example, displacements at fixed supports should indeed have zero displacements, and any symmetry in the model should be reflected in the stress and deflection results.

iv) *Static balance.* This is a fundamental check. The applied loads should be compared with the reactions. The check should include moments where appropriate. This check ensures that the applied loads and reactions are in balance, and ensures that the user specified loading definitions are properly interpreted by the program. When the applied loads and reactions are not in balance this is an indication of a serious error.

v) *Defaults.* All FEA software packages have built-in defaults. For certain input parameters default values or options are assumed if a value has not been input, or if an option has not been selected. Hence, checks should be performed to ensure that where defaults have been used, they are consistent with the assumptions of the analysis.

Methods used for post-processing of derived quantities from a FEA should be explained. The need and justification for applying correction factors for FEA results by comparison with design codes should be explained.

i) *Displacement results.* In the design of offshore structures the primary result parameter of interest is stress. Most design criteria are expressed as allowable stresses. Although deflection criteria are not as numerous as stress criteria in working stress design codes, they can be just as critical.

ii) *Stress results.* These results are presented attractively as stress contours in color plots in most FEA software, which provide a good qualitative indication of the adequacy of the density of the mesh. Smoothly changing contours usually indicates that the mesh is suitably fine. A change in stress of more than ±20% would be regarded as unsatisfactory for design purposes.

The stress state at a point is defined by several stress components depending on the element type. The state of stress in plated and shell structures is generally quite complex, and has to be combined in some way for design situations. Many failure theories have been developed wherein "failure" is said to have occurred when some equivalent stress exceeds the yield stress. The equivalent stress combines all the stresses acting at a point in the material. The most popular of these is the Von Mises stress.

The use of the equivalent stress for checking the critical buckling stress is not appropriate. For buckling checks, normal stress and shear stress, as appropriate, should be used. In some cases, the stress state may be biaxial and/or there may be significant shear stresses. To check these situations, it is usual to calculate the ratios of actual stress and critical stress for individual stress states, and combine the effects using interaction formulae.

iii) *Buckling Eigenvalues and Modes.* Eigenvalue buckling analysis predicts the theoretical buckling strength of an ideal linear elastic structure. This method corresponds to the textbook approach to elastic buckling analysis. Eigenvalue buckling analysis provides useful information for assessing the suitability of FEM analysis model and performing the nonlinear buckling analysis although it often yields unconservative results.

It is necessary to perform these checks to ensure that the loading, strength, and acceptance criteria are considered in arriving at the conclusions. This is a critical aspect of a finite element analysis since engineering decisions will typically be based on recommendations contained in this section.

i) *FEA results and acceptance criteria.* A statement confirming that all analysis procedure quality assessment checks have been executed satisfactorily should be included.

Despite the remarks made in the previous paragraph the results from alternative solution methods should also be treated cautiously. Analytical models incorporate idealizations, mistakes may be made in the calculations, textbooks and handbooks may contain errors, numerical solutions are subject to errors in coding and in data preparation, and experiments may be improperly performed and the results misinterpreted. Therefore, when the FEA results do not compare well with alternative methods, the possible reasons should be investigated.

The results should be presented so that they can be easily compared with the design/acceptance criteria. When the FEA results do not meet the acceptance criteria, possible reasons should be explored and documented. In case of large deviations, further justification regarding the validity of the FEA results should be provided.

ii) *Load Assessment.* In case of discrepancies in the results, the loading applied to the model should be reviewed as part of the investigation into the source of the problem. The appropriateness of the types of loads, load cases, magnitudes, directions, load combinations, load factors, boundary conditions, etc., should be reviewed.

The loads applied to a finite element model are approximations of the actual loads. The analysts should provide a general description on the method used to approximate the actual loads. If the load distribution is simplified to a more regular or uniform distribution, this should be justified to ensure that the simplified load distribution closely approximates the actual distribution in magnitude and direction. Details on load factors used in the analysis should also be provided. The information on whether the loads are based upon static loading conditions or combined loading conditions should also be provided.

Finally, an assessment of the accuracy of the applied loads should be used in describing the results from the analysis.

iii) *Strength assessment.* In design situations using traditional methods the practice is to apply a nominal design load to the structure and compare the computed stress with the allowable stress. The latter is usually some fraction of the yield stress or the buckling stress. In the modeling process several assumptions are made which may, or may not be conservative. An assessment of the conservatism should be made particularly in regard to the underlying assumptions implicit in the design criteria that are being applied. Often design criteria have evolved with design methods based on hand calculation. Different design criteria may be appropriate if FEA is used to compute stresses.

In making an assessment of the strength/resistance of the structure based on the results of a FEA, appropriate allowances should also be made for factors that were not accounted for in the analysis. Some of these factors include geometric and material imperfections, misalignments, manufacturing tolerance, residual stress, and corrosion.

The design criteria being applied may implicitly include an allowance for some, or all, of these factors.

iv) *Accuracy Assessment.* In assessing the accuracy of FEA results, factors to be considered include: the level of detail and complexity modeled, type of behavior modeled, mesh refinements, etc. In deciding the level of detail the analysts would necessarily have omitted some elements of the structure. The effect of these on the results should be assessed. The limitations of the element types used should also be assessed with respect to its capacity to model the required behavior.

Performing checks on the numerical accuracy of an FEA is difficult. Generally reliance is placed on a combination of good modeling practice and on parameters output by the FEA program.

The acceptability, or otherwise, of the ratio of the largest to smallest stiffness depends on the computer hardware and software and it is suggested that the guidance provided by the warning and error messages issued by the FEA program are heeded.

Application Examples

Examples for plate panels with an elliptical cutout subjected to an applied shear force are provided to demonstrate the eigenvalue buckling analysis and nonlinear buckling analysis.

Appendix C1, Figure 1 illustrates the geometry of a perforated plate panel subject to shear force. The opening is characterized by $\ell_0 \times b_0$, or length by width. Typically, an opening has a long rectangular shape.

FIGURE 1
Geometry of a Perforated Plate Panel

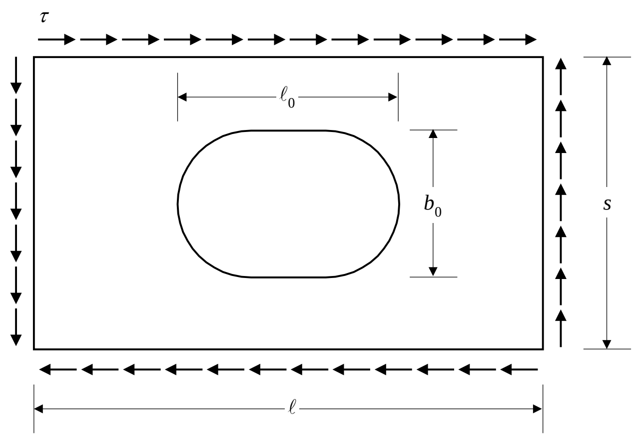

The geometry and material properties in the analysis are listed in Appendix C1, Table 1.

TABLE 1
Basic Analysis Variables

Variables	*Selected parameters*
Panels, $\ell \times s$	1450 × 800, 2200 × 800, 2400 × 800 mm
Plate thickness, t	10, 16, 20, 26 mm
Opening	None, 200 × 400, 400 × 600, 600 × 800 mm
Elastic modulus, E	2.06×10^5 MPa
Yield stress, σ_0	315 MPa

The FE model is shown in Appendix C1, Figure 2. In the FEM analysis, the initial imperfection is assumed to be of the form:

$$\frac{W_{p0}}{t} = \left[\delta_{10}\sin\left(\frac{\pi x}{\ell}\right) + \delta_{31}\sin\left(\frac{3\pi x}{\ell}\right)\right]\sin\left(\frac{\pi y}{s}\right)$$

where

δ_{10} = $2W^*/3t$

δ_{31} = $W^*/3t$

The amplitude of the imperfection is selected based on the statistics of ships' plating by Smith et al (1987)[52]. The effect of residual stress is ignored in the nonlinear buckling analysis.

Simply supported boundary conditions with all edges remaining straight during loading are assumed.

FIGURE 2
FEA Model

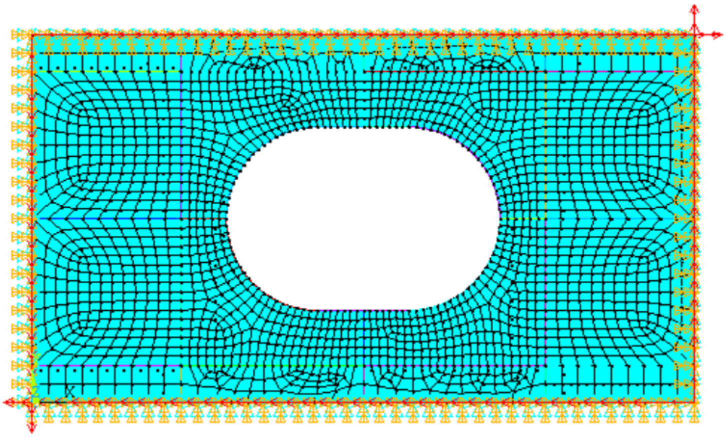

The plate panel is modeled using the Shell181 element type, which is well suited for linear, large rotation, and/or large strain nonlinear applications.

Appendix C1, Figures 3 and 4 provide the results from the eigenvalue buckling analysis and the nonlinear buckling analysis, where the reduction factor is defined as the elastic buckling stress or ultimate strength ratio between the perforated plate and the intact plate.

FIGURE 3
Elastic Buckling Reduction Factor

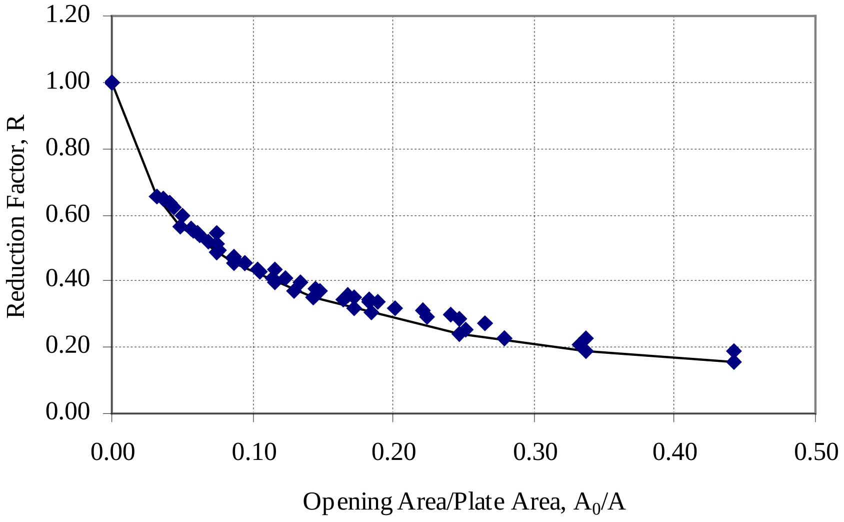

FIGURE 4
Ultimate Strength Reduction Factor

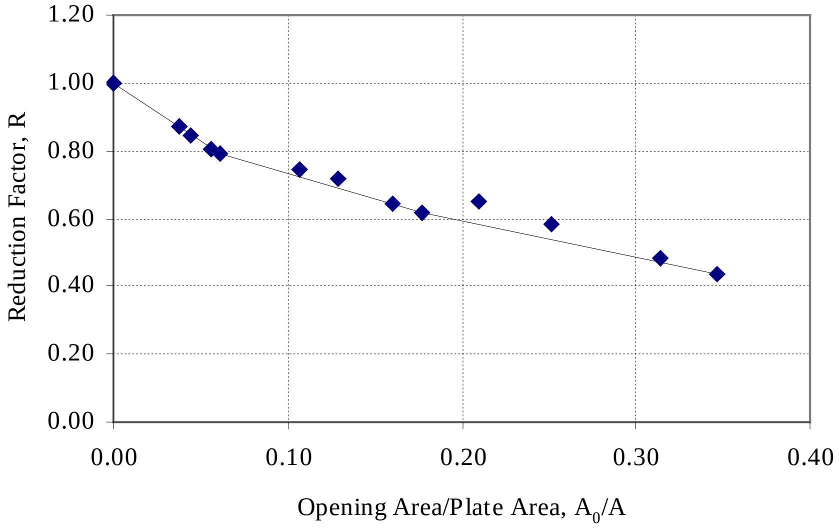

The results of the present eigenvalue buckling analysis are in quite good agreement with those by Yao et al[139,140] and Harada and Fujikubo[141]. The following requirements were satisfied in the present FEA for the ultimate strength analysis for perforated plates:

- The pre-buckling stress was uniform for the intact plate, and the stress concentration factor from the analysis was comparable to that obtained from an analytical solution for the perforated plate under the boundary conditions where the edges remain straight during loading.
- The eigenvalue for the intact plate was consistent with the analytical solution under the boundary conditions where the edges remain straight during loading.
- The ultimate strength is limited to the shear strength of material.

APPENDIX C2 References

1. ABS(2001). ABS *Rules for Building and Classing Mobile Offshore Drilling Units*.
2. ABS(2004). ABS *Rules for Building and Classing Steel Vessels*.
3. API(2000). API RP 2A-WSD, Recommended Practice for Planning, Designing and Constructing Fixed Offshore Platforms.
4. Hoadley, P W and Yura, J A (1985). Ultimate strength of tubular joints subjected to combined loads. OTC paper #4854, Houston, Texas, USA.
5. API(2000). Bulletin on Design of Stability Design of Cylindrical Shells, API BULLETIN 2U.
6. API(2000). Bulletin on Design of Flat Plate Structures, API BULLETIN 2V.
7. DnV(1995). DNV Classification Notes No. 30.1, Buckling strength analysis.
8. DnV(2002). DNV Recommendation Practice, DnV-RP-C201, Buckling Strength of Plated Structures.
9. IACS(2013) IACS Recommendation No. 47 "Shipbuilding and Repair Quality Standard".
10. Ricles, J M and Hebor, M (1999). Structural testing of corroded offshore tubular members. International Workshop on Corrosion Control for Marine Structures and Pipelines, Galveston, Texas, USA
11. ABS(2014). ABS *Rules for Building and Classing Floating Production Installations*.
12. ABS(2018). ABS *Rules for Building and Classing Offshore Installations*.
13. DnV(1996). *Rules for Classification of Mobile Offshore Units*.
14. ABS(2014). ABS *Rules for Building and Classing Single Point Moorings*.
15. Timoshenko, S P and Gere, J M (1961). "Theory of Elastic Stability", McGraw-Hill Book Company, Inc.
16. American Institute of Steel Construction (AISC), "Specification for the design, fabrication and erection of structural steel for buildings", *Manual of Steel Construction*, Eighth Edition.
17. Chen, W F, and Ross, D A(1977). "Tests of Fabricated Tubular Columns', Journal of the Structural Division, ASCE, Vol. 103, No. ST3.
18. Smith, C S, Kirkwood, W, and Swan, J W (1979). "Buckling Strength and Post-Collapse Behaviour of Tubular Bracing Members Including Damage Effects", Proceedings 2nd Intl. Conference on the Behaviour of Offshore Structures, BOSS, London.
19. Smith, C S, Somerville, W C, and Swan, J W (1981). "Residual Strength and Stiffness of Damaged Steel Bracing Members", OTC paper no. 3981, Houston, TX.
20. Steinmann and Vojta, J F (1989), 'Hydrostatic Beam Column Tests, (Phase II)', Final Report, API Project No. 87-56, CBI Technical Service Co.
21. Yeomans, N F (1976) 'Buckling Strength of Hot-Finished CHS-CIDECT program 2D', CIDECT Report 76/40.
22. Kiziltug, A Y, Grove, R B, Peters, S W, and Miller, C D (1985). "Collapse Tests of Short Tubular Columns Subjected to Combined Loads", Final Report to Joint Industry Group, CBI Industries, Inc.

23. Sherman, D R (1984), "Comparative Study of Flexural Capacity of Pipes", Final Report API Project No. 54201.11, Civil Engineering Department, University of Wisconsin-Milwaukee.

24. Sherman, D R (1986), "Bending Capacity of Fabricated Pipe at End Connections", Final Report to API Civil Engineering Department, University of Wisconsin - Milwaukee.

25. Korol, R M and Hudoba, J (1972). "Plastic Behaviour of Hollow Structural Sections", Proceedings ASCE, Structural Division 98, ST5, 1007-1023.

26. Korol, R M (1979). "Critical Buckling Strains of Round Tubes in Flexure", Int. J. Mech. Sci. 21, 719-730.

27. Kato, B and Akiyama, H (1976). "A Proposal for Design Formulae of Beam-Columns", ECCS, 2nd Int. Colloquium on Stability, Tokyo, Japan, pp. 41-60.

28. Galambos, T V (1998). "Guide to Stability Design Criteria for Metal Structures", the 5th Edition, John Wiley & Sons, INC.

29. ECCS(1978), European Recommendation for Steel Structures, European Convention for Constructional Steelwork, Brussel, Belgium.

30. AISC(1993), Load and Resistance Factor Design for Structural Steel Buildings, American Institute of Steel Construction, Chicago

31. Prion, H G L and Birkemoe, P C (1988). "Experimental Behaviour of Unstiffened Fabricated Tubular Steel Beam-Column", Report No. 88-03, Dept. Of Civil Engineering, University of Toronto, Ontario, Canada.

32. Ellis, J S (1958), "Plastic Behaviour of Compression Members", J. Mechanics and Physics of Solids, 6, pp. 282-300.

33. Wagner, A L, Mueller, W H and Erzurumlu, H (1977). "Ultimate Strength of Tubular Beam-Columns", Proceedings ASCE, Structural Division 103, ST1, pp. 9-12.

34. Miller, C D and Salikis, E P (1993), "Analysis of Cylindrical Shell Database and Validation of Design Formulations", API PRAC Project 90-56.

35. Miller, C D, Kinra, R K, and Marlow, R S (1982). "Tension and Collapse Tests of Fabricated Steel Cylinders," Proceedings Offshore Technology Conference, Paper No. OTC 4218, Houston, Texas.

36. Loh, J T (1990). "A Unified Design Procedure for Tubular Members, "Proceedings, Offshore Technology Conference, No. 6310, Houston.

37. Loh, J T (1989). "A Unified Design Procedure for Tubular Members," Exxon Production Research Co.,Offshore Div.

38. Das, P K (2000). "Buckling and Ultimate Strength Criteria of Stiffened Shells", ABS report OTD2000-03

39. Marzullo, M A and Ostapenko, A (1978). "Tests on Two High-Strength Short Tubular Columns", Proceedings, Offshore Technology Conference, OTC Paper No. 3086, Houston, TX.

40. Ostapenko, A and Grimm, D F (1980). "Local Buckling of Cylindrical Tubular Columns Made of Steel", Report No. 450-7, Fritz Engineering Laboratory, Lehigh University

41. Eder, M F, Grove, R B, Peters, S W, and Miller, C D (1984). "Collapse Tests of Fabricated Cylinders Under Combined Axial Compression and External Pressure", Final Report, American Petroleum Institute PRAC Project 82183-46.

42. ABS (2002). "A Study on the Buckling and Ultimate Strength of Plates in Floating Offshore Structures", ABS, RD2002-05

43. Guedes Soares, C (1988). "A Code Requirement for the Compressive Strength of Plate Elements", Marine Structures, Vol.1

44. Faulkner, D (1975). "A Review of Effective Plating for Use in the Analysis of Stiffened Plating in Bending and Compression", Journal of Ship Research, Vol.19.1

45. Valsgard, S (1983), "Numerical Design Prediction of the Capacity of Plates in Biaxial In-plane Compression", Computers & Structures, Vol.12, pp729-739

46. Porter, D M, Rockey, K C and Evans, H R (1975). "The Collapse Behavior of Plates Loaded in Shear", Structural Engineer, Vol.53.

47. Basler, K (1961). "Strength of Plate Girders in Shear", J. Structural Division, ASCE, ST7

48. Harding, J E (1983). "The Interaction of Direct and Shear Stresses on Plate Panels", In Plated Streuctures-Stability and Strength, edited by R. Narayanan.

49. Frieze, P A (2002). Assessment of ABS SVR Results Using Test Database", ABS Technical Report OTD 2002-05

50. Davidson, P C, Chapman, J C, Smith, C S and Dowling, P J (1989), "The Design of Plate Panels Subject to In-plane Shear and Biaxial Compression", RINA Trans.

51. Davidson, P C, Chapman, J C, Smith, C S and Dowling, P J (1991), "The Design of Plate Panels Subject to Biaxial Compression and Lateral Pressure", RINA Trans.

52. Smith, C S, Davidson, P C, Chapman, J C and Dowling, P J (1987), "Strength and Stiffness of Ships under In-plane Compression and Tension", RINA Trans.

53. Yao, T, Osamu, N, Fujikubo, M, Vargese, B and Muzutani, K (1996), "Buckling/Plastic Collapse Strength of Ship Bottom", J.NAJ, Vol. 181

54. Yao, T, Fujikubo, M, Vargese, B, Yamamura, K and Osamu, N (1997), "Buckling/Plastic Collapse Strength of Wide Rectangular Plate under Combined Pressure and Thrust", J.NAJ, Vol. 182

55. Yao, T and Khedmati, M (1999), "Estimation of Ultimate Strength of Ship Bottom Plating under Combined Transverse Thrust and Lateral Pressure", J.NAJ, Vol. 186

56. Johns, R (1976), "Plastic Behavior of Ship Structures", Trans. SNAME, Vol.84

57. Caldwell, J B (1955), "The Strength of Corrugated Plating for Ships' Bulkheads", Trans. RINA, 97, 495-522

58. Easley, J T (1975), "Buckling Formulas for Corrugated Metal Shear Diaphragms", ASCE Journal of the Structural Division, 101, 1403-1417

59. Paik, J K (1997), "Theoretical and Experimental Study on Ultimate Strength of Corrugated Bulkheads", ABS Technical Report.

60. Hughes, O (1983). *Ship Structural Design*, A Wiley-Interscience Publication

61. Bai,Y (2000), "Marine Structural Design", ABS IBC Training Course.

62. Ellinas, C P, Supple, W J and Walker, A C (1984). "Buckling of Offshore Structures", J.P.Kenny

63. Hughes, O (1983). *Ship Structural Design*, A Wiley-Interscience Publication

64. Mansour, A (1996). "Probability-based Ship Design Implementation of Design Guidelines for Ships: A Demonstration", SSC-SR1345

65. Mansour, A (2001). "Strength of Stiffened and Unstiffened Plates with Damage and Imperfection", ABS Report.

66. Smith, C S (1976). "Compressive Strength of Welded Steel Ship Grillages", RINA Trans.

67. Guedes Soares, C and Gordo, J M (1996). "Compressive Strength of Rectangular Plates Under Biaxial Load and Lateral Pressure", Thin-Walled Structures, Vol.24

68. Guedes Soares, C and Gordo, J M (1996). "Collapse Strength of Rectangular Plates Under Transverse Compression", J. Construct. Steel Res., Vol.3

69. Guedes Soares, C and Gordo, J M (1996). "Design Methods for Stiffened Plates under Predominantly Uniaxial Compression", Marine Structures, Vol.10

70. Ship Structure Committee (1995). “Reexamination of Design Criteria for Stiffened Plate Panels”, SSC-382

71. Stenphen, W B, Serrahn, C S and Chang, B (2002). “Background to New Edition of API Bulletin 2V: Design of Flat Plate Structures”, OTC 14187

72. Valenzuala, E, Wu, J F, Sun, H H and Liu, T J (2004). “ABS Floating Production Installations Guide Rule Change: FPSO Strength and Fatigue Assessment”, Proceeding of OMAE Specialty Symposium on Integrity of Floating Production, Storage & Offloading (FPSO) Systems, OMAE-FPSO’04-0093

73. Dowling, P J and Harding, J E (1982). “Experimental Behavior of Ring and Stringer-stiffened Shells”, Buckling of Shells in Offshore Structures, Ed. J.E. Harding, et al., London: Granada, 73-107.

74. Sridharan, S and Walker, A C (1980). “Experimental Investigation of Buckling Behavior of Stiffened Cylindrical Shells”, Dept of Energy U.K., Report OT-R7835, London.

75. Odland, J (1978). “Buckling Resistance of Unstiffened and Stiffened Circular Cylindrical Shell Structures”, Norwegian Maritime Research, 3, 2-22.

76. Miller, C D (1982). “Summary of Buckling Tests on Fabricated Steel Cylindrical Shells in USA”, Buckling of Shells in Offshore Structures, Ed. J.E. Harding et al., London: Granada, 429-471.

77. Miller, C D (1977). “Buckling of Axially-Compressed Cylinders”, Proc. ASCE Structural Division 103, ST3

78. Kendrick, S B (1972). Collapse of Stiffened Cylinders under External Pressure. Paper No.C190/72, Proc. Institution of Mechanical Engineers Conference on Vessel under Buckling Conditions, London, pp 33-42

79. Miller, C D and Kinra, R K (1981). “External Pressure Tests of Ring-Stiffened Fabricated Steel Cylinders”, J. Petroleum Technology.

80. Miller, C D et al (1983). “Collapse Tests of Fabricated Stiffened Steel Cylinders under Combined Loads”, Presented to the ASME Conference, Portland, Oregon, 20-23 Jun.

81. Faulkner, D, Stiansen, S G and Birrell, N D (1983). “Developments of a Reliability Based Design Code for the Structure of Tension leg Platforms”, Paper OTC-4648, OTC Conference, Houston.

82. ANSI/ASME BPV-I, VIII-1 (1992). ASME Boiler and Pressure Vessel Code.

83. BS5500 (1991). British Standard Specification for Unfired Fusion Welded Pressure Vessels.

84. API(2004). Bulletin on Design of Stability Design of Cylindrical Shells, API BULLETIN 2U.

85. Adamchak, J C (1979). “Design Equations for Tripping of Stiffeners Under In-plane and Lateral Loads”, DTNSRDC Report 79/064, Bethesda, Maryland, Oct. 1979.

86. Agelidis, N A, Harding, J E and Dowling, P J (1982). “Buckling Tests on Stringer-stiffened Cylinder Models Subject to Load Combinations, Det Norske Veritas, Report 282-0298.

87. Bushnell, D (1981). “Computerized Buckling Analysis of Shells”, Flight Dynamics Lab., Wright-Patterson Air Force Base, Ohio, Report AFWAL-TR-81-3049.

88. Chryssanthopoulos, M et al (1981). “Imperfection Sensitivity Analysis of Ultimate Stress of Stringer-stiffened Cylinders under Axial Compression and External Pressure”, Det Norske Veritas, Report 81-1198, Hϕvik, Norway.

89. Das, P K, Faulkner, D and Zimmer R A (1992). “Selection of Robust Strength Models for Efficient Design of Ring and Stringer Stiffened Cylinders Under Combined Loads”, Proceedings of OMAE-92, Calgary.

90. Das, P K, Faulkner, D and Guedes da Silva, A(1991). “User's Manual for Strength Analyses and Failure Surface Routines of Orthogonally Stiffened Cylindrical Shell Structural Components Under Various Loading Conditions”, Dept of Naval Architecture and Ocean Engineering, University of Glasgow, Report No. NAOE-91-27.

91. Das, P K and Faulkner, D (1991). "Local Buckling of Orthogonally Stiffened Cylindrical Shell Structural Components", Dept of Naval Architecture and Ocean Engineering, University of Glasgow, Report No. NAOE-91-30.

92. Das, P K, Faulkner, D and Zimmer R A (1992). "Efficient Reliability Based Design of Ring and Stringer Stiffened Cylinders Under Combined Loads", Proceedings of Behavior of Offshore Structures (BOSS) '92, London, July 1992, 14 pp.

93. Das, P K, Faulkner, D and Guedes da Silva, A (1991). "Limit State Formulations and Modeling for Reliability Based Analysis of Orthogonally Stiffened Cylindrical Shell Structural Components", Dept of Naval Architecture and Ocean Engineering, Univ. of Glasgow, Report No. NAOE-91-26, Aug. 1991.

94. Dowling, P J, et al (1980): "Report on the Testing on Large and Small Scale Stiffened Shells under Axial Compression", Dept of Energy, London, Report OT-R8107.

95. Dowling, P J, et al (1982). "Buckling of Orthogonally Stiffened Cylindrical Shells Used in Offshore Engineering", Buckling of Shells, Ed. E. Ramm, Berlin: Springer-Verlag.

96. Ellinas, C P, Batista, R C and Croll, J G A (1981). "Overall Buckling of Stringer-stiffened Cylinders", Proc. ICE, Part 2, 71, 479-512.

97. Ellinas, C P and Croll, J G A (1981). Discussion of "Analysis of the Behavior of Axially Compresses Stringer Stiffened Cylindrical Shells", by A.C. Walker and S. Sridharan, Proc. Instn Civ. Engrs, Part 2, 70.

98. Ellinas. C P and Croll. J G A (1983): "Experimental and Theoretical Correlations for Elastic Axially-compressed Cylinders", J. Strain Analysis 18, 41-67.

99. Ellinas, C P, Supple, W J and Walker, A C (1984). *Buckling of Offshore Structures*. J.P.Kenny

100. Faulkner, D, Adamchak, J C, Snyder, M and Vetter M F (1973). "Synthesis of Welded Grillages to Withstand Compression and Normal Loads", Computers and Structures, vol. 3, pp 221-246, 1973.

101. Faulkner, D (1976). "Buckling Research Needs for Efficient and Safe Design of Offshore Steel Structures", University of Glasgow Report NAOE-76-03, 5 November 1976.

102. Faulkner, D (1977). "Some Thoughts on the Nature of Hazards Affecting Structures in Deeper Waters", Journal SUT, Vol. 3.

103. Faulkner, D (1987). "Toward a Better Understanding of Compression Induced Tripping". Steel and Aluminium Structures", 3, R. Narayanan (Ed.), Elsevier Applied Science, pp 159-175.

104. Faulkner, D (1983). "The Collapse Strength and Design of Submarines", RINA. Intl. Symposium, Naval Submarines, London.

105. Faulkner, D (2000). "Ring Frame Design Procedures for Orthogonally Stiffened Cylindrical Shells", University of Glasgow Report No. NAOE-92-20.

106. Green, D R and Nelson, H M (1982). "Compression Tests on Large Scale, Stringer-stiffened Tubes", Buckling of Shells in Offshore Structures, Ed. J.E. Harding et al., London: Granada, 25-43.

107. Harding, J E and Dowling P J (1982). "Analytical Results for the Behavior of Ring and Stringer-stiffened Shells", Buckling of Shells in Offshore Structures, Ed. J.E. Harding, et al., London: Granada, 231-256.

108. Harding, J E, et al (1983). "The Buckling Design of Stringer-stiffened Shells Subject to Combined Pressure and Axial Loading", presented at the 15th Annual OTC Conf., Houston, Texas.

109. Kinra, R K (1978). "Hydrostatic and Axial Collapse Tests of Stiffened Cylinders". J. Petroleum Technology, 668-680.

110. Lennon, R F and Das, P K (1987). "The Effect of Cold Forming and Welding Locked in Stress States on the Buckling Resistance of Orthogonally Stiffened Cylinders", Proc. of Intl Conference on Advances in Marine Structures, Dunfermline, April 1997.

111. McCall, S and Walker, A C (1982). "Buckling Tests on Stringer-stiffened Cylinder Models Subject to Load Combinations," Det Norske Veritas, Report 82-0299.

112. Odland, J (1979). "General Buckling of Stringer-stiffened Shells", Det Norske Veritas, Report 79-0042

113. Samuelson, L A (1982). "Practical Analysis Methods for Design of Circular Cylinders with Logitudinal Stiffeners and Subjected to Axial Compression", Buckling of Shells, Ed. E. Ramm, Berlin: Springer-Verlag.

114. Singer, J (1980). "Buckling Experiments on Shells – A Review of Recent Developments", Presented at Euromech Colloqium 128, Stability, Buckling and Post-buckling Behavior; Foundations and Analysis, Delft, 31 Mar-2 Apr 1980.

115. Steen, E, Xirouchakis, P and Valsgard, S. (1982). "Design Proposals for Buckling of Stringer-stiffened Cylindrical Shells under Axial Compression and External Pressure", Det Norske Veritas, Report 82-0268.

116. Steen, E and Valsgard, S (1981). "General Buckling of Orthogonally Stiffened Cylindrical Shells under various Load Conditions", Det Norske Veritas, Report 81-0611.

117. Syngellakis, S and Walker, A C (1981). "Elastic Local Buckling of Longitudinally Stiffened Cylinders", Stability Problems in Engg Structures and Components, Ed. T.H. Richards and P. Stanley, Essex: Applied Science Publishers, 159-178.

118. Valsgard, S and Steen, E (1980). "Simplified Strength Analysis of Narrow-paneled Stringer-stiffened Cylinders under Axial Compression and Lateral Load", Det Norske Veritas, Report 80-0590.

119. Valsgard, S and Foss, G (1982). "Buckling Research in Det Norske Veritas" Buckling of Shells in Offshore Structures, Ed. J.E. Harding et al., London: Granada, 491-548.

120. Videiro, P M (1980). "Reliability-based Design of Marine Structures", Doctoral Thesis, Department of Marine Structures, Faculty of Marine Technology, The Norwegian University of Science and Technology, NTNU, Trondheim, Norway, 1998.

121. Walker, A C and Sridharan, S (1980). "Analysis of the Behavior of Axially Compressed Stringer-stiffened Cylindrical Shells", Proc. ICE., Part 2 69, 447-472.

122. Walker, A C, et al (1982). "Theoretical Analysis of Stringer and Ring Stiffened Shells", Buckling of Shells in Offshore Structures, Ed. J.E. Harding, et al., London: Granada, 183-208.

123. Walker, A C and Sridharan, S (1979). "Buckling of Longitudinally Stiffened Cylindrical Shells", BDSS "79, Paper 72, London, 341-356.

124. Weller, T, Singer, J and Batterman, S C (1974). "Influence of Eccentricity of Loading on Buckling of Stringer-stiffened Cylindrical Shells", Thin Shell Structures: Theory Experiment and Design, Ed. Y.C. Fung, and E.E. Sechler, New Jersey: Prentice-Hall, 305-324.

125. White, J D and Dwight, J B (1977). "Weld Shrinkage in Large Stiffened Tubulars", Proc. of Conference on Residual Stresses in Welded Structures, Welding Institute, Cambridge, December.

126. AWS D1.1(2000), "Structural Welding Code – Steel", American Welding Society, 17th Edition.

127. HSE(1990). Offshore Installations: Guidance on Design, Construction and Certification, Fourth edition, HMSO.

128. BOMEL(1999). Tubular Joints Design Guide - Chapter 2: Static Strength. Dec. 1999. Confidential to Sponsors (including ABS).

129. Hoadly, P A and Yura, J A (1983). "Ultimate strength of tubular joints subjected to combined loads : Phase II". PMFSEL Report No. 83-3. University of Texas at Austin.

130. Weinstein, R M and Yura, J A (1985). "The effect of chord stresses on the static strength of DT tubular connections". PMFSEL Report No. 85-1. University of Texas at Austin.

131. Boone, T J and Yura, J A (1982). "The chord stress effects on the static strength of tubular joints". PMFSEL Report No. 82-1. University of Texas at Austin.

132. Swensson, K and Yura, J A (1986). "The static strength of double-tee tubular joints: load interaction effects". PMFSEL Report No. 86-3. University of Texas at Austin.

133. Dexter, E M and Lee M M K (1994). "Effect of overlap on strength of K Joints in CHS tubular members". 6th Int. Symp. On Tubular Structures, Melbourne.

134. Gazolla, F et al (1999). "Strength Prediction of Axially Loaded Overlap Tubular K Joints". Proc. 9th ISOPE, Breast, France.

135. Sawada, Y et al (1979). "Static and fatigue tests on T joints stiffened by an inner ring". OTC 3422, Houston

136. Murtby, D S R et al (1992). "Structural efficiency of internally ring-stiffened steel tubular joints". Journal of Structural Engineering, ASCE, 118(11)

137. Basu, R I, Kirkhope, K J and Srinivasan (1996). Guideline for Evaluation of Finite Elements and Results, SSC-387

138. ANSYS Release 8.1 Documentation Preview, ANSYS, Inc., 2004

139. Yao, T, Fujikubo, M, Murakami, C, Moriguchi, T (1999). "Buckling strength of perforated rectangular plates under combined loads". Journal of the Kansai Society of Naval Architects of Japan (in Japanese), 233, 723 – 729.

140. Yao, T, Hayashi, S, Murakami, C, Kuwahara T (2001). "Buckling/ultimate strength of perforated rectangular plate under thrust". Journal of the Society of Naval Architects of Japan (in Japanese), 723 – 729.

141. Harada, M, Fujikubo, M (2001). "Estimation of buckling and ultimate strength of rectangular plate with cutout". Journal of the Society of Naval Architects of Japan (in Japanese), 723 – 729.

142. DnV(2002). DNV Recommendation Practice, DnV-RP-C202, Buckling Strength of Shells.